Proceedings of the Zoological Institute RAS
Vol. 321, No. 4, 2017, pp. 433–484

УДК 56.569

THERIAN POSTCRANIAL BONES FROM THE UPPER CRETACEOUS BISSEKTY FORMATION OF UZBEKISTAN

A.O. Averianov[1, 2]* and J.D. Archibald[3]

[1]*Zoological Institute of the Russian Academy of Sciences, Universitetskaya Emb. 1, 199034 Saint Petersburg, Russia; e-mail: dzharakuduk@mail.ru*

[2]*Institute of Geology and Petroleum Technology, Kazan Federal University, Kremlevskaya Str. 4/5, 420008 Kazan, Russia*

[3]*Department of Biology, San Diego State University, San Diego, California, 92182-4614, USA; e-mail: darchibald@mail.sdsu.edu*

ABSTRACT

The Upper Cretaceous (upper Turonian) Bissekty Formation of Uzbekistan produces the most diverse Cretaceous therian fauna including one stem marsupial and eleven stem placental taxa known from cranial and dental elements. Some isolated postcranial elements from the Bissekty Formation can be confidently attributed to some of these taxa based on morphology and size. The humeral fragments, astragalus, and calcanei attributed to the deltatheroidan *Sulestes karakshi* Nessov, 1985 are similar to these bones in other stem marsupials. Postcranial bones referred to Zhelestidae Nessov, 1985 and Asioryctitheria Novacek et al., 1997 possess plesiomorphic therian morphologies, which are also present in some stem marsupials. All fragments of scapula from the Bissekty Formation show a plesiomorphic morphology with a trough-like infraspinous fossa placed medially to the supraspinous fossa. Bones attributed to the stem placental *Paranyctoides quadrans* (Nessov, 1982) and to the zalambdalestid *Kulbeckia kulbecke* Nessov, 1993 indicate arboreal and cursorial specializations, respectively. In particular, *Kulbeckia* Nessov, 1993 is similar to *Zalambdalestes* Gregory et Simpson, 1926 in having long and distally fused tibia and fibula and a long calcaneal tuber. Its distal humerus has a deep trochlea, large medial trochlear keel, and large capitular tail separated from a cylindrical capitulum by a shallow groove. The upper ankle joint of *Kulbeckia* has the complete separation of medial and lateral astragalotibial articulations.

Key words: Cretaceous, Eutheria, evolution, Mammalia, Metatheria, morphology, postcranial skeleton, Theria

ПОСТКРАНИАЛЬНЫЕ КОСТИ ТЕРИЕВ ИЗ ВЕРХНЕМЕЛОВОЙ БИССЕКТИНСКОЙ СВИТЫ УЗБЕКИСТАНА

А.О. Аверьянов[1, 2]* и Дж.Д. Арчибальд[3]

[1]*Зоологический институт Российской академии наук, Университетская наб. 1, 199034 Санкт-Петербург, Россия; e-mail: dzharakuduk@mail.ru*

[2]*Институт геологии и нефтегазовых технологий, Казанский Федеральный Университет, Кремлевская ул. 4/5, 420008, Казань, Россия*

[3]*Отдел биологии, Университет штата Сан-Диего, Сан-Диего, Калифорния, 92182-4614, США; e-mail: darchibald@mail.sdsu.edu*

РЕЗЮМЕ

Из верхнемеловой (верхний турон) биссектинской свиты Узбекистана известна наиболее разнообразная фауна меловых терий, включающая один таксон стволовых сумчатых и одиннадцать таксонов стволовых плацентарных, известных по черепным и зубным остаткам. Некоторые изолированные посткраниальные

**Corresponding author / Автор-корреспондент*

элементы из биссектинской свиты могут быть надежно отнесены к некоторым из указанных таксонов на основании морфологии и размеров. Фрагменты плечевой, таранной и пяточной костей, отнесенные к дельтатероиду *Sulestes karakshi* Nessov, 1985, сходны с аналогичными костями стволовых сумчатых. Посткраниальные кости, отнесенные к Zhelestidae Nessov, 1985 и Asioryctitheria Novacek et al., 1997, характеризуются плезиоморфной для териев морфологией, которая наблюдается также у некоторых стволовых сумчатых. Все фрагменты лопатки из биссектинской свиты имеют плезиоморфную морфологию с желобообразной подосной ямкой, расположенной медиальнее надосной ямки. Кости, отнесенные к стволовому плацентарному *Paranyctoides quadrans* (Nessov, 1982) и к залямбдалестиду *Kulbeckia kulbecke* Nessov, 1993, указывают на специализацию к древесному и бегающему образу жизни соответственно. В частности, *Kulbeckia* Nessov, 1993 сходна с *Zalambdalestes* Gregory et Simpson, 1926 по наличию длинных и сращенных дистально берцовых костей и длинного пяточного бугра. На дистальном конце ее плечевой кости имеются глубокий блок, большой медиальный блоковый гребень и большой капитулярный вырост, отделенный от цилиндрического капитулюма неглубокой бороздкой. На голеностопном суставе *Kulbeckia* полностью разделены медиальная и латеральная фасетки для сочленения таранной и большой берцовой костей.

Key words: меловой период, Eutheria, эволюция, Mammalia, Metatheria, морфология, посткраниальный скелет, Theria

INTRODUCTION

The Upper Cretaceous (Turonian) Bissekty Formation in Uzbekistan has produced one of the most diverse Mesozoic mammalian faunas, comprised of one multituberculate, one symmetrodont, one stem marsupial, and eleven stem placental taxa (Archibald and Averianov 2003, 2005a, 2006, 2012; Averianov and Archibald 2006, 2013; Averianov et al. 2010). The mammalian assemblage from the Bissekty Formation and the slightly older and less known mammalian assemblage from the Cenomanian Khodzhakul Formation of Uzbekistan (Averianov and Archibald 2005) are the earliest known eutherian dominated faunas, showing significant diversification of stem placental mammals by the beginning of the Late Cretaceous. The eutherian mammals from the Bissekty Formation are represented by *Paranyctoides* Fox, 1979 of uncertain affinities, a number of taxa of Asioryctitheria Novacek et al., 1997 and Zhelestidae Nessov, 1990, and the zalambdalestid *Kulbeckia* Nessov, 1993. This is the highest diversity of stem placental mammals known from a single Cretaceous fauna. Together with mammalian cranial and dental remains, intensive screening of the fossiliferous strata of Bissekty Formation at Dzharakuduk (Fig. 1a, b) produced several hundred postcranial elements, attributable to Multituberculata Cope, 1884 (Kielan-Jaworowska and Nesov 1992; Chester et al. 2010) and Theria Parker et Haswell, 1897. Although isolated, these postcranial bones are often excellently preserved providing a rare opportunity to study the postcranial morphology of Mesozoic therians in detail.

Nesov briefly mentioned and figured some therian postcranial elements from the Bissekty Formation (Nesov 1982: pl. 2, figs 1, 4; Nesov 1985: pl. 2, figs 8, 9; pl. 3, fig. 13; Nesov 1987: pl. 1, figs. 7, 8). Fragments of distal humeri, proximal and distal femora, and tarsal bones from the Bissekty Formation have been studied by Szalay and Sargis (2006) and Chester et al. (2010, 2012), who identified the presence of several metatherian and eutherian taxa. Newly identified vertebrae as well as fragmentary elements of the fore and hind limb from the Bissekty Formation are described in the present paper. There are also isolated vertebral centra, sternebrae, metapodials, and phalanges that are likely mammalian, but which are not included in this study because they are not very informative. Some mammalian postcranial specimens from the Bissekty Formation have been published under field URBAC numbers (Szalay and Sargis 2006; Chester et al. 2010, 2012). These specimens are housed now in the USNM collection. The new and old collection numbers are provided on the complete list of the studied postcranial specimens in Supplemental Table 1.

Institutional abbreviations. CCMGE, Chernyshev's Central Museum of Geological Exploration, Saint Petersburg; USNM, National Museum of Natural History, Smithsonian Institution, Washington DC, USA; ZIN, Zoological Institute, Russian Academy of Sciences, Saint Petersburg, Russia.

Table 1. Measurements (in mm) of therian postaxial cervical vertebrae from the Upper Cretaceous Bissekty Formation of Uzbekistan. Measurements: ACH – anterior height of centrum; ACW – anterior width of centrum; ANW – anterior width of neural arch (between lateral margins of prezygapophyses); CL – centrum length; NAL – neural arch length (between anterior and posterior margins of dorsal roof of neural canal); PCH – posterior height of centrum; PCW – posterior centrum width; PNW – posterior width of neural arch (between lateral margins of postzygapophyses).

Specimen	ACH	ACW	ANW	CL	NAL	PCH	PCW	PNW
USNM 642672	1.9	3.5	–	2.5	1.7	–	3.6	6.0
USNM 642673	2.0	3.9	~6.7	~2.3	1.9	1.9	3.7	6.4
USNM 642674	1.2	3.0	4.3	2.4	–	1.5	3.0	–
ZIN 88925	2.0	3.7	–	3.0	–	2.0	3.6	–

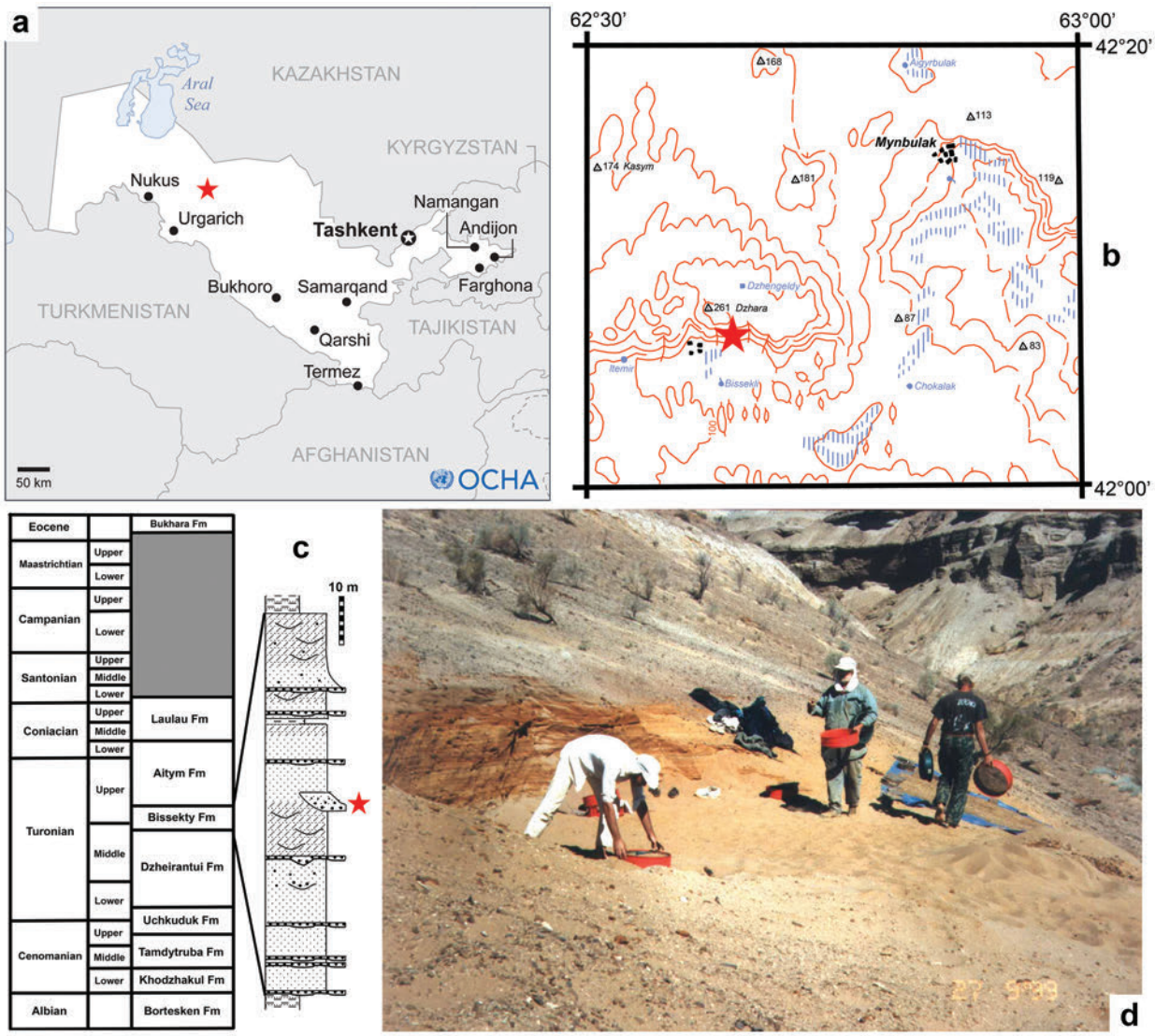

Fig. 1. Location of the Dzharakuduk locality complex (indicated by star) on a map of Uzbekistan and neighboring regions **(a)** and on a more detailed map of the region around Mynbulak **(b)**. Stratigraphic scheme of the Cretaceous strata in the central Kyzylkum Desert, Uzbekistan with section of the Bissekty Formation at Dzharakuduk, with the position of the site CBI-14, marked by an asterisk **(c)**. Dry screening of fossiliferous sediments at CBI-14 site in 1999 by members of URBAC expedition **(d)**, photo by A. Averianov.

METHODS

The mammalian postcranial specimens described here were collected by L.A. Nesov and colleagues in 1977–1994 and by the URBAC (Uzbekistan/Russian/British/American/Canadian) joint paleontological expeditions in 1997–2006 in the Turonian Bissekty Formation at Dzharakuduk, central Kyzylkum Desert, Uzbekistan (Archibald et al. 1998; Nesov et al. 1998). At Dzharakuduk the Bissekty Formation is exposed along an escarpment that extends from about 42°06´22.60´´N and 62°37´09.00´´E to 42°05´44.22´´N and 62°41´06.49´´E (Fig. 1b). The Bissekty Formation comprises an up to 80 m thick succession of medium-grained, poorly lithified, cross-bedded fluvial sandstones and clast-supported, well-cemented intraformational conglomerates (Redman and Leighton 2009) (Fig. 1c). The geological age is bracketed using invertebrate fossils from marine units overlying and underlying the Bissekty Formation, as well as by the comparison with the Late Cretaceous vertebrate complexes of Central Asia (Averianov and Sues 2012). The unit is assigned a late Turonian age, approximately 90.4–88.6 Ma (Gradstein et al. 2004).

Fossils were recovered by surface collecting at the richest sites in 1977–1994 with subsequent dry and wet screening of 300 metric tons of matrix between 1997 and 2006 (Fig. 1d), which produced approximately 1500 mammalian specimens (Archibald and Averianov 2005a).

The anatomical terminology generally follows Evans (1993) and Szalay (1993). For the sake of brevity, we refer to the monotypic taxa by the generic names only.

We used molar size as a proxy for body mass in these Cretaceous therians. The first molars are the least variable among the molar series and thus most suitable for body mass estimation (Gingerich 1974). The body mass prediction is more accurate based on m1 than on M1 (Gingerich et al. 1982; Gingerich and Smith 1985). This is fortunate because mammalian upper molars are far less common compared to lower molars in fluviatile deposits, including the Bissekty Formation. We calculated the size of m1 for eutherians from the Bissekty Formation and m2 for the metatherian *Sulestes* Nessov, 1985, because in metatherians m1 is homological with the eutherian dp5 (Averianov et al. 2010) which is generally smaller than m2–3. We used two regression equations, one calculated for insectivorous-like mammals by Bloch et al. (1998) (1) and the other calculated for all primates by Conroy (1987) (2):

(1) $\ln Y = 1.628 \ln X + 1.726$

(2) $\ln Y = 1.784 \ln X + 2.54$

where X is length multiplied by width of m1 (m2 in *Sulestes*) in mm^2, and Y is body mass in g. For the tooth width we used the greater of two values, trigonid width or talonid width. Calculated body mass values for 45 therian specimens of 11 species from the Bissekty Formation are given in Supplemental Tables 2 and 3. The average value of body mass and standard error for multiple samples are presented in Supplemental Table 4. *Parazhelestes robustus* Nesov, 1993, for which m1 is unknown (Archibald and Averianov 2012), is not included. Based on other parts of the dentition, this species is intermediate in size between *Parazhelestes mynbulakensis* (Nesov, 1985) and *Eoungulatum kudukensis* Nesov et al., 1998.

The body mass estimated using the first equation is approximately three times smaller than the values produced by the second equation (Supplemental Table 4). The estimated body mass values, based on the first equation, undoubtedly constitute a serious underestimation of the actual body weight. Postcranial elements attributed to *Kulbeckia* based on morphology and size correspond to the same elements in a specimen of *Rattus rattus* (Linnaeus, 1758) with a body mass 92 g (ZIN 104198). The body mass estimation from the first equation for *Kulbeckia* gives a value several times smaller, ~30 g (Supplementary Table 4). The second equation produces a mean value of body mass ~80 g for *Kulbeckia*, which seems more likely. We think that the reason for the underestimating body mass in the first equation is inclusion of many derived extant soricomorph taxa in the dataset by Bloch et al. (1998), which have a high level of metabolism and small body size relative to the size of their teeth. Tenrecoids, which were not included in the Bloch et al. dataset, possess a comparatively small tooth size relative to body mass, providing a more suitable model for the body mass estimation of Mesozoic stem placentals, which likely had a similar level of metabolism.

The body mass estimations based on postcranial bones are more reliable than those from dentition because postcranial bones are involved in weight bearing (Moncunill-Solé et al. 2015). There have been several attempts to estimate body mass from postcranial remains (Gingerich 1990; Scott 1990; Anyonge 1993), but they utilized complete long bones, unknown for

Table 2. Measurements (in mm) of therian thoracic and lumbar vertebrae from the Upper Cretaceous Bissekty Formation of Uzbekistan. Measurements: ACH – anterior height of centrum; ACW – anterior width of centrum; ANW – anterior width of neural arch (between lateral margins of prezygapophyses); CL – centrum length; NSL – neural spine length (between anterior and posterior margins); PCH – posterior height of centrum; PCW – posterior centrum width; PNW – posterior width of neural arch (between lateral margins of postzygapophyses).

Specimen	ACH	ACW	ANW	CL	NSL	PCH	PCW	PNW
				Thoracic vertebrae				
USNM 594513	2.8	3.4	2.9	3.7	2.4	1.8	3.4	1.95
USNM 594518	1.9	3.3	–	3.5	2.8	1.7	3.5	–
USNM 594579	1.5	2.4	–	3.2	1.6	1.7	2.7	2.1
USNM 594690	2.6	4.0	4.5	4.4	2.8	2.3	3.8	–
USNM 605212	1.1	2.6	–	3.4	–	1.4	2.6	–
USNM 642700	2.0	4.4	4.4	4.6	4.5	1.9	4.3	3.8
ZIN 82557	2.4	4.0	–	5.2	2.5	2.2	4.2	~3.9
ZIN 82564	2.2	4.7	–	~6.5	3.7	–	–	–
ZIN 103874	–	–	–	–	1.5	3.1	5.3	–
ZIN 103875	2.1	3.0	3.1	3.0	–	1.9	3.5	–
				Lumbar vertebrae				
USNM 642671	0.8	2.2	2.5	1.9	1.3	1.0	1.9	2.2
ZIN 88878	1.5	3.1	–	3.4	–	1.5	3.3	–

the Bissekty therians, and mostly pertain to much larger mammals. For large mammals, body mass predictions based on teeth and postcranial bones can differ dramatically (Millien and Bovy 2010).

For attribution of isolated tarsal bones, a method of linear regression between molar size and length of tarsal bones has been used (Cifelli 1983; Coillot et al. 2013; Hooker 2014; Penkrot and Zack 2016). However, the available data on associated Cretaceous therian tarsals and dentition is insufficient for construction of the linear regression model.

We used postcranial skeletons of three small extant mammals for size comparisons with the Bissekty therians: Radde's shrew, *Sorex raddei* Satunin, 1895 (ZIN 70913, adult male, Krasnodar Territory, Russia, body weight 10.9 g), a black rat, *Rattus rattus* (ZIN 104198, adult male, Estonia, body weight 92 g), and a European hedgehog, *Erinaceus europaeus* Linnaeus, 1758 (ZIN 52645, adult male, Leningrad Province, Russia). The body weight for the first two specimens was registered during collection. The body mass of *E. europaeus* may vary significantly depending on available food. In Finland the body weight of adult hedgehogs varied between 500 and 950 g (Kristoffersson 1971). An average value, 725 g, is conditionally accepted for ZIN 52645.

All scatterplots were performed using STATISTICA 7.1 ©StatSoft, Inc. 1984–2005.

Morphological Description and Comparison

Atlas and axis. Seven left and one right halves represent the atlas. USNM 594713 has the more complete anterior articular fovea (Fig. 2c), while the dorsal arch is most complete on USNM 594520 (Fig. 2a, b). These two specimens, as well as ZIN 103871, ZIN 104118, and ZIN 104119, fit the size of *Rattus rattus*. USNM 594587 is somewhat smaller, but larger than the atlas of *Sorex raddei*. ZIN 88917 and 103873 are the largest specimens, which are smaller than the atlas of *Erinaceus europaeus*. All atlas fragments have similar morphology. The anterior articular fovea has an auriculate shape. It is deeply concave and extends across the medial surface of the neural arch. ZIN 103873 preserves the medial end of the anterior articular fovea documenting that it does not extend onto the atlas intercentrum. The posterior articular fovea is oval-shaped and flat to slightly concave, or more concave (USNM 594713; Fig. 2e, f). The dorsal arch (USNM 594520; Fig. 2a, b) curves gently with a constant width throughout its height. Its base

Table 3. Measurements (in mm) of caudal vertebrae from the Upper Cretaceous Bissekty Formation of Uzbekistan. Measurements: ACH – anterior height of centrum; ACW – anterior width of centrum; ANW – anterior width of neural arch (between lateral margins of prezygapophyses); CL – centrum length; PCH – posterior height of centrum; PCW – posterior centrum width; PNW – posterior width of neural arch (between lateral margins of postzygapophyses).

Specimen	ACH	ACW	ANW	CL	PCH	PCW	CL/ACW
			Anterior caudals				
USNM 590598	1.6	2.3	–	3.9	1.8	2.5	1.67
USNM 594567	2.1	3.2	3.1	5.7	2.3	3.2	1.78
USNM 642637	1.4	2.2	–	3.0	1.5	2.2	1.37
USNM 642638	2.8	3.5	4.1	9.4	3.2	4.3	2.69
USNM 642641	5.6	6.7	–	9.7	5.7	6.0	1.48
ZIN 88905	1.6	2.4	3.1	4.1	2.2	1.8	1.71
ZIN 88910	1.9	2.2	–	6.3	2.0	2.5	2.86
ZIN 103877	–	2.5	–	5.2	1.8	2.4	2.08
			Posterior caudals				
USNM 594719	2.5	3.6	–	12.4	2.5	3.3	3.44
USNM 594720	2.2	2.6	–	9.9	1.9	2.2	3.81
USNM 642635	2.2	2.7	–	9.9	1.8	3.0	3.67
USNM 642636	2.0	2.3	–	8.2	1.8	2.3	3.57
USNM 642639	1.8	2.4	2.2	7.7	1.6	2.2	3.21
USNM 642640	1.4	1.7	–	8.1	1.3	1.6	4.77
ZIN 88865	1.6	2.0	–	4.6	1.8	2.2	2.30
ZIN 88903	1.4	1.7	–	6.8	1.3	1.8	4.00
ZIN 88904	1.6	2.0	–	5.1	1.5	3.0	2.55
ZIN 103878	2.7	3.6	–	10.4	2.8	3.1	2.89
ZIN 103879	1.2	1.5	–	6.2	1.0	1.5	4.13

occupies the middle third of the atlas length. The transverse process is broken on all specimens. The base of transverse process is flattened dorsoventrally and similar in anteroposterior length to the dorsal arch. There are no transverse and atlantal foramina. Medially (not shown), there is a very narrow space between the anterior and posterior articular foveae, suggesting that an intercentrum (not preserved) would be very short anteroposteriorly compared with the neural arch in *Barunlestes* Kielan-Jaworowska, 1975 (Kielan-Jaworowska 1978: fig. 2D).

The atlantes from the Bissekty Formation are generally similar to the atlas of *Maelestes* Wible et al., 2007 (Wible et al. 2009: fig. 20). The latter differs from the Bissekty atlantes in that the dorsal arch is placed closer to the posterior end of the neural arch and is markedly widening medially. In *Maelestes* the transverse process has a more rounded cross section

Table 4. Measurements (in mm) of therian scapula fragments from the Upper Cretaceous Bissekty Formation of Uzbekistan. Measurements: GL – glenoid length; GW – glenoid width.

Specimen	GL	GW
	Size class I	
ZIN 103866	3.2	1.5
	Size class II	
USNM 642633	3.4	1.9
	Size class III	
ZIN 103867	4.6	–
USNM 642630	–	2.7
	Size class IV	
USNM 642634	5.7	3.6

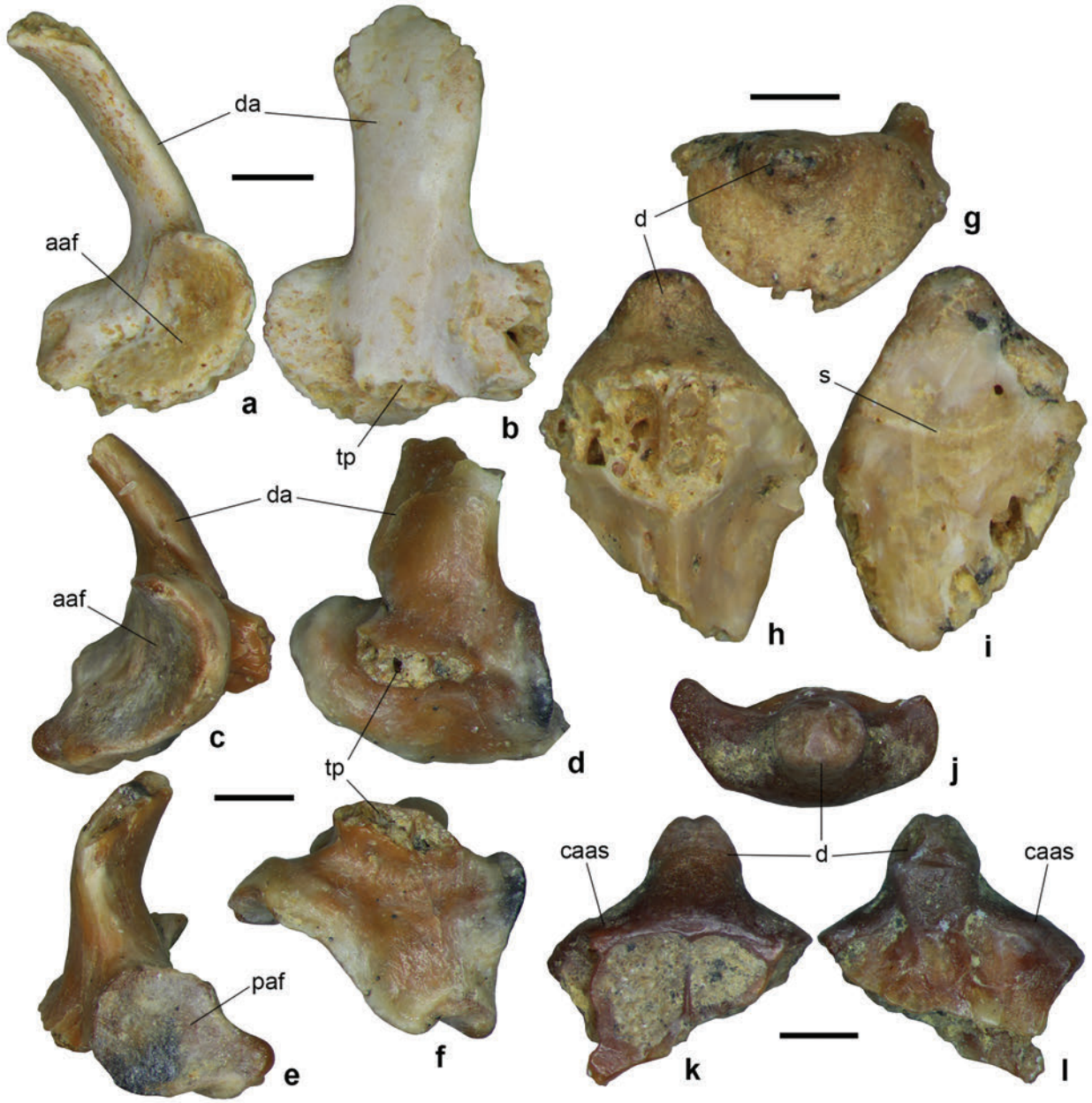

Fig. 2. Fragments of atlas and axis from the Upper Cretaceous Bissekty Formation of Uzbekistan. **a–b** – USNM 594520, left neural arch of atlas, in anterior **(a)** and lateral **(b)** views. **c–f** – USNM 594713, left neural arch of atlas, in anterior **(c)**, lateral **(d)**, posterior **(e)**, and ventral **(f)** views. **g–i** – USNM 594554, fragment of axis odontoid process, in anterior **(g)**, ventral **(h)**, and dorsal **(i)** views. **j–l** – ZIN 104120, axis fragment, in anterior **(j)**, ventral **(k)**, and dorsal **(l)** views. *Abbreviations*: aaf – anterior articular fovea; caas – centrum anterior articular surface; d – dens; da – dorsal arch; paf – posterior articular fovea; s – suture separating the proatlas centrum and the atlas centrum; tp – transverse process. Scale bars each equal 1 mm.

and the sulcus of the vertebral artery is ventral to the transverse process (anterior to this process in USNM 594520; not discernible in other specimens). The atlas of *Ukhaatherium* Novacek et al., 1997 (Horovitz 2003: fig. 3) is similar to USNM 594520 in the position of the sulcus for vertebrate artery, between the dorsal arch and the anterior articular fovea, and in the general shape of the preserved part. The

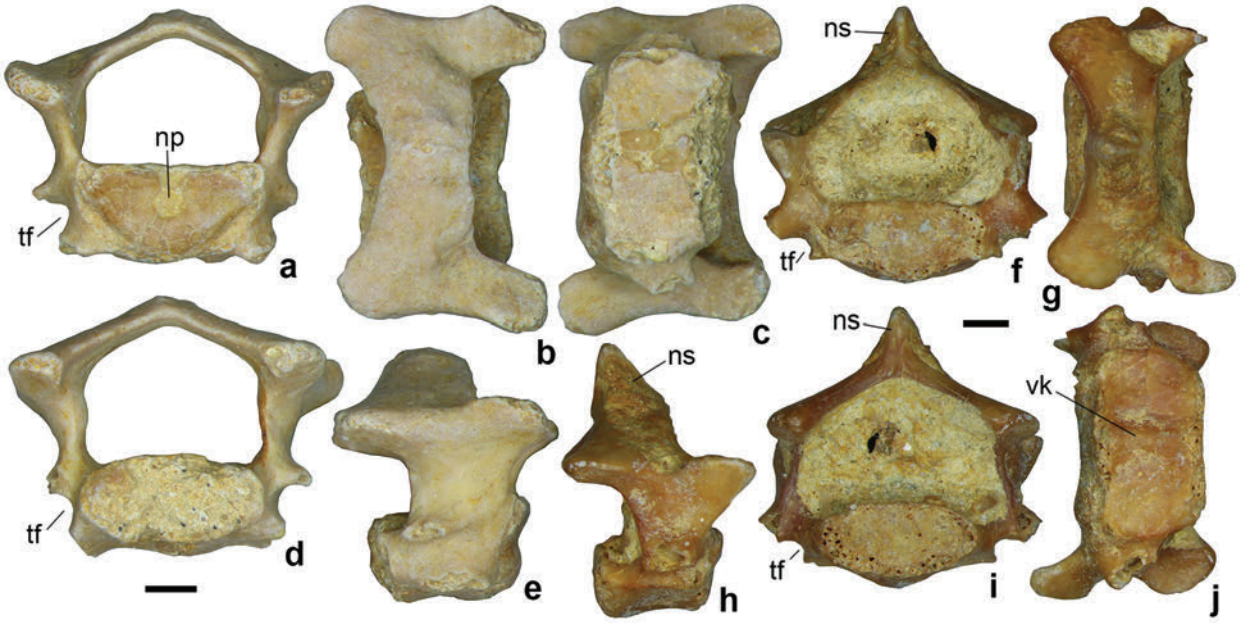

Fig. 3. Postaxial cervical vertebrae from the Upper Cretaceous Bissekty Formation of Uzbekistan. **a**–**e** – USNM 642673, in anterior (**a**), dorsal (**b**), ventral (**c**), posterior (**d**), and lateral (**e**) views. **f**–**j** – USNM 642672, in anterior (**f**), dorsal (**g**), lateral (**h**), posterior (**i**), and ventral (**j**) views. *Abbreviations*: np – notochordal pit; ns – neural spine; tf – transverse foramen; vk – ventral keel. Scale bars each equal 1 mm.

atlas of *Asioryctes* Kielan-Jaworowska, 1975 (Kielan-Jaworowska 1977: fig. 1A) differs from the Bissekty atlantes in having the dorsal arch closer to the posterior end of neural arch (unclear in *Ukhaatherium*), anteroposteriorly it has a shorter neural arch, and a more pronounced sulcus for the vertebral artery, which is placed anterior to the transverse process, as in *Ukhaatherium* and Bissekty atlantes. Atlantes of both *Asioryctes* and *Ukhaatherium* are similar to the Bissekty atlantes in having a dorsoventrally flattened transverse process, in contrast to the more rounded cross-section of the transverse process in *Maelestes*. The atlas of *Barunlestes* (Kielan-Jaworowska 1978: fig. 2) differs from all mentioned taxa and specimens from the Bissekty Formation in having a short neural arch, wedge-shaped in lateral view, and in the presence of a transverse canal. The sulcus of the vertebral artery is anterior to the dorsal arch.

There are two axial fragments from the Bissekty Formation. USNM 594554 (Fig. 2g–i) preserves the incomplete odontoid process with the dorsal suture apparently separating the proatlas centrum and the atlas centrum (Jenkins 1969; Evans 1993) (Fig. 2i). The specimen belonged to an animal intermediate in size between *Rattus rattus* and *Erinaceus europaeus*. The dens is pointed, with the dorsal side projecting more anteriorly compared with the ventral side. All ventral and lateral sides of the dens are covered by a smooth articular surface for the atlas intercentrum (maximum width of this surface is 2.8 mm). This articular surface was not connected with the anterior articular surface of the axial centrum, which is not preserved. On the dorsal side, there is a pair of vascular foramina anterior to the suture. Posterior to the suture there is a pair of shallow oval depressions in the floor of neural canal. On the ventral side there is a distinct median ridge flanked by two small slit-like foramina. These foramina are positioned in the deep lateral depressions occupying the space between the median ridge and anterior articular surfaces of the axis centrum.

USNM 594554 is generally similar to CCMGE 6/11758, an axis referable to a large zhelestid from the Khodzhakul Formation of Uzbekistan (Nesov et al. 1994: pl. 1, fig. 5; Averianov and Archibald 2005). In particular, in both specimens the articular surface of the dens is not confluent with the anterior articular surface of the centrum. However, in USNM 594554 the dens is much shorter, without a neck, with non-parallel lateral sides, lacking the tongue-like exten-

sion of the articular surface on the ventral side, and in having shallower dorsal depressions. The low median ridge, flanked by lateral depressions, and separate articulate surfaces of the dens and axial centrum, are also present in the axis of *Maelestes* (Wible et al. 2009: fig. 21). In *Maelestes* the axial dens is relatively longer, compared to USNM 594554.

ZIN 104120 is a fragment of a much smaller axis, preserving the dens and the anterior articular surfaces of the axial centrum, which, in contrast with USNM 594554, are connected with the articular surface of the dens (Fig. 2j–l). There are shallow depressions separated by a wide median ridge on the dorsal side. On the ventral side two smaller depressions are separated by a much narrower median ridge. This construction is generally similar to that in CCMGE 6/11758. Among stem placentals, the anterior articular surfaces of the axis centrum are linked to each other in *Asioryctes* (Kielan-Jaworowska 1977) and separate in *Maelestes* (Wible et al. 2009). These surfaces are described as confluent for *Zalambdalestes* Gregory et Simpson, 1926 and *Barunlestes* (Kielan-Jaworowska 1978: p. 10), but on the reconstruction of the axis of *Barunlestes* they are shown as separate (Kielan-Jaworowska 1978: fig. 4A). *Barunlestes* is coded as having separate surfaces in the analysis by Wible et al. (2009). In the axis of *Asioryctes* (Kielan-Jaworowska 1977: fig. 1B) there is a similar narrow ventral ridge, but the depressions are less pronounced. In the axis of *Maelestes* (Wible et al. 2009: fig. 21) the ventral median ridge is distinctly wider and there is no median ridge on the dorsal side. In ZIN 104120 the dens is anterodorsally directed, as in *Zalambdalestes*, while in *Barunlestes* it is more horizontal (Kielan-Jaworowska 1978: figs. 3A, 4A). Based on the linked anterior articular surfaces, ZIN 104120 likely belongs to Asioryctitheria.

Postaxial cervical vertebrae. There are four postaxial cervical vertebrae in the collection, four of which have the neural arch. The smallest specimen (USNM 642674) fits the size of *Rattus rattus*. Two other specimens (USNM 642672; Fig. 3f–j and USNM 642673; Fig. 3a–e) are slightly larger (Table 1). The largest specimen (ZIN 88925) is smaller than the cervicals of *Erinaceus europaeus*. The vertebrae have a dorsoventrally flattened centrum and a high delicate neural arch enclosing a large neural canal. The neural canal is about 1.5–2 times higher than the centrum. The cervical ribs (not complete on any specimen) are coosified with the centrum and form the transverse foramen between the rib's tuberculum and capitulum, and the vertebra's centrum (Fig. 3a, d, f, i). The centrum articular surface is oval-shaped or D-shaped, convex ventrally (USNM 642673 anterior surface (Fig. 3a) and USNM 642674 both surfaces). Presence of a ventral centrum keel does not affect the shape of articular surface; it is present in one specimen with D-shaped articular surfaces (USNM 642674) and in one specimen with oval-shaped articular surfaces (USNM 642672; Fig. 3j). The ventral surfaces of other centra are flat. The centrum articular surfaces are slanted so the anterior surface is faced anteroventrally and posterior surface – posterodorsally. This slanting is most pronounced in ZIN 88925, which might be one of the most anterior postaxial cervicals, possibly number three. In this vertebra there is a distinct notochordal pit in the center of anterior and posterior articular surfaces. A larger notochordal pit, connected to the dorsal centrum surface by a vertical groove, is present in USNM 642673 (Fig. 3a). In the latter vertebra, the posterior centrum articular surface was apparently not coosified with the centrum suggesting that it is a juvenile specimen. In USNM 642673 and ZIN 88925 there is a pair of vascular foramina in the middle of dorsal centrum surface (this surface is not prepared in two other specimens).

The neural arch (most complete in USNM 642672 and USNM 642673) is arcuate, with the minimum anteroposterior length at the midline. The prezygapophyses are distinct processes, whereas the postzygapophyses are not separated from the neural arch into distinct processes. The zygapophyseal articular surfaces are oval-shaped, with the long axis anteroposterior. The prezygapophyseal articular surfaces are somewhat larger than the postzygapophyseal surfaces. USNM 642674 has no neural spine, whereas in USNM 642673 (Fig. 3e) it is a short, low ridge and in USNM 642672 (Fig. 3h) it is a relatively high process with a triangular shape in lateral view.

In *Maelestes* cervical seven has a rounded ventral surface (Wible et al. 2009). In the postaxial cervicals from the Bissekty Formation the ventral surface of the centrum is either rounded or has a median ridge. The transverse foramen is present on all postaxial cervical vertebrae in Monotremata and Multituberculata (Kielan-Jaworowska and Gambaryan 1994). In *Maelestes* as well as in most extant therians there is no transverse foramen on cervical seven (Lessertisseur and Saban 1967; Evans 1993; Wible et al. 2009).

All Bissekty specimens have the transverse foramina suggesting that cervical seven is not present in the sample. In *Ukhaatherium* cervical four has a low, stout neural spine and cervical seven has a smaller neural spine (Horovitz 2003). In most postaxial cervicals from the Bissekty Formation the neural spine is either absent or very small; it is relatively large only in one specimen (USNM 642672).

The inferior lamellae on the posterior cervical vertebrae are present in *Asioryctes* (Kielan-Jaworowska 1977) and absent in *Juramaia* Luo et al., 2011 and *Zalambdalestes* (Luo et al. 2011; Wible et al. 2009). None of the postaxial cervical vertebrae from the Bissekty Formation has the inferior lamellae, but the most posterior cervicals may not be present in the sample.

Thoracic vertebrae. The thoracic vertebrae in mammals show considerable variation through the series. By direction of neural spine they can be divided into the preanticlinal vertebrae in which the neural spine is posterodorsally directed, an anticlinal vertebra with a vertical neural spine, and postanticlinal vertebrae in which the neural spine is anterodorsally directed (Evans 1993). The anterior thoracic vertebrae, which articulate with the sternum via ribs, have more or less horizontal zygapophyseal articular surfaces. The diaphragmatic and more posterior thoracic vertebrae have ribs not attached to the sternum (Lessertisseur and Saban 1967). These vertebrae are similar to lumbar vertebrae in having a more vertical orientation of zygapophyseal articular surfaces and the presence of an accessory process (anapophysis) ventral to the postzygapophysis. These are thoracolumbar vertebrae.

There is a single preanticlinal thoracic vertebra in the sample (ZIN 103875: Fig. 4a–e), matching the size of *Rattus rattus*. The length of the centrum is short, equaling the anterior centrum width. The poorly preserved centrum articular surfaces are D-shaped with a flat anterior surface and slightly concave posterior surface. The ventral centrum surface is rounded. The neural canal is oval-shaped and similar in size to the centrum articular surfaces. The small and poorly preserved diapophysis (for attachment of the tuberculum of the rib) is located at the anterior margin of the neural arch near the middle of its height (Fig. 4d). The postzygapophyseal articular surface is long anteroposteriorly, concave, and facing ventrolaterally. The neural spine is directed more posteriorly than dorsally. There is a distinct anapophysis, which is connected by a horizontal ridge to the diapophysis (Fig. 4d). The poor development of the diapophysis and presence of the anapophysis suggest that ZIN 103875 might be the last preanticlinal vertebra.

There are three thoracic vertebrae with vertical neural spine, as it is evident from its preserved base (ZIN 82564, USNM 642700, and ZIN 103874). These specimens are likely anticlinal vertebrae. These vertebrae have no parapophysis on the neural arch and have a ridge-like diapophysis on the centrum (not preserved in ZIN 103874), suggesting that the vertebrae were articulating with a single-headed rib. This means that these vertebrae are postdiaphragmatic (thoracolumbar) vertebra and the diaphragmatic vertebra was located anterior to the anticlinal vertebra (e.g., see Argot 2003: fig. 5). The anapophysis is present in USNM 642700 (Fig. 4i) and lacking in the two other vertebrae. In spite of their similar position in the thoracic series, all three vertebrae have quite different morphology. ZIN 82564 has a long and very shallow centrum with articular surfaces lower than the neural canal height. The ridge-like parapophysis (costal fovea) is located in the anterior part of the centrum. In USNM 642700 the relative size of neural canal and centrum articular surfaces is similar to the previous specimen, but the centrum is shorter and the ridge-like parapophysis extends along most of the centrum length (Fig. 4i). In ZIN 103874 the centrum is much shorter and the neural canal is small, distinctly smaller than the centrum articular surfaces. The prezygapophyseal articular surface is oriented at an angle of 60° to the vertical axis. The postzygapophyseal articular surface is long and oval-shaped. In all vertebrae of this kind the neural spine is confined to the posterior half of the neural arch. In ZIN 82564 and ZIN 103874 there is a single large vascular foramen on the ventral side of the centrum near the midline.

The remaining thoracolumbar vertebrae fall into two distinct morphotypes. The first morphotype, represented by two specimens (USNM 594690 and USNM 594518; Fig. 4k–o), shows a typical thoracolumbar morphology. The neural spine is anterodorsally inclined (postanticlinal vertebrae). The ridge-like diapophysis occupies most of the centrum length. The neural canal is smaller than the centrum articular surfaces. The prezygapophyses have concave articular surface. There is no anapophysis. In USNM 594690 the anterior articular surfaces is D-shaped

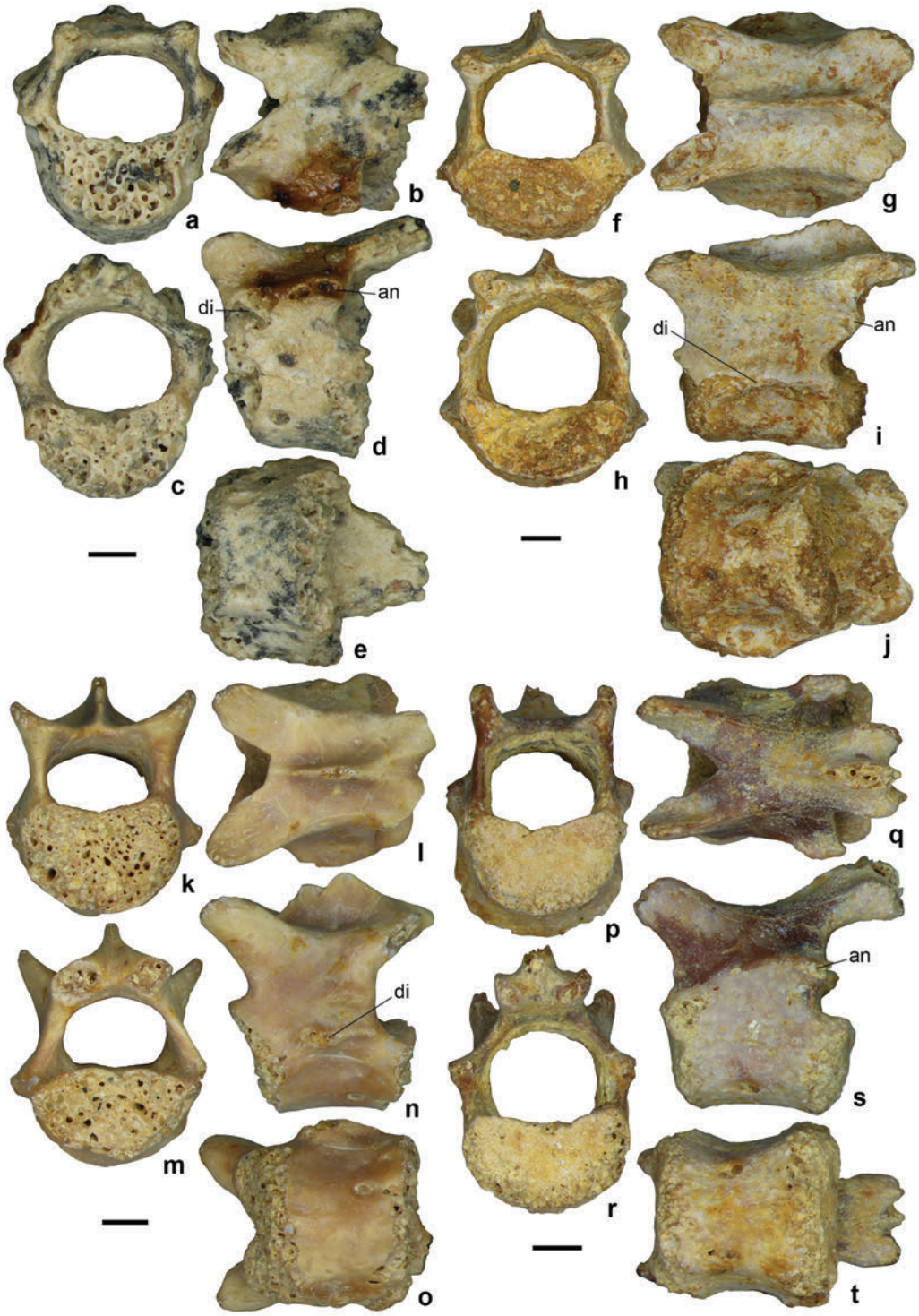

Fig. 4. Thoracic vertebrae from the Upper Cretaceous Bissekty Formation of Uzbekistan. **a–e** – ZIN 103875, in anterior **(a)**, dorsal **(b)**, posterior **(c)**, lateral **(d)**, and ventral **(e)** views. **f–j** – USNM 642700, in anterior **(f)**, dorsal **(g)**, posterior **(h)**, lateral **(i)**, and ventral **(j)** views. **k–o** – USNM 594690, in anterior **(k)**, dorsal **(l)**, posterior **(m)**, lateral **(n)**, and ventral **(o)** views. **p–t** – USNM 594513, in anterior **(p)**, dorsal **(q)**, posterior **(r)**, lateral **(s)**, and ventral **(t)** views. *Abbreviations*: an – anapophysis; di – diapophysis. Scale bars each equal 1 mm.

with the concave dorsal margin. In USNM 594518 it is more triangular and there is a median ridge on the centrum ventral surface.

The four other specimens (ZIN 82557, USNM 594513, USNM 594579, and USNM 605212) show a quite distinct morphology. The neural spine is confined to the posterior end of the neural arch, mostly above the postzygapophysis, and was likely directed posterodorsally, as in the preanticlinal thoracic vertebrae. But the diapophysis is lacking and there is a prominent anapophysis, connected by a horizontal ridge to the parapophysis (anterior costal fovea), which is poorly preserved on all specimens (Fig. 4s). The neural canal is taller than the centrum articular surfaces. The prezygapophyseal articular surfaces are convex and oriented more vertically than horizontally, suggesting that these vertebrae are postdiaphragmatic. These specimens represent three size classes, small (USNM 584579 and USNM 605212), medium (USNM 594513) and large (ZIN 82557) (Table 2). The large specimen is slightly larger than *Rattus rattus*. The small specimens have centrum articular surfaces more compressed dorsoventrally. A fragmentary neural arch ZIN 103876 is likely belonging to this morphotype.

In *Ukhaatherium* dorsal vertebra 12 was considered a lumbar vertebra because it bears the root of a dorsoventrally very slender and anteroposteriorly wide transverse process (Horovitz 2003). However, this might be not a base of broken transverse process, but a ridge-like diapophysis, as in thoracolumbar vertebrae from the Bissekty Formation. If so, dorsal 12 in *Ukhaatherium* might be a thoracolumbar vertebra. Most mammals have at least 12 thoracic vertebrae (Lessertisseur and Saban 1967; Narita and Kuratani 2005). In *Ukhaatherium* the anapophysis is present starting with the thoracic vertebra 9 (Horovitz 2003). In the thoracolumbar vertebrae from the Bissekty Formation the anapophysis is variably present. A thoracic vertebra of *Barunlestes* (Kielan-Jaworowska 1978: fig. 5) is similar with the thoracolumbar vertebrae from the Bissekty Formation, specifically with USNM 642700 (Fig. 4f–j), in having a long ridge-like diapophysis and large anapophysis.

Lumbar vertebrae. There are two lumbar vertebrae in the sample. USNM 642671 is an almost complete vertebra (Fig. 5). It is the smallest mammalian vertebra from the Bissekty Formation (Table 2), but about twice larger than the lumbar vertebrae of *Sorex raddei*. The anterior centrum articular surface was not fused with the centrum. The anterior end of the centrum has three distinct surfaces, two smaller lateral facets set at an angle to the larger medial facet. The posterior articular surface is fused with the centrum and has a rhomboid shape. There is a wide median ridge on the ventral surface of the centrum, flanked by lateral depressions (Fig. 5e). The neural canal is larger than the centrum articular surfaces. The prezygapophyses are widely separated. The prezygapophyseal articular surfaces are concave and inclined at an angle of 40° to the vertical axis. The transverse process, although not complete, was clearly directed anterolaterally. Its base occupies the anterior half of the neural arch just above the centrum. There is a distinct anapophysis (Fig. 5d). Only the base of the neural spine is preserved, which is confined to the posterior part of the neural arch. The neural spine was evidently directed posterodorsally.

ZIN 88878, missing the posterior part of the neural arch, is about 1.8 times larger than USNM 642671. It has similar morphology, but the pedicel of the neural arch is shorter anteroposteriorly, allowing for a larger intervertebral foramen. The centrum is markedly flattened dorsoventrally, with oval-shaped articular surfaces. There is a prominent median ridge on the centrum's ventral side and a single large vascular foramen on the left side of this ridge. The base of the broken transverse process occupies about half of the centrum length. The direction of the transverse process cannot be estimated. There is no evidence of the anapophysis, but it might be present on the missing part of the neural arch. The neural canal is relatively smaller than in USNM 642671. The prezygapophyses are widely spaced. The concave prezygapophyseal facet is oriented at an angle of 70° to the vertical axis, which is unusually horizontal for a lumbar vertebra.

Both lumbar vertebrae from the Bissekty Formation are remarkable for their short centrum. In most extant therians the centrum of lumbar vertebrae is distinctly more elongated. The morphology of the neural spine in USNM 642671 is very similar to the second morphotype of thoracolumbar vertebrae from the Bissekty Formation, exemplified by specimens ZIN 82557, USNM 594513, USNM 594579, and USNM 605212. At least some taxa of Bissekty mammals had thoracolumbar and lumbar vertebrae with the neural spine directed posterodorsally. The neural spine of lumbar vertebrae is directed anterodorsally in *Ukhaatherium* and posterodorsally in *Barunlestes* (Kielan-Jaworowska 1978; Horovitz 2003).

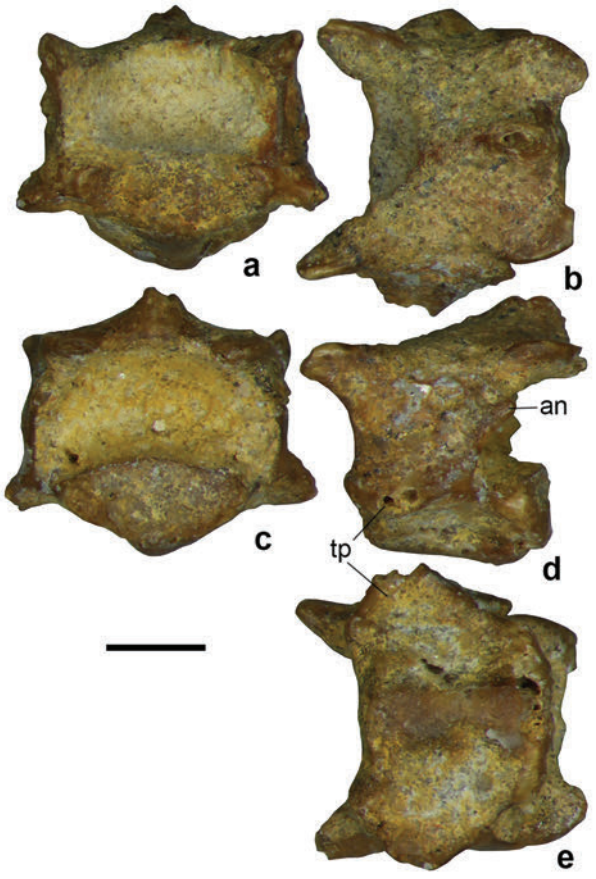

Fig. 5. USNM 642671, lumbar vertebra from the Upper Cretaceous Bissekty Formation of Uzbekistan. **a** – anterior view; **b** – dorsal view; **c** – posterior view; **d** – lateral view; **e** – ventral view. *Abbreviations*: an – anapophysis; tp – transverse process. Scale bar equals 1 mm.

Caudal vertebrae. The caudal vertebrae are the most numerous mammalian vertebrae from the Bissekty Formation. The caudal vertebrae in mammals show gradual simplification through the series with the most posterior vertebrae representing simple rods (Lessertisseur and Saban 1967; Evans 1993). Anterior caudal vertebrae differ from the posterior caudal vertebrae by retention of functional zygapophyses possessing articular surfaces.

USNM 642641 with the most developed neural arch is likely the first caudal (Fig. 6a–e). It is notable for its enormous size; this is the largest mammalian vertebrae from the Bissekty Formation (Table 3). The centrum is distinctly wider but much shorter than the first caudal vertebra of *Didelphis marsupialis* Linnaeus, 1758. The centrum length is only 1.48 times greater than the anterior centrum width. The anterior articular surface of the centrum is hexagonal in shape with a large pit lacking ossified cortical bone in the center. The posterior articular surface of the centrum is pentagonal in shape and has a similar pit. On the ventral surface of the centrum there is a shallow median ridge flanked by two higher lateral ridges, which are connected with the extensive facets (hypapophyses) for the haemal arches along the anterior and posterior body margins, and interrupted in the middle of the centrum. There is a well-developed transverse process, which is directed posterolaterally, as in the first caudal of *Didelphis marsupialis*. The base of the transverse process is located in the middle of the centrum length and height and its length is more than half of the centrum length. On the lateral side of the centrum there is a strong ridge anterior and posterior of the transverse process forming the lateral margin of the centrum's pentagonal or hexagonal articular surface. The neural canal (for the coccygeal nerve) is very small, with the width twice greater than the height anteriorly. Moreover, most of the neural canal is filled by a median ridge along the dorsal surface of the centrum. This ridge increases in height posteriorly and in the posterior half of the vertebra the neural canal becomes an inverted V-shaped slit between this ridge and neural arch. There are very large prezygapophyses directed dorsolaterally each with a prominent labially deflected metapophysis (mammillary process) (Fig. 6a, b, d). The prezygapophyseal articular surface is concave and oriented to an angle of 41° to the vertical axis. The prezygapophyses are closely spaced. There is a low neural spine along the entire length of the neural arch. It slightly increases in height at the posterior preserved portion of the neural arch. The postzygapophyses are missing.

USNM 642637 is an anterior caudal vertebra with the centrum even shorter than in the USNM 642641 (Fig. 6f–j). It has the centrum length to anterior centrum width ratio of 1.37. The centrum articular surfaces are rectangular (anterior) or oval (posterior). The facets for the haemal arches are better developed on the anterior margins. These facets are connected by two longitudinal ridges with a flattened surface between them. The base of the transverse process occupies most of the centrum length. Likely the transverse process was a broad plate directed laterally, as in the first caudal of *Rattus rattus*. The neural canal is smaller than the centrum articular surfaces, but still large for a caudal vertebra. The prezygapophy-

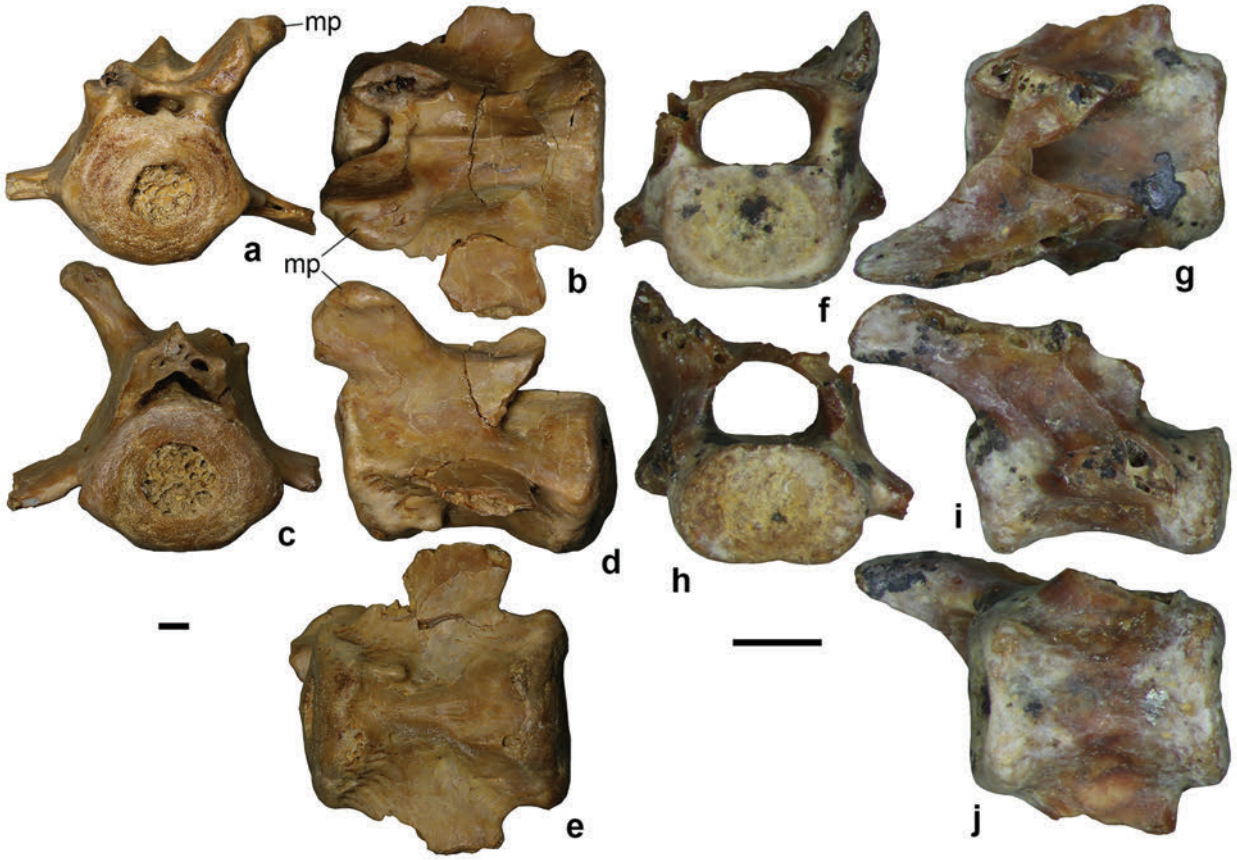

Fig. 6. Anterior caudal vertebrae from the Upper Cretaceous Bissekty Formation of Uzbekistan. **a–e** – USNM 642641, in anterior **(a)**, dorsal **(b)**, posterior **(c)**, lateral **(d)**, and ventral **(e)** views. **f–j** – USNM 642637, in anterior **(f)**, dorsal **(g)**, posterior **(h)**, lateral **(i)**, and ventral **(j)** views. *Abbreviation*: mp – metapophysis. Scale bars each equal 1 mm.

ses were widely spaced. The prezygapophysis is long with a flat articular surface oriented at an angle of 55° to the vertical axis. There is no metapophysis. There is no neural spine on the preserved part of the neural arch. Based on short centrum, broad transverse process, and long prezygapophysis, USNM 642637 is likely the first caudal vertebra.

Three specimens from the Bissekty Formation, with the centrum length to anterior centrum width ratio of 1.67 (USNM 590598), 1.71 (ZIN 88905), and 1.78 (USNM 594567) are among the anterior caudal vertebrae, but likely not the first caudals. The articular surfaces of centra are pentagonal or oval. In USNM 590598 there is a median ridge on the centrum's ventral surface. The centrum's ventral surface is rounded in two other specimens. There are no haemal facets on either specimen, suggesting that the haemal arches were already absent in this region. The neural canal is small in ZIN 88905 and very small in two other specimens. As in USNM 642641, there is a median ridge along the dorsal surface that fills most of the space of the neural canal. This ridge is relatively weak in ZIN 88905 and very large in USNM 594567, leaving inverted V-shaped slit for the neural canal. The prezygapophyses are closely spaced. There is a low neural spine in USNM 594567. The neural spine is lacking in two other specimens.

Three specimens with the centrum length to anterior centrum width ratio of 2.08 (ZIN 103877), 2.69 (USNM 642638; Fig. 7a–e), and 2.86 (ZIN 88910), are more posterior in the caudal series than the previously described specimens. USNM 642638 is the largest of these specimens with articular surfaces comparable in size to *Didelphis marsupialis*, but having a shorter centrum length. These caudal vertebrae have well-developed prezygapophyses with distinct concave articular facets and large metapophyses. In ZIN 88910 the prezygapophyseal articular facet is

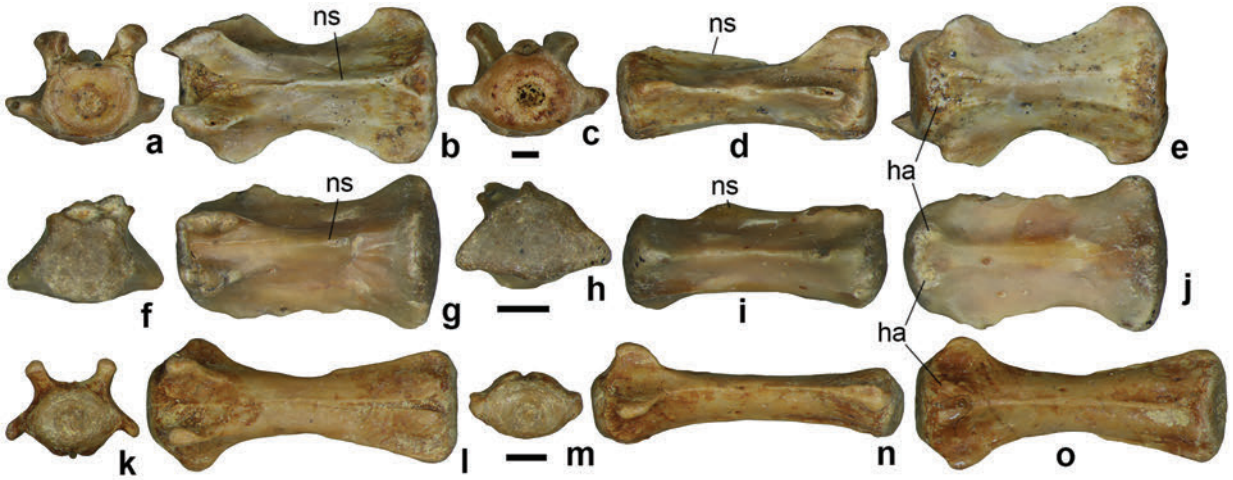

Fig. 7. Caudal vertebrae from the Upper Cretaceous Bissekty Formation of Uzbekistan. **a**–**e** – USNM 642638, anterior caudal vertebra, in anterior **(a)**, dorsal **(b)**, posterior **(c)**, lateral **(d)**, and ventral **(e)** views. **f**–**j** – ZIN 88904, posterior caudal vertebra, in anterior **(f)**, dorsal **(g)**, posterior **(h)**, lateral **(i)**, and ventral **(j)** views. **k**–**o** – USNM 642639, posterior caudal vertebra, in anterior **(k)**, dorsal **(l)**, posterior **(m)**, lateral **(n)**, and ventral **(o)** views. *Abbreviations*: ha – haemal arch; ns, neural spine. Scale bars each equal 1 mm.

very large, while in USNM 642638 it is very small (Fig. 7b). In ZIN 103877 the prezygapophyses were asymmetrical, with the left one being larger. The prezygapophyses are closely spaced. In ZIN 88910 and USNM 642638 there is a long notch between the bases of the prezygapophyses on the neural arch (Fig. 7b). The neural arch is complete on all specimens and the postzygapophyses are totally lacking. Thus, these vertebrae had zygapophyseal articulation with the previous vertebra but not with the subsequent vertebra. Such morphology, transitional between the anterior and posterior caudals, is present on caudal six of *Rattus rattus* and caudal three of *Erinaceus europaeus*. The neural spine is long, distinct, and low in ZIN 88910 and USNM 642638 (Fig. 7b) and very short, virtually absent in ZIN 103877. The neural canal is extremely small, less than a small needle in width. The centrum articular surfaces are pentagonal. On the ventral centrum surface there is a shallow central depression flanked by lateral ridges connected with the poorly developed facets for haemal arches anteriorly (Fig. 7e). There are distinct anterior and posterior transverse processes near the anterior and posterior centrum end, respectively. The largest of these processes is anterior in ZIN 103877 and posterior in USNM 642638 (Fig. 7b, e).

The next morphotype is exemplified by two posterior caudal vertebrae with the centrum length to anterior centrum width ratio of 2.30 (ZIN 88865) and 2.55 (ZIN 88904; Fig. 7f–j). They have wide anterior and posterior transverse processes and a rudimentary neural arch that occupies about half of the centrum length. The neural canal is extremely small and possibly closed posteriorly. The prezygapophyses are broken but apparently were very small. There is a single median ridge on the ventral centrum surface. In ZIN 88865 there are no haemal facets. In ZIN 88904 the rudimentary halves of the haemal arch are apparently fused with the centrum and form short anterior processes (Fig. 7j). In ZIN 88904 the posterior articular surface of the centrum is triangular (Fig. 7i), incorporating the posterior edge of the posterior transverse processes.

The four, more elongated posterior caudal vertebrae, with the centrum length to anterior width ratio of 2.89 (ZIN 103878), 3.21 (USNM 642639), 3.57 (USNM 642636), and 3.81 (USNM 594720), have a reduced neural arch and widely separated anterior and posterior transverse processes. The neural canal is absent. The prezygapophyses are small and widely separated. Instead of a neural arch there is a distinct median ridge with a flat triangular surface at the posterior end (USNM 642636 and USNM 594720) or rudimentary postzygapophyses (ZIN 103878). In USNM 642639 there is faint dorsal medial ridge anteriorly and median groove posteriorly (Fig. 7m). The anterior transverse processes are wider than the posterior transverse processes, which are poorly

differentiated from the centrum. There is a median ridge on the ventral side of the centrum. The small anterior ventral processes (fused haemal arches) are variably developed, sometimes with a flat triangular area between them.

Five more posterior caudal vertebrae, with the centrum length to anterior width ratio of 3.44 (USNM 594719), 3.67 (USNM 642635), 4.00 (ZIN 88903), 4.13 (ZIN 103879), and 4.77 (USNM 642640) are different from the previous morphotype in the lack or poor development of the transverse processes. USNM 594719 with the centrum length of 12.4 mm is the longest caudal vertebra in the sample (Table 3). The median ridge on the ventral centrum surface is poorly developed or lacking. The prezygapophyses are small knobs. There are no fused haemal arches or haemal facets.

There are also several incomplete posterior caudal vertebrae from the Bissekty Formation that do not offer additional information.

Scapula. There are eleven fragments of scapulae. Nine fragments preserve the neck, at least part of the glenoid, and the base of the blade. All these specimens belong to the plesiomorphic therian morphotype of scapula exemplified by *Ukhaatherium* and *Maelestes* (Horovitz 2003; Wible et al. 2009). The two other specimens are represented by the glenoid only. One of them (USNM 642634) is consistent in morphology with the previous morphotype. The second glenoid fragment (USNM 642633) shows somewhat different morphology. The eleven fragments of scapula form four size classes, from the smallest to the largest: class I (ZIN 103866), class II (ZIN 103869, ZIN 103870, USNM 642632, USNM 642631, and USNM 642633), class III (ZIN 103867 and USNM 642630), and class IV (ZIN 103868, ZIN 103872, and USNM 642634). Class II is slightly smaller than scapulae of *Rattus rattus* and class IV is smaller than *Erinaceus europaeus*. One or both glenoid measurements are available for five of the specimens (Table 4).

In the majority of extant therians the scapular blade is flat, with a perpendicular scapular spine and the infraspinous and supraspinous fossae in the same plane (coplanar) (Wible et al. 2009). In contrast, in the Bissekty therians, as well as in *Ukhaatherium* and *Maelestes*, the scapular spine is inclined towards the plane of the infraspinous fossa at an angle of ~60–70°. The trough-like infraspinous fossa is deeply concave and slightly offset medially relative to the plane of the supraspinous fossa, i.e. both fossae are not in the same plane. In lateral view, because of the angle of the scapular spine the infraspinous fossa is partially obscured (Fig. 8m). As a result, the scapula has an S-shaped cross section at the mid-height of the scapular blade. In more complete specimens (ZIN 103868, ZIN 103870), the infraspinous fossa is distinctly larger than the supraspinous fossa.

The scapular neck deflects medially from the scapular blade so the subscapular surface is convex in the neck region. More dorsally, the subscapular surface is convex at the infraspinous fossa and slightly concave at the supraspinous fossa. When preserved, the scapular blade is relatively narrow anteroposteriorly, constricting some at the neck and then expanding again at the glenoid. The base of the metacromion process is either the same thickness as the remainder of the scapular spine (ZIN 103867, ZIN 103872, URBAC 06-028) or much wider (ZIN 103866, ZIN 103868, and ZIN 103870). The likely present acromion process is not preserved on any specimens.

In most specimens, the scapular part of the glenoid surface is elliptical, with a round posterior margin and the anterior surface tapering towards the narrower coracoid part of the glenoid surface. The long axis of the glenoid ellipse is parallel to the plane of the infraspinous fossa and forms an angle with the supraspinous fossa. Viewed laterally or medially the edge of the glenoid ranges from gently (ZIN 103866, ZIN 103867; Fig. 8g, i) to more sharply concave (USNM 642634, USNM 642633: Fig. 8u, v). The coracoid part of the glenoid (supraglenoid tubercle) is prominent and hook-like, with a variably developed coracoid process, which deflects medially.

The scapular fragment USNM 642633, represented by the glenoid and the proximal part of the scapular neck (Fig. 8x–z*), differs from the other specimens in having a more rounded outline of the glenoid surface separated by a narrowing between it and the supraglenoid tubercle, in having the base of spine placed closer to the glenoid surface, and in a marked tuberosity in the acromioscapular notch.

In *Ukhaatherium* and *Maelestes* the scapular spine is directed posteriorly, almost parallel to the infraspinous fossa (Horovitz 2003; Wible et al. 2009). In the scapulae from the Bissekty Formation, the scapular spine is directed posterolaterally, but the distal part of the spine, missing in all specimens, may turn posteriorly. This change in the scapular spine orientation appears to be present in *Ukhaatherium* (Horovitz 2003: fig. 4).

Fig. 8. Fragments of scapula from the Upper Cretaceous Bissekty Formation of Uzbekistan. **a**–**e** – ZIN 103868, left scapula, in posterior (**a**), medial (**b**), anterior (**c**), lateral (**d**), and distal (**e**) views. **f**–**j** – ZIN 103867, right scapula, in posterior (**f**), lateral (**g**), anterior (**h**), medial (**i**), and distal (**j**) views. **k**–**o** – ZIN 103870, right scapula, in distal (**k**), posterior (**l**), lateral (**m**), anterior (**n**), and medial (**o**) views. **p**–**t** – ZIN 103866, left scapula, in distal (**p**), posterior (**q**), medial (**r**), anterior (**s**), and lateral (**t**) views. **u**–**w** – USNM 642634, left scapula, in medial (**u**), lateral (**v**), and distal (**w**) views. **x**–**z*** – USNM 642633, right scapula, in lateral (**x**), medial (**y**), posterior (**z**), and distal (**z***) views. *Abbreviations*: cp – coracoid process. Scale bars each equal 1 mm.

There are certain similarities between USNM 642633 and the proximal fragment of the scapula of the zalambdalestid *Barunlestes* (Kielan-Jaworowska 1978: fig. 9; pl. 7, fig. 2). Both have a rounder scapular portion of the glenoid and the supraglenoid tubercle is smaller than in other specimens from the Bissekty Formation. The tuberosity at the base of the acromion process in USNM 642633 apparently corresponds to the enlarged ventral part of the spine described for *Barunlestes* (Kielan-Jaworowska 1978: 17). The

scapula of *Barunlestes* differs from USNM 642633 in that the coracoid process is larger than the supraglenoid tubercle in the former, while in USNM 642633 both are of similar size. USNM 642633 is likely referable to the zalambdalestid *Kulbeckia* known from the Bissekty Formation by cranial and dental remains (Archibald and Averianov 2003).

Humerus. There are two proximal humeral fragments with well-preserved head and tubercles, several shaft fragments lacking proximal and distal ends, and several fragments with the distal end. The two proximal fragments, USNM 642648 and USNM 642654, have similar morphology but differ in size (Table 5). The globular humeral head overhangs the shaft anteriorly. The tubercles do not project proximally above the head, as in *Maelestes*, *Ukhaatherium*, and *Barunlestes* (Kielan-Jaworowska 1978; Horovitz 2003; Wible et al. 2009). The size difference between the greater and lesser tubercles is not great. In USNM 642648 there a shallow groove on the greater tubercle (insertion of m. supraspinatus), while on the other specimen the surface of the greater tubercle is smooth. The tubercles are separated posteriorly by a wide and shallow intertubercular groove. In the larger specimen, USNM 642654, there is a distinct depression between the tubercles on the proximal side, posterior to the head, and proximal to the intertubercular groove (Fig. 9a). In this specimen there is also a very prominent pectoral crest of the greater tubercle (Fig. 9e), which is absent in USNM 642648. A similarly strong pectoral crest is present in *Ukhaatherium* (Horovitz 2003: fig. 8A, B).

Chester et al. (2010) identified three metatherian groups and seven eutherian groups based on 15 distal humerus fragments from the Bissekty Formation. Among the eutherian groups, one was referred to Zalambdalestidae and five to Zhelestidae. There are no additional humeral specimens preserving the distal end, but some information can be added from the shaft fragments. USNM 642653 fits approximately the size of metatherian group 2 (Chester et al. 2010). It is remarkable in having an enormous rectangular lateral epicondylar crest (Fig. 9f, g), which is developed as in adult specimens of *Didelphis virginiana* (Kerr, 1792) (Szalay and Sargis 2001: fig. 2D, E). A small but deep olecranon fossa shows no perforation on the preserved portion. Humeri from both metatherian groups 2 and 3 may belong to *Sulestes*, the first representing the juvenile individuals. USNM 642652 agrees in most of its preserved details to the zalambdalestid humerus ZIN 85309 (Chester et al. 2010: fig. 7), but is about 20% smaller and has an unperforated radial fossa. It may belong to a juvenile individual of *Kulbeckia*. The large humeral fragment USNM 642655 fits the size of zhelestid group 5 (Chester et al. 2010), but differs in having a much larger medial epicondyle with a large entepicondylar foramen and a distinct depression distal to that foramen on its anterior side (Fig. 9h). The lateral epicondylar crest is well developed.

The metatherian group 1 of Chester et al. (2010: fig. 3) includes two distal fragments of small humeri USNM 642656 and USNM 642657. These specimens were referred to Metatheria based on a spherical capitulum, a short groove separating the capitulum and trochlea, and a well-developed lateral epicondylar crest (broken on both specimens). A similarly spherical capitulum and a groove separating capitulum and trochlea (zona conoidea) are present in the stem placental *Deccanolestes* Prasad et Sahni, 1988 and arboreal Paleocene euarchontans (Boyer et al. 2010). These characters as indicated by Chester et al. (2010) relate to arboreal locomotion and do not indicate unequivocally the metatherian nature of the specimens. These specimens, as well as fragments of small femora with arboreal specializations (see below), can be attributed to *Paranyctoides*, one of the smallest eutherian in the Bissekty assemblage (Averianov and Archibald 2016).

USNM 642659, the single representative of eutherian group 1 of Chester et al. (2010), may belong to Asioryctitheria. In general proportions it is similar with the humerus of *Ukhaatherium* (Horovitz 2003: fig. 8C–E).

Radius. Four proximal radius fragments, three left and one right, can be attributed to two morphotypes that differ in morphology and size (Table 6). ZIN 103882 (Fig. 10a–e) and ZIN 104124 are similar in size to the radius of *Rattus rattus*. The proximal end

Table 5. Measurements (in mm) of therian proximal humerus fragments from the Upper Cretaceous Bissekty Formation of Uzbekistan. Measurements: PL – proximal end length; PW – proximal end width.

Specimen	PL	PW
	Size class I	
USNM 642648	2.9	3.8
	Size class II	
USNM 642654	4.9	6.1

Fig. 9. Fragments of humerus from the Upper Cretaceous Bissekty Formation of Uzbekistan. **a**–**e** – USNM 642654, right proximal humerus, in proximal **(a)**, lateral **(b)**, anterior **(c)**, medial **(d)**, and posterior **(e)** views. **f**–**g** – USNM 642653, right shaft fragment, in anterior **(f)** and posterior **(g)** views. **h**–**I** – USNM 642655, left shaft fragment, in anterior **(h)** and posterior **(i)** views. *Abbreviations*: entf – entepicondylar foramen; gt – greater tubercle; lec – lateral epicondylar crest; lt – lesser tubercle; pc – pectoral crest. Scale bars each equal 1 mm.

Table 6. Measurements (in mm) of therian radius fragments from the Upper Cretaceous Bissekty Formation of Uzbekistan. Measurements: PL – proximal end length; PW – proximal end width.

Specimen	PL	PW
	Size class I	
ZIN 103882	1.4	2.3
ZIN 104124	1.5	2.2
	Size class II	
ZIN 104122	2.1	3.0
ZIN 104123	2.1	2.8

Table 7. Measurements (in mm) of therian ulna fragments from the Upper Cretaceous Bissekty Formation of Uzbekistan. Measurements: PL – proximal end length; PW – proximal end width.

Specimen	PL	PW
	Size class I	
ZIN 103884	0.9	1.1
	Size class II	
ZIN 103883	2.1	1.5
USNM 594693	–	1.3

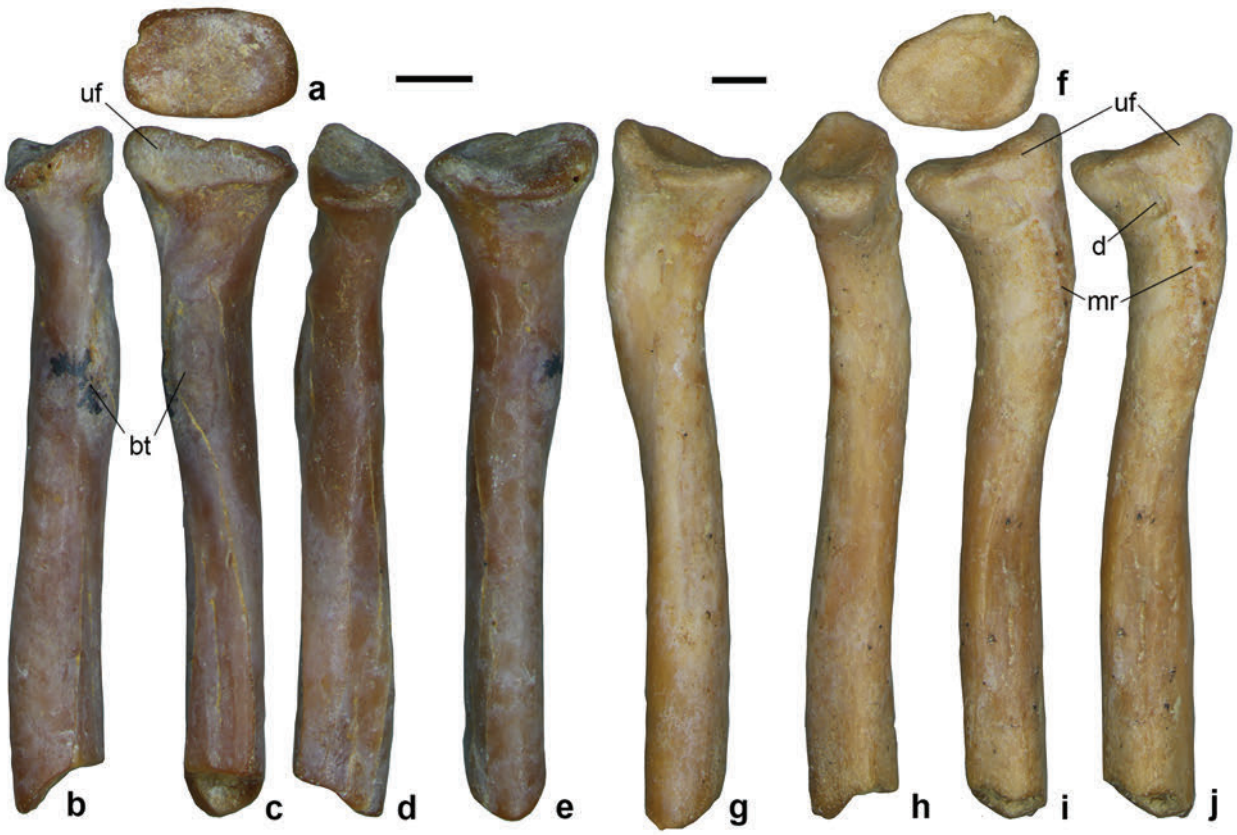

Fig. 10. Fragments of radius from the Upper Cretaceous Bissekty Formation of Uzbekistan. **a**–**e** – ZIN 103882, right radius, in proximal **(a)**, medial **(b)**, posterior **(c)**, lateral **(d)**, and anterior **(e)** views. **f**–**j** – ZIN 104122, left radius, in proximal **(f)**, anterior **(g)**, lateral **(h)**, posterior **(i)**, and posteromedial **(j)** views. *Abbreviations*: bt – bicipital tuberosity; d – depression; mr – medial ridge; uf – ulnar facet. Scale bars each equal 1 mm.

is oval (ZIN 104124) or trapezoidal (ZIN 103882) in proximal view, with a shallow articular fovea (capitular depression). The proximal articular surface is almost perpendicular to the shaft. The proximal end is wider than the shaft in anterior and posterior views; in medial and lateral views it has a similar width. The posterior side of the proximal end is occupied by the ulnar facet (the articular circumference; Fig. 10c). The shaft is slightly curved in the neck region in the medial or lateral view and almost straight in the anterior or posterior view. Just distal to the neck on the posterior side there is a very large bicipital tuberosity

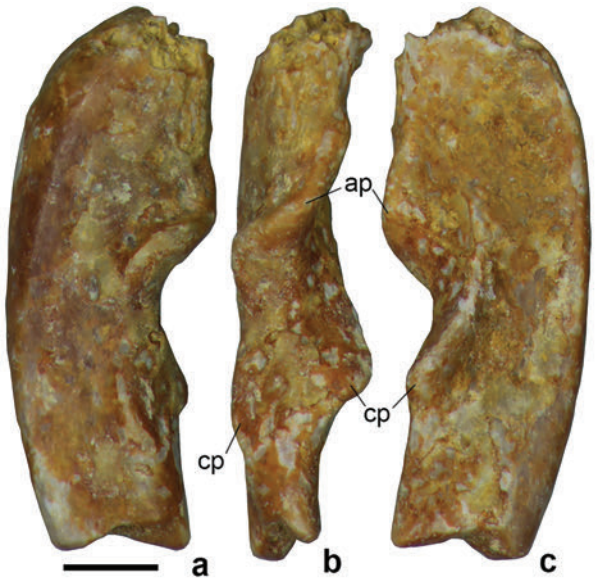

Fig. 11. ZIN 103883, fragment of right ulna from the Upper Cretaceous Bissekty Formation of Uzbekistan. **a** – lateral view; **b** – anterior view; **c** – medial view. Abbreviations: ap – anconeal process; cp – coronoid process. Scale bar equals 1 mm.

(Fig. 10b, c), much larger than in *Rattus rattus*. The bicipital tuberosity of the radius is connected proximally with the interosseous crest and curves distally along the preserved shaft fragment.

ZIN 104122 (Fig. 10f–j) and ZIN 104123 are somewhat larger (Table 6) than ZIN 103882 and ZIN 104124. The proximal articulation surface is more oval than trapezoid and not perpendicular to the shaft, facing dorsolaterally. The neck is slightly curved in the medial or lateral views and strongly curved in the anterior or posterior views. In ZIN 104122 there is no bicipital tuberosity. On the posterior side, there is a small but distinct depression just distal to the ulnar facet and a short longitudinal ridge medial to this depression (Fig. 10i, j). In ZIN 104123, in contrast, there is a prominent ridge in place of the bicipital tuberosity and a larger ridge on the medial side of the shaft.

The radius of *Maelestes* (Wible et al. 2009: fig. 28) has a straight neck, as in the first morphotype, but lacks the bicipital (radial) tuberosity. In *Ukhaatherium* the radius has a S-shaped profile in lateral view (Horovitz 2003: fig. 1A), as in the second morphotype, and has a bicipital tuberosity.

Ulna. There are several proximal ulnar fragments from the Bissekty Formation. Only two specimens completely preserve the trochlear (semilunar) notch and olecranon process. ZIN 103883 belongs to a small mammal, about twice smaller than *Rattus rattus* (Table 7). The anconeal process, and lateral and medial projections of the coronoid process are poorly developed (Fig. 11). There is a shallow radial notch between the medial and lateral coronoid processes. The olecranon is only slightly shorter proximodistally than the trochlear notch. ZIN 103884 is a tiny specimen, about twice smaller than the previous one (Table 7). The trochlear notch is somewhat deeper, but bordered only proximally with the projections of the coronoid process but not elevated beyond the shaft. The bone is gently deflected posteriorly. In USNM 594693 the olecranon process is distinctly shorter than the trochlear notch (not completely preserved).

In *Ukhaatherium* the ulna has poorly developed anconeal and coronoid processes (Horovitz 2003: fig. 1A), as in specimens from the Bissekty Formation. In contrast with *Ukhaatherium*, the ulnar tuberosity cannot be identified in specimens from the Bissekty Formation. The anconeal and coronoid processes are much better developed, with a deep trochlear notch in *Barunlestes* (Kielan-Jaworowska 1978: fig. 12A).

Innominate bone. There are numerous acetabular fragments composed of ilium and ischium and several fragments of the iliac blade. No parts of the pubis could be identified as contributing to the acetabulum. Most fragments of the ilial body, including more complete specimens ZIN 103885-103888, have a similar morphology. The largest specimens are ZIN 103885 and ZIN 103888, which are slightly larger than the ilium of *Rattus rattus*. The anterior end of the iliac crest is not preserved in either specimen, but the lateral flaring of wing of the ilium is evident in more anteriorly complete specimens. The iliac body is constricted dorsoventrally between the acetabular region and the region articulating with the sacrum. The posterior dorsal iliac spine is well developed. The medial surface of the iliac wing, articulating with the sacrum, can be smooth (ZIN 103887) or sculptured (ZIN 103885: Fig. 12b), but is in the same plane as the medial bone surface, or forming a deeper pocket-like articulation, as in ZIN 103888. ZIN 103889 is distinct from the other ilial fragments by the presence of a large preacetabular tubercle for *m. rectus femoris* (iliopectinal eminence) on the lateral side in front of the acetabulum (Fig. 12d, e), which is proportionally larger than in *Rattus rattus*. In other specimens there is no trace of the preacetabular tubercle. ZIN 103889

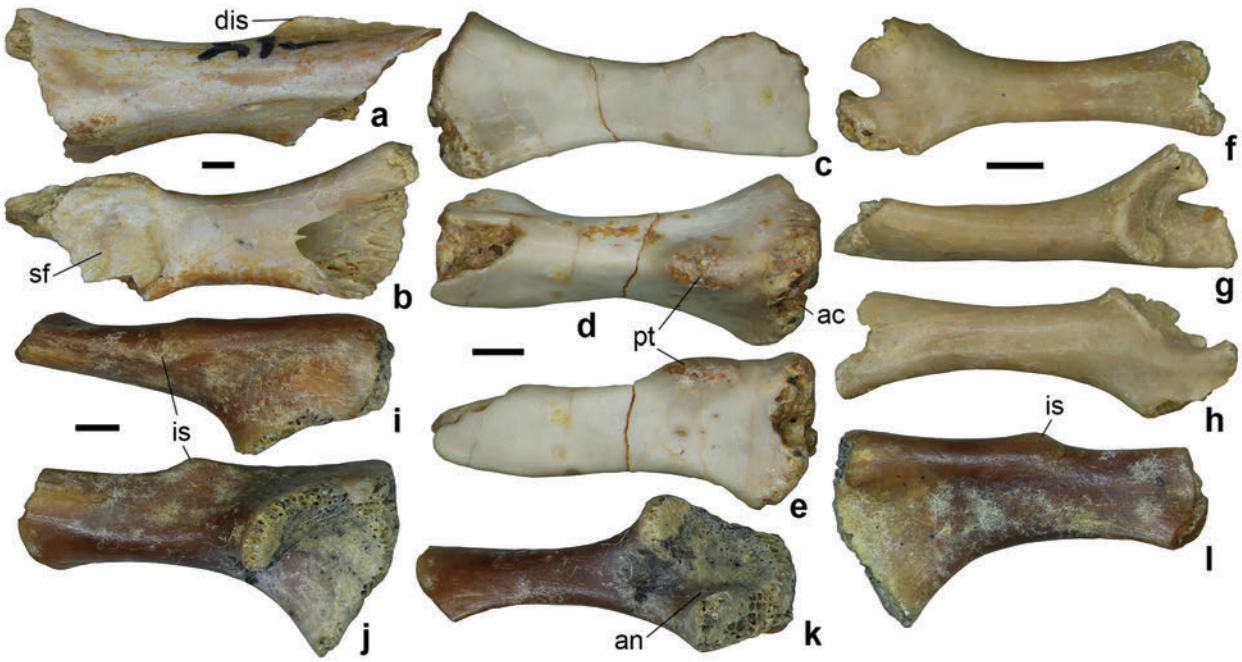

Fig. 12. Fragments of pelvic bones from the Upper Cretaceous Bissekty Formation of Uzbekistan. **a**–**b** – ZIN 103885, right ilium, in lateral **(a)** and medial **(b)** views. **c**–**e** – ZIN 103889, left ilium, in medial **(c)**, lateral **(d)**, and ventral **(e)** views. **f**–**h** – USNM 594696, right ischium, in lateral **(f)**, medial **(g)**, and ventral **(h)** views. **i**–**l** – USNM 642670, right ischium, in dorsal **(i)**, lateral **(j)**, ventral **(k)**, and medial **(l)** views. *Abbreviations*: ac – acetabulum; an – acetabular notch; dis – dorsal iliac spine; is – ischiatic spine; pt – preacetabular tubercle for *m. rectus femoris*; sf – sacrum facet. Scale bars each equal 1 mm.

is the only fragment of the ilium preserving part of the acetabular articular surface for the femur (Fig. 12d).

Among more complete ischium fragments, USNM 642669 and USNM 642670 are of similar size, fitting the size of the ischium in *Rattus rattus*. ZIN 103890 is a somewhat smaller specimen. USNM 642670 comes from an immature individual with the pelvic bones not fused. There are distinct facets for the ilium and apparently for the acetabular bone (Fig. 12j). In the acetabulum of USNM 642670 there is a prominent lunate surface for articulation with the femur. The anterior margin of the lunar surface is projecting laterally. Ventrally it is separated from the rest of the bone by a prominent acetabular notch (Fig. 12k). There is a distinct ischiatic spine along the dorsal margin of ischium posterior to the acetabulum (Fig. 12j, l). USNM 594696 is a tiny specimen, about twice smaller than the previous one. It has a quite different morphology. The body of ischium is rod-like, markedly constricted posterior to the acetabulum (Fig. 12f–h). There is no ischial spine. The acetabulum is perforated by a large foramen (Fig. 12f, g). There is a rather long ventral process for articulation with the pubis and/or acetabular bone. There is no acetabular notch (Fig. 12h).

In *Ukhaatherium* there is no preacetabular tuber for *m. rectus femoris* on ilium and there is an acetabular notch on the ischium (Horovitz 2003).

Femur. Chester et al. (2012) described 14 fragmentary femora from the Bissekty Formation. These fragments were separated, based on size and morphology, into six groups for the proximal fragments and four groups for the distal fragment. There are several additional proximal femoral fragments of various size, but most of them are missing the head and trochanters and do not offer additional information. Additional specimens can be distributed among size groups recognized by Chester et al. (2012) (Tables 8 and 9). In the specimens with a more complete femoral shaft, there is no third trochanter. Three specimens, however, preserve the femoral head and are briefly described here. ZIN 103891 preserves only the femoral head and greater trochanter. It is attributed to the size class V (Table 8). The articular surface of the head extends laterally and posteriorly. The greater trochanter is complete and lower than the femoral

Table 8. Measurements (in mm) of therian proximal femur fragments from the Upper Cretaceous Bissekty Formation of Uzbekistan. Measurements: HL – femoral head length; PW – proximal end width.

Specimen	HL	PW
	Size class I	
USNM 642645*	1.51	3.37
ZIN 103893	1.5	–
	Size class II	
ZIN 85321*	1.95	4.88
	Size class III	
ZIN 85324*	2.42	5.87
ZIN 103892	2.3	-
ZIN 85322*	2.19	6.61
	Size class IV	
USNM 642646*	2.40	6.44
ZIN 97885*	2.61	6.84
ZIN 103891	3.2	–
	Size class V	
ZIN 85325*	4.14	9.72
ZIN 97886*	4.04	8.96

*Measurements from Chester et al. (2012).

head, as in group 6 and possibly in group 5 (Chester et al. 2012). ZIN 103892 is very similar in size (size class III; Table 8) and morphology to ZIN 85324 (Chester et al. 2012: fig. 8). The trochanteric fossa is quite deep. The large lesser trochanter projects medially. The proximal surfaces of the head and greater trochanter are destroyed. ZIN 103893 is a small femur fitting the size of proximal group 1 (size class I; Table 8). However, it differs in morphology from the previously described morphotypes of proximal femur from the Bissekty Formation (Chester et al. 2012). The articular surface of the head extends laterally and only very slightly posteriorly. The femoral neck is virtually absent. The tip of the greater trochanter is not preserved. Its posterior crest wraps around the pocket-like lateral part of the trochanteric fossa (Fig. 13a, b). The remainder if the trochanteric fossa is quite shallow. A very similar wrapping posterior crest of the great trochanter is present in a tiny proximal fragment ZIN 103894. It is about 80% of the size of ZIN 103893 but apparently came from a juvenile individual because the head and greater trochanter apparently were not fused to the shaft. Both of these latter specimens may belong to a single taxon.

Table 9. Measurements (in mm) of therian distal femur fragments from the Upper Cretaceous Bissekty Formation of Uzbekistan. Measurements: DL – distal end length; DW – distal end width.

Specimen	DL	DW
	Size class I	
USNM 642642*	1.33	2.04
	Size class II	
USNM 642647	2.6	4.7
USNM 642643*	3.05	4.06
	Size class III	
ZIN 85327*	4.74	6.13
USNM 642644*	4.26	6.47
USNM 642703*	-	6.42

*Measurements from Chester et al. (2012).

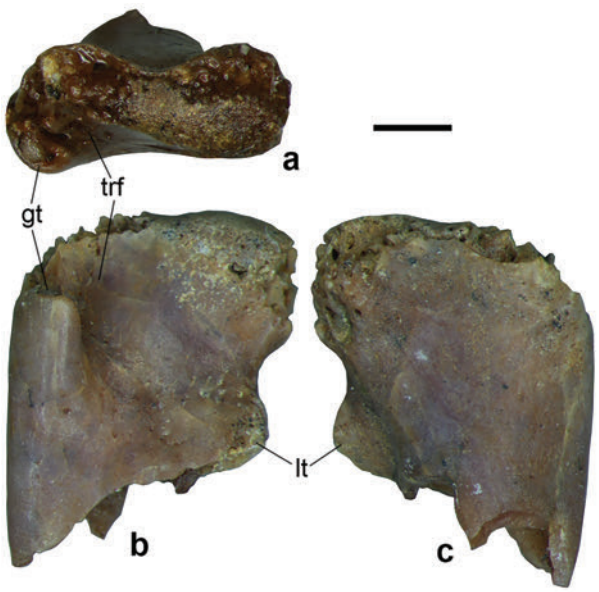

Fig. 13. ZIN 103893, proximal fragment of left femur from the Upper Cretaceous Bissekty Formation of Uzbekistan. **a** – proximal view; **b** – posterior view; **c,** anterior view. *Abbreviations*: gt – greater trochanter; lt – lesser trochanter; trf – trochanteric fossa. Scale bar equals 1 mm.

A single additional distal femoral fragment (USNM 642647) is referred to the size class II (Table 9). The distal end is not flared laterally. The patellar groove is present, but its depth cannot be estimated because the distal condyles are abraded anteriorly. It is markedly different from USNM 642643 (Chester et al. 2012: fig. 3) in having very shallow lateral condyles, which only little extend posteriorly beyond the shaft.

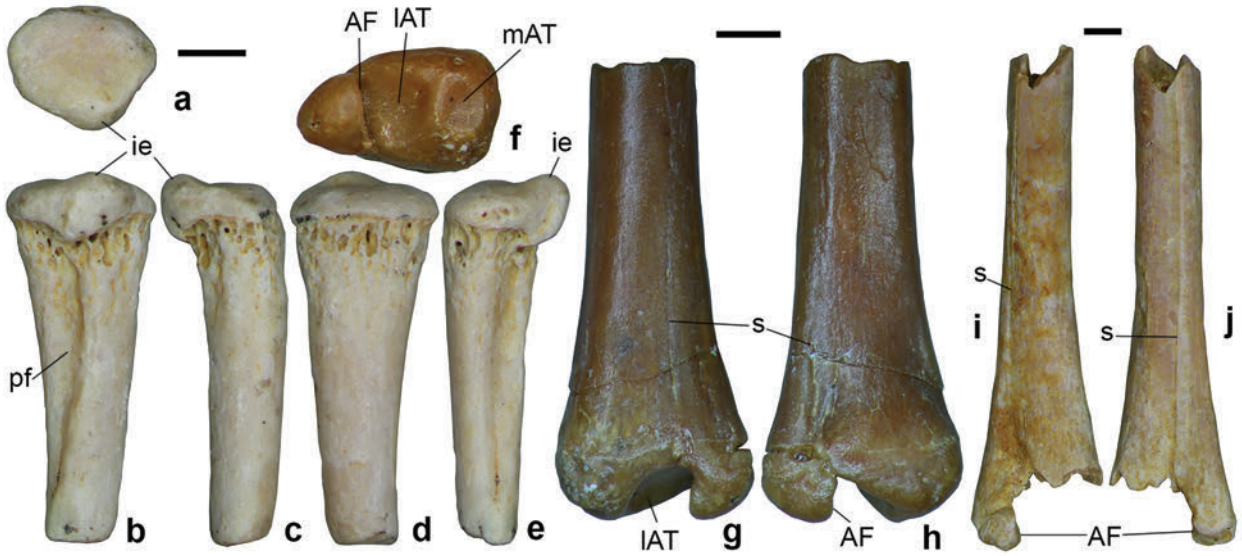

Fig. 14. Fragments of tibia and fibula from the Upper Cretaceous Bissekty Formation of Uzbekistan. **a**–**e** – ZIN 82559, left tibia, in proximal **(a)**, posterior **(b)**, medial **(c)**, anterior **(d)**, and lateral (e) views. **f**–**h** – USNM 642702, right tibiofibula, in distal **(f)**, posterior **(g)**, and anterior **(h)** views. **i**–**j** – ZIN 103881, right tibiofibula, in anterior **(i)** and posterior **(j)** views. *Abbreviations*: AF – astragalofibular facet; ie – intercondyloid eminence; lAT – lateral astragalotibial facet; mAT – medial astragalotibial facet; pf – posterior fossa; s – suture between tibia and fibula. Scale bars each equal 1 mm.

Table 10. Measurements (in mm) of therian proximal tibia fragments from the Upper Cretaceous Bissekty Formation of Uzbekistan. Measurements: PL – proximal end length; PW – proximal end width.

Specimen	PL	PW
	Size class I	
ZIN 82559	1.8	2.2
	Size class II	
ZIN 103880	4.0	4.4

In all known proximal femoral fragments from the Bissekty Formation the greater trochanter is lower or at level with the femoral head. In *Barunlestes* it is higher than the femoral head (Kielan-Jaworowska 1978: fig. 14A). In *Barunlestes* the articular surface is limited to the spherical femoral head, whereas in the specimens from the Bissekty Formation the articular extends posterolaterally towards the greater trochanter. The femur of *Barunlestes* has a third trochanter, which is not observed in more complete fragments from the Bissekty Formation. The third trochanter is also absent in *Ukhaatherium* (Horovitz 2003).

A distal fragment of a small femur USNM 642642 was referred to a metatherian by Chester et al. (2012: fig. 2) based on lack of a distinct patellar groove and shallow asymmetrical condyles. The lateral condyle is much wider and contributes to the lateral flaring of the lateral side of the femur. Both characters are related to an arboreal mode of life (Chester et al. 2012). As noted by Chester et al. (2012), these specimen fit the size of small humeri USNM 642656 and USNM 642657 with arboreal characteristics. These specimens are attributed here to *Paranyctoides* and the femoral fragment USNM 642642 may well belong to this taxon.

Tibia and fibula. There are two proximal fragments of tibia, ZIN 82559 and ZIN 103880, of different size (Table 10). The second specimen is about the size of *Rattus rattus*. In both specimens the proximal condyle is not completely ossified with the shaft. The tibial tuberosity is lacking (ZIN 82559) or small (ZIN 103880). The proximal condyle slightly overhangs the shaft on the posterior side. The shaft is slightly curved posteriorly. In ZIN 82559 the lateral and medial condyles are poorly differentiated and placed in the same plane. The lateral condyle is about twice larger. There is a distinct intercondyloid eminence along the posterior margin of the proximal condyle. In ZIN 103880 the intercondyloid eminence is very low and placed between the condyles. The lateral condyle is placed higher than the medial condyle. In

ZIN 82559 there is a distinct but short posterior fossa limited medially and distally by a strong ridge (Fig. 14b). In ZIN 103880 the posterior fossa is much shallower and extends down the whole preserved shaft fragment.

ZIN 103881 and USNM 642702 represent distal portions of the co-ossified tibia and fibula (Fig. 14f–h). The latter specimen was discussed and illustrated by Szalay and Sargis (2006: figs 16A, 17G–I). Nesov (1987: pl. 1, fig. 8) figured a third fragment of a co-ossified tibia and fibula from the Bissekty Formation. ZIN 103881 is distinctly smaller than the tibia of *Rattus rattus* and belongs to an immature individual with the sutures between tibia and fibula clearly visible (Fig. 14i, j). The preserved fragment is remarkably straight and elongated suggesting that the whole bone was rather long. The shaft gradually widens distally in anterior or posterior view, but has an almost constant width in lateral or medial view. In anterior view the fibula is very thin in the middle of the shaft but increases in width distally (Fig. 14i). In posterior view about one third of the bone width is composed of the fibula. The lateral malleolus composed of the fibula is preserved but the distal end of the tibia and medial malleolus are broken away. The lateral malleolus has a distinct articular astragalofibular facet on the medial side. USNM 642702 is slightly smaller than the previous specimen, with the length and width of the distal end 1.9 and 3.2 mm, respectively. It is more mature in that the sutures between the tibia and fibula are more subdued (Fig. 14g, h). The cochlea tibiale (lateral astragalotibial facet) and lateral and medial malleolae are similar in width. There is a distinct round medial astragalotibial facet on the distal side of the medial malleolus.

The short posterior tibial fossa, bordered by a strong medial ridge, observed in ZIN 82559, is reminiscent of the fossa in the symmetrodont *Zhangheotherium* Hu et al., 1997 (Luo and Ji 2005: fig. 5E). In *Barunlestes* the fibula is fused with the distal half of the tibial shaft with no visible suture (Kielan-Jaworowska 1978: pl. 11, fig. 1) unlike specimens from the Bissekty Formation referred to *Kulbeckia* in which a suture is evident. The middle of the tibial shaft is unknown for Bissekty Formation specimens, so the nature of fusion with the fibula in this region is unknown.

Astragalus. There are only three astragali from the Bissekty Formation, all described previously by Szalay and Sargis (2006) (Table 11). One specimen, USNM 642687 (Szalay and Sargis 2006: fig. 8) was associated with the calcanei of the metatherian group V and provisionally attributed to the Deltatheroida. It is distinct in having smooth and continuous surfaces of the three articulating areas on dorsal surface, with the lateral and medial portion of the facets extending distally on the neck with a broad non-articular area between them. The astragalar canal is present.

Table 11. Measurements (in mm) of therian astragalus from the Upper Cretaceous Bissekty Formation of Uzbekistan. Measurements: L – maximum length; W – maximum width.

Specimen	L	W
Sulestes karakshi		
USNM 642687	4.3	3.1
Kulbeckia kulbecke		
USNM 642675	3.35	2.6
USNM 642676	3.3	2.7

USNM 642687 similar to the astragalus of *Asioryctes* (Kielan-Jaworowska 1977) and *Ukhaatherium* (Horovitz 2000: fig. 5) in the absence of a pulley-shaped astragalar trochlea, which we view as a symplesiomorphy of these taxa. As in marsupials and in contrast with most placentals, in USNM 642687, *Ukhaatherium*, and Adapisoriculidae (Smith et al. 2010: fig. 1) the astragalofibular facet and the medial astragalotibial facet form wide angles relative to the lateral astragalotibial facet. The neck of the astragalus in USNM 642687, as well as in *Asioryctes* and *Ukhaatherium*, is situated approximately in the middle of the astragalus. In USNM 642687 the astragalar neck is short and not constricted relative to the head, in contrast with *Ukhaatherium* and most other eutherians. The astragalar neck and head are of the similar width in *Zalambdalestes* (Kielan-Jaworowska 1978: fig. 15A). As was suggested by Szalay and Sargis (2006), this specimen likely belongs to *Sulestes*.

Two other specimens, USNM 642675 and USNM 642676, were associated with the distal fragment of tibiofibula USNM 642702 (Szalay and Sargis 2006: figs. 16, 17). According to these authors, there are no calcanei from the Bissekty Formation that would fit these astragali. However, they described a possible zalambdalestid calcaneus and suggested that tibiofibula USNM 642702 might belong to a zalambdalestid. The upper ankle joint represented by these specimens is unique in the complete separation of medial and lateral astragalotibial articulations. The astragalus of *Zalambdalestes* (Kielan-Jaworowska 1978: fig. 15)

has a medial trochlear ridge about twice shorter than the lateral trochlear ridge, closely approximating this condition. In *Zalambdalestes*, the medial and lateral astragalotibial facets are likely not connected, as in USNM 642675 and USNM 642676. If so, this would support attribution of these specimens to a zalambdalestid *Kulbeckia*.

Calcaneus. Szalay and Sargis (2006) described 19 calcanei from the Bissekty Formation, which were classified in several samples and taxonomic groups. Two specimens described in that paper do not come from the Bissekty Formation. ZIN 85353 (Szalay and Sargis 2006: figs. 9A, 10A, 11G–M) and ZIN 85346 (Szalay and Sargis 2006: figs. 9N, 10N, 11F–F, 15) come from the Cenomanian Khodzhakul Formation at localities Sheikhdzheili and Chelpyk, respectively, South West Kyzylkum Desert, Uzbekistan. Two specimens were published under the same number, URBAC 04-117, one referred to a metatherian (Szalay and Sargis 2006: figs. 1A, 2A, 3), and another to a eutherian (Szalay and Sargis 2006: figs. 9G, 10G). The current numbers for these specimens are USNM 642693 and USNM 642694, respectively.

Szalay and Sargis (2006) identified five metatherian and seven eutherian groups based on calcanei from the Bissekty Formation. Among the latter, eutherian groups I and VII include specimens that do not come from the Bissekty Formation (see above), Eutherian group II was referred to the Zalambdalestidae, and the remaining eutherian groups to the Zhelestidae. Dental remains demonstrate a preponderance of eleven eutherian species and only one metatherian from the Bissekty Formation compared to seven eutherians and five metatherians based on calcanei. The likelihood that both figures are correct is vanishingly small. Unsurprisingly, we find the multiple lines for taxonomic identification based on dental remains to be more compelling and thus suspect that some of the calcanei earlier referred to metatherians in fact belong to eutherians. The second most common mammalian group after Zhelestidae is Asioryctitheria. Szalay and Sargis (2006) did not attribute any calcanei to Asioryctitheria, suggesting on numbers alone that some of those attributed to metatherians in fact belong to Asioryctitheria. Some morphological data also support this attribution. Szalay and Sargis (2006) considered a ventrally deflecting calcaneal tuber to be a metatherian character, yet the Mongolian asioryctitherian *Ukhaatherium* (Horovitz 2000) is similar in having a ventrally deflecting calcaneal tuber.

With twelve newly recovered specimens, a sample of 31 calcanei from the Bissekty Formation was available for this study (Table 12). This sample can be divided into two distinct morphotypes. The first morphotype includes eight calcanei and corresponding to metatherian groups I–V of Szalay and Sargis (2006). It is distinct in having a ventrally deflecting tuber calcanei and a calcaneocuboid facet not perpendicular to the long axis of calcaneus. Among these specimens, USNM 642693 (metatherian group I; Szalay and Sargis 2006: fig. 3) differs from other specimens in having the large peroneal process extending more distally compared to the calcaneocuboid facet, and with the sustentacular facet extending along the dorsal margin of the calcaneocuboid facet (Fig. 15f). Szalay and Sargis (2006) reconstructed the astragalus in USNM 642693 as having a minimal superposition on the calcaneus, but rather placed mostly medial to it. This reconstruction is based on the purported orientation of the calcaneus in the pes, which is difficult to assess from an isolated bone. A conventional dorsal view of the specimen (Szalay and Sargis 2006: fig. 3C) shows much greater superposition of the astragalus on the calcaneus.

In the remaining specimens of the first morphotype (groups I–V), the peroneal process is smaller and does not extend distally beyond the calcaneocuboid facet, and the sustentacular facet does not extend along the dorsal margin of the calcaneocuboid facet. In USNM 642682 the peroneal process is complete, contra interpretation in Szalay and Sargis (2006: fig. 5), and projects directly ventrally. A similarly ventrally deflecting peroneal process is well preserved in a slightly larger specimen USNM 642688. Both specimens were referred to metatherian group III by Szalay and Sargis (2006). In USNM 642692 (metatherian group II; Szalay and Sargis 2006: fig. 4), the peroneal process is mostly broken, but could be of the same size and direction, as in the previous specimens. Szalay and Sargis (2006) considered the tuber calcanei as being significantly deeper in metatherian group III compared with the groups I–II. However, the tuber calcanei is mostly broken in these specimens and we do not see much difference in the depth of tuber calcanei. Nearly complete specimens USNM 642686 (Fig. 15a–e) and ZIN 88902 are similar in most respects with the metatherian groups II–III of Szalay and Sargis (2006).

The two larger specimens, referred to the metatherian group IV (USNM 642685; Szalay and

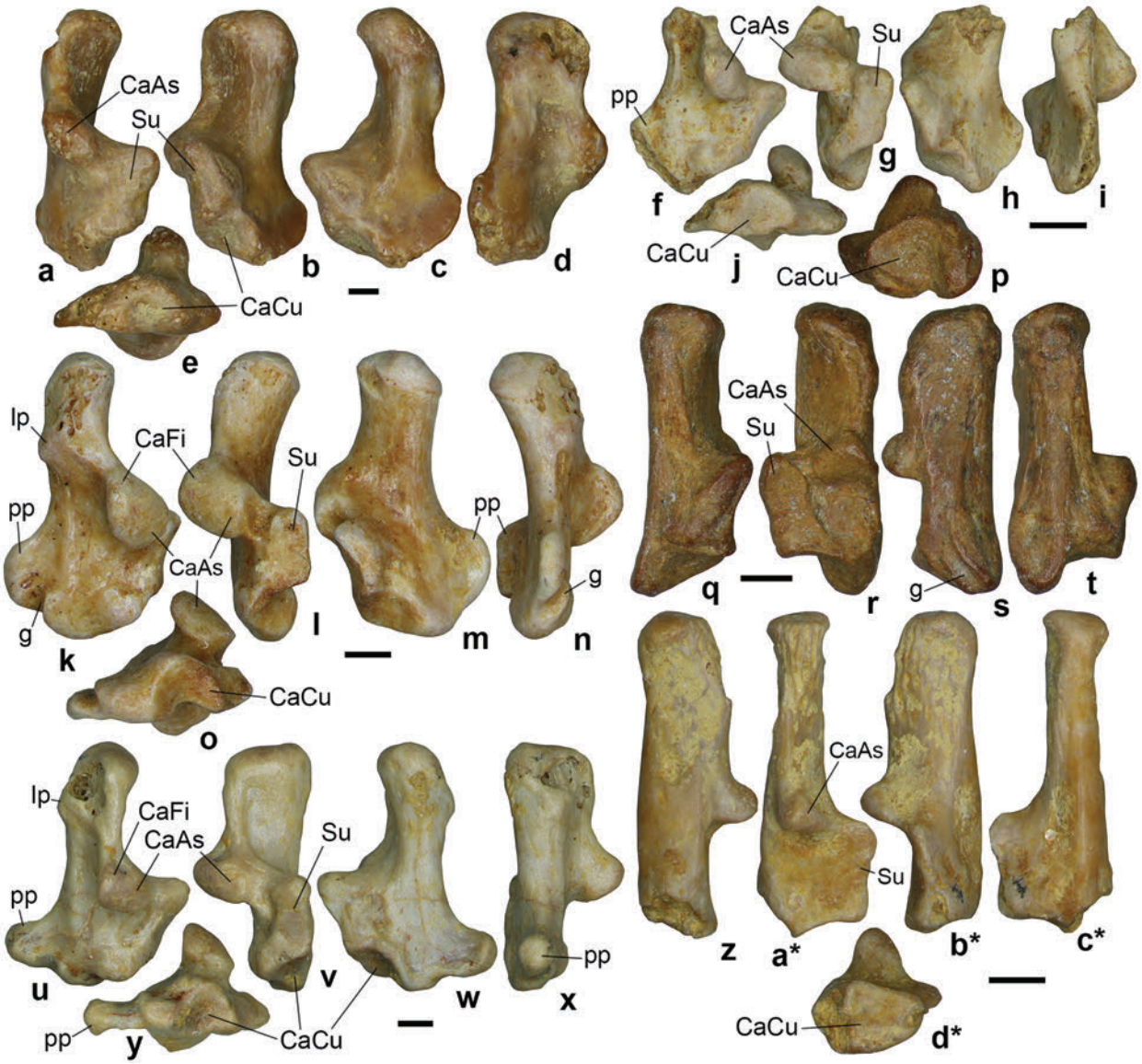

Fig. 15. Calcanei from the Upper Cretaceous Bissekty Formation of Uzbekistan. **a**–**e** – USNM 642686, right calcaneus, in dorsal **(a)**, dorsomedial **(b)**, medial **(c)**, ventral **(d)**, and distal **(e)** views. **f**–**j** – USNM 642693, right calcaneus, in lateral **(f)**, dorsal **(g)**, dorsomedial **(h)**, ventral **(i)**, and distal **(j)** views. **k**–**o** – USNM 642685, right calcaneus, in lateral **(k)**, dorsal **(l)**, medial **(m)**, ventral **(n)**, and distal **(o)** views. **p**–**t** – USNM 642698, left calcaneus, in distal **(p)**, medial **(q)**, dorsal **(r)**, lateral **(s)**, and ventral **(t)** views. **u**–**y** – USNM 642689, right calcaneus, in lateral **(u)**, dorsal **(v)**, medial **(w)**, ventral **(x)**, and distal **(y)** views. **z**–**d*** – USNM 642681, right calcaneus, in lateral **(z)**, dorsal **(a*)**, medial **(b*)**, ventral **(c*)**, and distal **(d*)** views. *Abbreviations*: CaAs – calcaneoastragalar facet; CaCu – calcaneocuboid facet; CaFi – calcaneofibular facet; g – peroneus longus groove; lp – calcaneal lateral process; pp – peroneal process; Su – sustentacular facet. Scale bars each equal 1 mm.

Sargis 2006: fig. 6) and metatherian group V (USNM 642689; Szalay and Sargis 2006: fig. 7), were considered as possibly belonging to deltatheroidans. These specimens differ from the previous ones by the presence of the calcaneal lateral process and the groove for the tendon of the peroneus longus. These specimens differ one from another mostly in the shape of the peroneal process. In the slightly smaller specimen USNM 642685 the peroneal process is a flat triangular plate (Fig. 15k, m), whereas in the

Table 12. Measurements (in mm) of therian calcaneus from the Upper Cretaceous Bissekty Formation of Uzbekistan. Measurements: L – maximum length; W – maximum width.

Specimen	L	W
Sulestes karakshi		
USNM 642685	6.6	4.1
USNM 642689	7.3	4.5
Paranyctoides quadrans		
USNM 642693	–	3.4
Asioryctitheria		
ZIN 88902	5.9	3.1
USNM 642686	5.9	3.8
USNM 642682	–	4.0
USNM 642692	–	4.5
Zhelestidae size class I		
ZIN 88890	4.0	1.5
ZIN 104111	4.2	2.0
ZIN 88889	–	1.9
Zhelestidae size class II		
USNM 642695	5.0	2.3
USNM 642690	5.0	–
USNM 642697	5.3	2.2
USNM 642680	–	2.2
ZIN 104112	–	2.2
Zhelestidae size class III		
ZIN 85344	5.5	2.3
USNM 642684	5.4	2.4
ZIN 103895	5.5	2.8
USNM 642698	5.7	2.6
ZIN 104110	–	2.4
USNM 642694	–	2.5
Zhelestidae size class IV		
USNM 642679	6.3	2.9
USNM 642691	6.4	3.2
USNM 642699	6.6	3.1
USNM 642678	6.8	3.0
USNM 642696	7.0	2.9
USNM 642683	–	2.9
Kulbeckia kulbecke		
USNM 642681	5.8	2.0

larger specimen USNM 642689 it is a stout and narrower process (Fig. 15u, w). A transversely broad calcaneoastragalar facet, noted for USNM 642689 by Szalay and Sargis (2006: p. 180), is actually divided into two facets, which meet at an obtuse angle. The lateralmost of these facets is likely the calcaneofibular facet (Fig. 15u). A small calcaneofibular facet is likely present also in USNM 642685 (Fig. 15i). In this character, as well as in overall configuration, USNM 642689 is very similar with the calcaneus of *Deltatheridium* Gregory et Simpson, 1926 (Horovitz 2000: fig. 9), and may indeed belong to the deltatheroidan *Sulestes*, as was proposed by Szalay and Sargis (2006). The difference between this specimen and a smaller USNM 642685 in the shape of the peroneal process and calcaneocuboid facet may be explained by ontogenetic and individual variation. The change of the shape of peroneal process occurs in the ontogenesis of extant Didelphidae (Szalay 1994: fig. 4.2). Both specimens are referred here to *Sulestes*.

Szalay and Sargis (2006) thought that the calcaneal lateral process, documented in USNM 642685 and USNM 642689, referred to *Sulestes*, was characteristic for all calcanei attributed by them to the Metatheria. In additional specimens with the same morphology and completely preserved tuber calcanei, USNM 642686 (Fig. 15a–d) and ZIN 88902, there is no calcaneal lateral process. This process was likely absent also in the less complete specimens. This process is also absent in the asioryctitherian *Ukhaatherium* (Horovitz 2000: fig. 4). The calcaneus of *Ukhaatherium* is generally similar with the calcanei from the Bissekty Formation attributed by Szalay and Sargis (2006) to the metatherian groups II and III. It differs from the latter specimens in the morphology of the calcaneocuboid facet, which is perpendicular to the long axis of the calcaneus. Most likely the calcanei of the metatherian groups II and III belong to asioryctitherians known from the Bissekty Formation by dental remains (Archibald and Averianov 2006). The smallest specimen USNM 642693, referred to the metatherian group I, which is morphologically distinct from the previous group in having a large distally projecting peroneal process and sustentacular facet extending along the dorsal margin of calcaneocuboid facet, may belong to the relatively small sized stem placental *Paranyctoides quadrans* (Nesov, 1982), described from the Bissekty Formation (Archibald and Averianov 2001; Averianov and Archibald 2013).

USNM 642681 (Szalay and Sargis 2006: fig. 12), the sole representative of the eutherian group II, was referred to the Zalambdalestidae. This calcaneus is distinct in having a cone-like calcaneoastragalar facet, a proportionally longer tuber calcanei, and a large and nearly transversely oriented calcaneocuboid facet. Szalay and Sargis (2006: p. 185) considered the peroneal process in this specimen as "nearly completely reduced." However, the peroneal process is mostly broken (Fig. 15z–c*), although it appears to be smaller than in the calcanei referred to the Zhelestidae. The calcaneus of *Zalambdalestes* (Kielan-Jaworowska 1978: fig. 15; pl. 9, figs. 1c–f) is similar to USNM 642681 in having a long tuber calcanei but differs in a distinctly more reduced peroneal process. USNM 642681 most likely belongs to the zalambdalestid *Kulbeckia* described from the Bissekty Formation (Archibald and Averianov 2003).

The remaining 21 calcanei specimens from the Bissekty Formation, including those referred to the eutherian groups III–VI by Szalay and Sargis (2006), have similar morphology and attributable to the Zhelestidae (Fig. 15p–t). These calcanei are characterized by straight, relatively short and massive tuber calcanei, a larger peroneal process, and the calcaneocuboid process perpendicular to the long axis of the calcaneus. A short peroneous longus groove might be present on the peroneal process in some specimens (USNM 642679, USNM 642698; Fig. 15s).

TAXONOMIC ATTRIBUTION OF ISOLATED POSTCRANIAL ELEMENTS

As discussed in the previous section, taxonomic attribution of some isolated therian postcranial bones from the Bissekty Formation can be done on morphological grounds. These data are summarized in Table 13. The next attempt to identify isolated postcranial elements from the Bissekty Formation is based on size comparison. The graph presented in Fig. 16 provides a picture of the size disparity between the Bissekty therians. Among the Bissekty therians four size groups can be recognized. Group I includes five taxa with body mass below 50 g. *Uchkudukodon nessovi* (McKenna et al., 2000) is the smallest taxon in this group and *Bulaklestes kezbe* Nesov, 1985 is the largest. *Daulestes kulbeckensis* Trofimov et Nesov, 1979, *D. inobservabilis* (Nesov, 1982), and *Paranyctoides quadrans* are intermediate in size. All these species except *Paranyctoides* are asioryctitherians

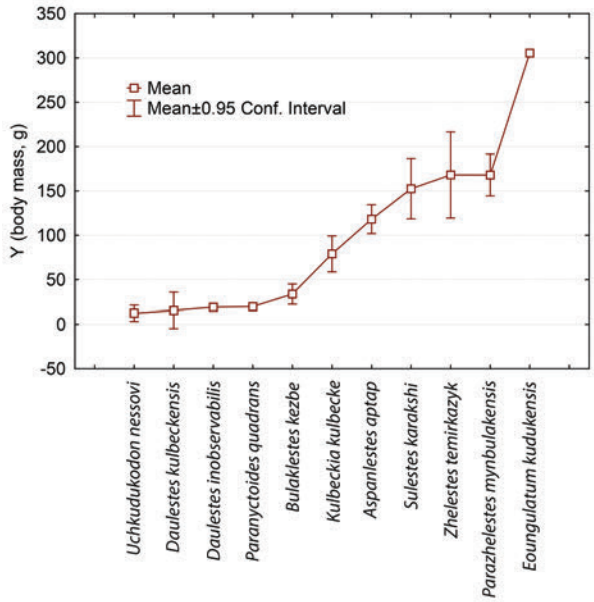

Fig. 16. Body mass estimation for the therians from the Upper Cretaceous Bissekty Formation of Uzbekistan based on lower molars and regression model for primates (Conroy, 1987).

(Archibald and Averianov 2006). The body mass of the Mongolian asioryctitherian *Ukhaatherium* has been identified as 32 g based on skull length (Horovitz 2003), which is similar with the Bissekty asioryctitherians. Group II includes a single species, the zalambdalestid *Kulbeckia kulbecke* Nesov, 1993, with a body mass between 50 and 100 g. Group III includes three zhelestid species (*Aspanlestes aptap* Nesov, 1985, *Zhelestes temirkazyk* Nesov, 1985, and *Parazhelestes mynbulakensis*) and one deltatheroidan (*Sulestes karakshi* Nesov, 1985). All have a body mass between 100 and 200 g. The largest taxon in the sample, the zhelestid *Eoungulatum kudukensis* with the body mass over 300 g is the sole representative of group IV. *Parazhelestes robustus*, for which a body mass could not be determined, would fall between *Parazhelestes mynbulakensis* and *Eoungulatum kudukensis*, being somewhat closer to the size of the latter species.

The taxonomic attribution of isolated vertebrae is most difficult because usually there is some size variation within the series, especially among caudal vertebrae. However, two specimens are exceptional because of their size: a very small lumbar vertebra USNM 642671 and a very large anterior caudal vertebra USNM 642641. The latter fits the size of *Didelphis marsupialis*. There is only one mammal in

Table 13. Taxonomic attribution of therian isolated postcranial elements from the Upper Cretaceous Bissekty Formation of Uzbekistan.

Element	Specimens	Attribution based on
	Sulestes karakshi	
Humerus shaft	USNM 642653	Morphology
Humerus distal	USNM 642658, ZIN 85305	Morphology[1]
Astragalus	USNM 642687	Morphology[2]
Calcaneus	USNM 642685, 642689	Morphology[3]
	Paranyctoides quadrans	
Humerus distal	USNM 642656, 642657	Morphology and size[4]
Femur distal	USNM 642642	Morphology and size[5]
Calcaneus	USNM 642693	Size[6]
	Aspanlestes aptap	
Scapula	USNM 642630, ZIN 103867	Size
	Eoungulatum kudukensis	
Anterior caudal	USNM 642641	Size
	Zhelestidae indet.	
Humerus distal	USNM 642660, 642661, 642662, 642663, 642664, 642665, 642666, 642667, 642668	Morphology[7]
Calcaneus	USNM 642677, 642678, 642679, 642680, 642683, 642684, 642690, 642691, 642694, 642695, 642696, 642697, 642698, 642699, ZIN 85344, 88889, 88890, 103895, 104110, 104111, 104112, 104113	Morphology[8]
	Uchkudukodon nessovi	
Ulna	ZIN 103884	Size
	Asioryctitheria indet.	
Axis	ZIN 104120	Morphology and size
Distal humerus	USNM 642659	Size[9]
Femur distal	USNM 642643, 642647	Size
Calcaneus	USNM 642682, USNM 642686, USNM 642688, USNM 642692, ZIN 88902	Morphology[10] and size
	Kulbeckia kulbecke	
Scapula	USNM 642633	Morphology and size
Humerus distal	USNM 642652, ZIN 85309	Morphology[11]
Femur proximal	USNM 642646, ZIN 97885	Size
Femur distal	USNM 642644, ZIN 85327	Size
Tibia-fibula	CCMGE 8/12455, USNM 642702, ZIN 103881	Morphology[12]
Astragalus	USNM 642675, 642676	Morphology[12]
Calcaneus	USNM 642681	Morphology[13]

[1]Metatherian groups 2 and 3 of Chester et al. (2010). [2]Metatherian group V of Szalay and Sargis (2006). [3]Metatherian groups IV and V of Szalay and Sargis (2006). [4]Metatherian group 1 of Chester et al. (2010). [5]Metatherian distal femur of Chester et al. (2012). [6]Metatherian group I of Szalay and Sargis (2006). [7]Zhelestid groups 1–5 of Chester et al. (2010). [8]Eutherian groups III and IV of Szalay and Sargis (2006). [9]Eutherian group 1 of Chester et al. (2010). [10]Metatherian groups II and III of Szalay and Sargis (2006). [11]Zalambdaelstid distal humerus of Chester et al. (2010). [12]Probably zalambdalestid crus and astragali of Szalay and Sargis (2006). [13]Eutherian group II of Szalay and Sargis (2006).

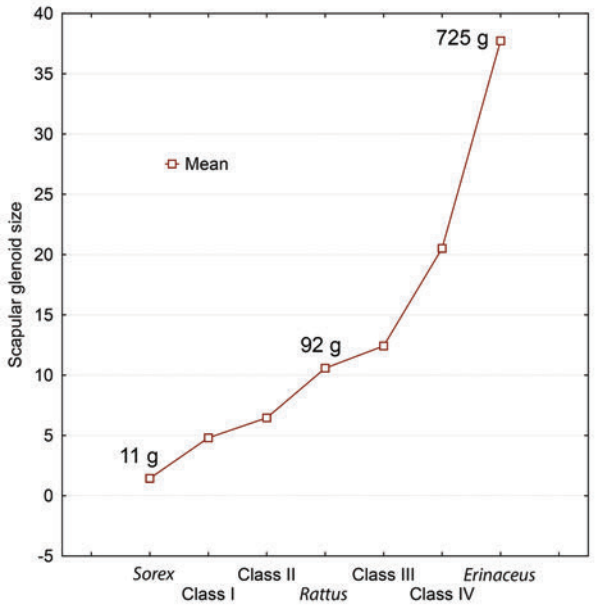

Fig. 17. The size of scapular glenoid (glenoid length multiplied by glenoid width, in mm^2) in Bissekty therians (class sizes I–IV), *Sores raddei*, *Rattus rattus*, and *Erinaceus europaeus*. The scapular glenoid size for the class III is calculated from two incomplete specimens of similar size.

the assemblage that could be as large, the zhelestid *Eoungulatum kudukensis* (Fig. 16). Therefore, the anterior caudal USNM 642641 is attributable to *Eoungulatum* Nesov et al., 1998. The attribution of the lumbar vertebra USNM 632671 is less certain. It may belong to one of the asioryctitherians, or to *Paranyctoides*.

The scapular fragments can be separated into four distinct size classes (Table 4; Fig. 17). The size class II includes a single specimen (USNM 642633), attributed to *Kulbeckia* based on morphology. The size class I (ZIN 103866) may belong to either an asioryctitherian or *Paranyctoides*. The size class III (USNM 642630, ZIN 103867) includes scapulae of animals with a body mass around 100 g. The single suitable taxon for this size group is a zhelestid *Aspanlestes* Nesov, 1985. The next size class IV (USNM 642634) may belong to a larger zhelestid, or to *Sulestes*.

Although there are many fragments of the humerus in the sample, most of the distal fragments are too incomplete to allow measurement. The two proximal humeral fragments differ significantly in size (Table 5; Fig. 18). The smaller specimen (USNM 642648) may belong to an asioryctitherian or *Paranyctoides*, the larger (USNM 642654) to a zhelestid or *Sulestes*.

The four proximal radial fragments fall into two size groups (Table 6; Fig. 19). Specimens of the first

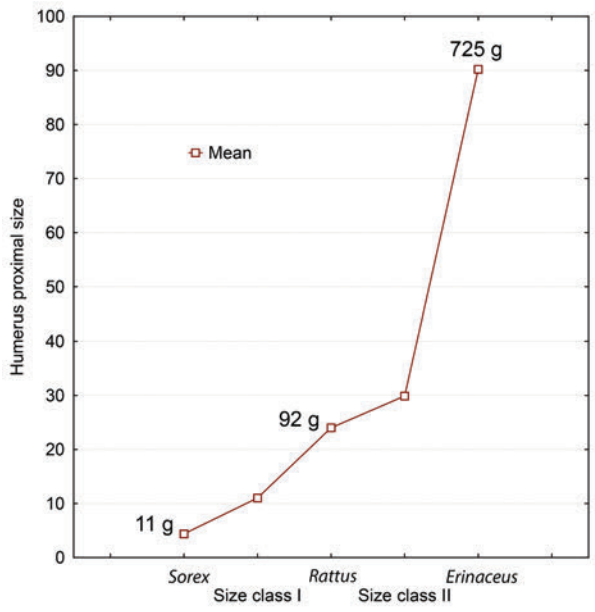

Fig. 18. The size of proximal humerus (proximal end length multiplied by proximal end width, in mm^2) in Bissekty therians (class sizes I–II), *Sores raddei*, *Rattus rattus*, and *Erinaceus europaeus*.

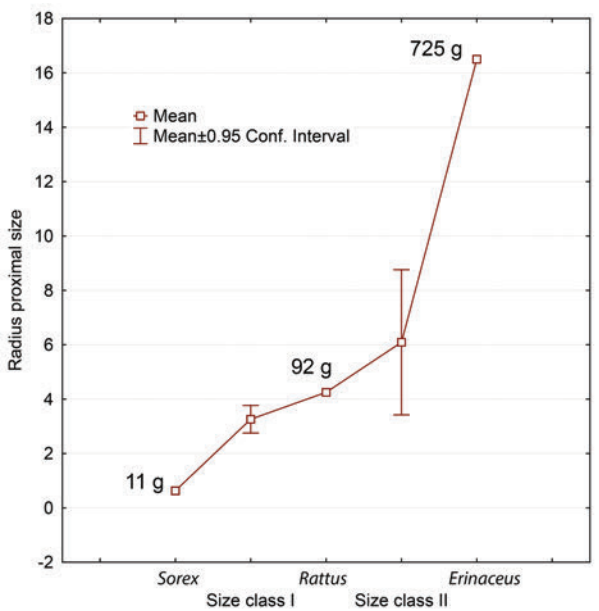

Fig. 19. The size of proximal radius (proximal end length multiplied by proximal end width, in mm^2) in Bissekty therians (class sizes I–II), *Sores raddei*, *Rattus rattus*, and *Erinaceus europaeus*.

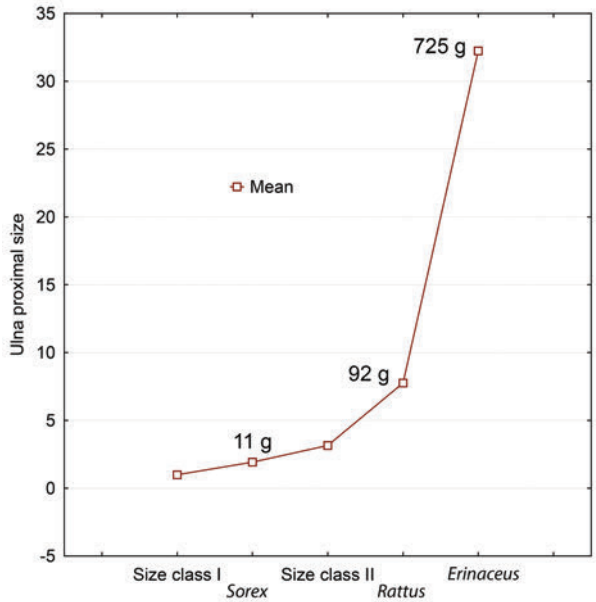

Fig. 20. The size of proximal ulna (proximal end length multiplied by proximal end width, in mm²) in Bissekty therians (class sizes I–II), *Sores raddei*, *Rattus rattus*, and *Erinaceus europaeus*.

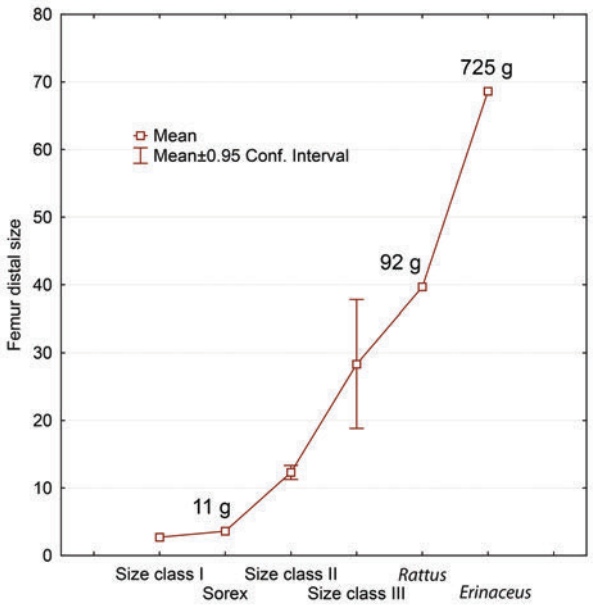

Fig. 22. The size of distal femur (distal end length multiplied by distal end width, in mm²) in Bissekty therians (class sizes I–III), *Sores raddei*, *Rattus rattus*, and *Erinaceus europaeus*.

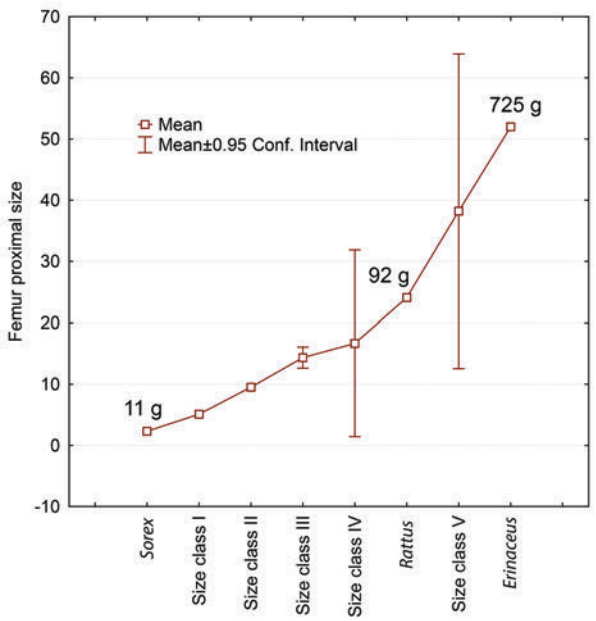

Fig. 21. The size of proximal femur (femoral head length multiplied by proximal end width, in mm²) in Bissekty therians (class sizes I–V), *Sores raddei*, *Rattus rattus*, and *Erinaceus europaeus*.

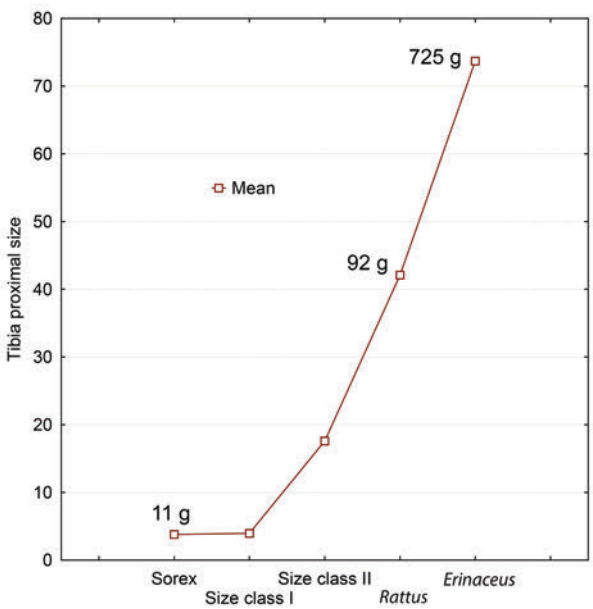

Fig. 23. The size of proximal tibia (proximal end length multiplied by proximal end width, in mm²) in Bissekty therians (class sizes I–II), *Sores raddei*, *Rattus rattus*, and *Erinaceus europaeus*.

size class (ZIN 103882, ZIN 104124) may belong to a large asioryctitherian or *Kulbeckia*. The second size class (ZIN 104122, ZIN 104123) is suitable for zhelestids and *Sulestes*.

A tiny fragment of proximal ulna (ZIN 103884; Table 7; Fig. 20) is smaller than the ulna of *Sorex raddei* (body mass 10.9 g) and likely belongs to the smallest therian in the Bissekty Formation, asioryctitherian *Uchkudukodon* Archibald et Averianov, 2006 (Fig. 16). The second measured proximal ulnar fragment (ZIN 103883: Fig. 20) may belong to a larger asioryctitherian or *Paranyctoides*.

Four of five size classes of proximal femur are placed between *Sorex raddei* and *Rattus rattus* (Table 8; Fig. 21). The size classes I–III may belong to asioryctitherians and *Paranyctoides*, size class IV to *Kulbeckia*. The larger proximal femoral fragments (size class IV) may belong to a zhelestid or *Sulestes*.

The smallest distal femoral fragment (USNM 642642; Table 9; Fig. 22), attributed to *Paranyctoides*, is about the size of *Sorex raddei* (10.9 g). The larger distal femoral fragments may belong to Asioryctitheria (size class II) and *Kulbeckia* (size class III).

One of the two proximal tibial fragments (ZIN 82559; Table 10; Fig. 23) is close in size to *Sorex raddei*. It may belong to an asioryctitherian or *Paranyctoides*. A larger specimen (ZIN 103880) is smaller than tibia of *Rattus rattus* (Fig. 23) and may belong to an asioryctitherian or *Kulbeckia*.

IMPLICATIONS FOR EVOLUTION OF POSTCRANIAL SKELETON IN THERIA

In this section we review postcranial characters that can be documented for the materials from the Bissekty Formation as they relate to variations in postcrania in stem therians, stem placentals, stem marsupials, and the closest outgroups for the Theria.

In all atlas fragments from the Bissekty Formation there is no transverse foramen. The transverse foramen is absent in the atlas of Monotremata, most Marsupialia, in asioryctitherians *Asioryctes* and *Ukhaatherium*, and in the cimolestid *Maelestes* (Kielan-Jaworowska 1977; Kielan-Jaworowska and Gambaryan 1994; Horovitz 2003; Wible et al. 2009). This foramen is present in the zalambdalestid *Barunlestes* (Kielan-Jaworowska 1978) and most extant placentals. At least some of atlas fragments from the Bissekty Formation might belong to zhelestids, the dominant mammal group in the assemblage. If so, zhelestids would have a plesiomorphic therian condition – lack of a transverse foramen in the atlas. Some authors considered the presence/absence of the transverse foramen in the atlas as equivalent to the presence/absence of the atlantal rib (Ji et al. 2002, 2006; Kielan-Jaworowska et al. 2004), which is misleading. In the Bissekty eutherians, as well as in most other stem placentals and most marsupials, the atlantal rib is absent (fused with the atlas and becoming the atlantal transverse process), and the transverse foramen is absent. In *Barunlestes* and most extant placentals the atlantal rib is also absent, but the transverse foramen is present.

In the atlantes from the Bissekty Formation, as well as in other known stem placentals (*Asioryctes*, *Ukhaatherium*, *Maelestes*, *Barunlestes*), the vertebral artery ran anterior to the dorsal arch, which is about twice shorter anteroposteriorly than the neural arch. In most extant placentals, the dorsal arch is as wide as the neural arch and the vertebral artery pierces the dorsal arch via the atlantal foramen. The atlantal foramen is absent in stem marsupials and variably present in extant marsupials (Marshall and Sigogneau-Russell 1995; Horovitz and Sánchez-Villagra 2003). Thus, absence of the atlantal foramen is a therian plesiomorphy and this foramen appeared independently in crown marsupials and placentals.

The suture between the proatlas and the centrum 1 is still visible in the apparently adult axis USNM 594554 from the Bissekty Formation (Fig. 2i). This suture is absent in the otherwise similar axis CCMGE 6/11758 from the Khodzhakul Formation and in the axis ZIN 104120 from the Bissekty Formation, as well as in adult or juvenile specimens of extant therians (Jenkins 1969). Presence of the proatlas-centrum 1 suture is apparently a plesiomorphic character for therians or an earlier clade, which is retained in some stem placentals. CCMGE 6/11758, which likely belonged to a large zhelestid (Averianov and Archibald 2005), is interesting in the presence of a distinct suture between the centrum 1 and 2. This suture is present in adult tritylodonts, monotremes, *Asioryctes*, *Zalambdalestes*, and *Barunlestes*, as well as in some juvenile therians (Jenkins 1969; Kielan-Jaworowska 1977, 1978).

The anterior articular surfaces of the axis in USNM 594554 from the Bissekty Formation and in CCMGE 6/11758 from the Khodzhakul Formation, as well as in *Maelestes* (Wible et al. 2009) and *Barunlestes* (Wible et al. 2009) are not ventrally

confluent with the dens. In another axial fragment from the Bissekty Formation (ZIN 104120) and in *Asioryctes* (Kielan-Jaworowska 1977) the anterior articular surfaces of the axis are confluent with each other and to the articular surface of the dens. The confluence of the anterior articular facets of the axis is an apomorphy of Theria according to Horovitz and Sánchez-Villagra (2003: character 12(1)). This character has a more complex distribution in the analysis by Wible et al. (2009: character 344) where no clear phylogenetic signal was indicated. In extant therians both of these variants are present (Lessertisseur and Saban 1967). The phylogenetic significance of this character is uncertain.

The presence of three morphologically different variants of anticlinal thoracic vertebra as well as the abundance of the postanticlinal thoracic vertebrae in the sample suggests taxonomic variations in the anticlinal vertebra of Bissekty therians. Some thoracolumbar vertebrae and at least one lumbar vertebra from the Bissekty Formation have the neural spine posterodorsally directed. This morphology suggests absence of the anticlinal vertebrae at least in some of Bissekty mammals. Anticlinal vertebra are known in haramiyidans (Bi et al. 2014), morganucodontids (Jenkins and Parrington 1976), multituberculates (Kielan-Jaworowska and Gambaryan 1994; Sereno 2006; Yuan et al. 2013; Zhou et al. 2013), symmetrodonts (Li and Luo 2006; Ji et al. 2009), and in most extant therians (Slijper 1946). The anticlinal vertebra is absent in docodonts (Luo et al. 2015), monotremes, eutriconodonts (Luo et al. 2007a), and *Fruitafossor* Luo et Wible, 2005 (Luo and Wible 2005). Within the crown Placentalia absence of anticlinal vertebrae was considered as a parallel synapomorphy for Xenarthra, Pan-Tethytheria, and Dermoptera (O'Leary et al. 2013). Presence of anticlinal vertebrae indicates flexibility of the lower back region and can be variably present in closely related taxa (Argot 2004). The condition in *Barunlestes* is unclear: the neural spine is dorsally directed on the first lumbar vertebra and posterodorsally directed in more posterior lumbar vertebrae (Kielan-Jaworowska 1978). In stem marsupials the anticlinal vertebra is within the first lumbar vertebrae (Argot 2004) or absent (Szalay and Trofimov 1996), while in crown marsupials and eutherians it is within the thoracic series. Presence of postanticlinal thoracic vertebrae in the Bissekty Formation suggests that when the anticlinal vertebra is present, it is within the thoracic series.

There are only two lumbar vertebrae from the Bissekty Formation that based on size and morphology belong to different species. Both specimens have the lumbar rib synostosed with the vertebra to form a transverse process. Separate lumbar ribs are present in tritylodonts, docodonts, gobiconodonts, *Pseudotribos* Luo et al., 2007, *Fruitafossor*, and *Akidolestes* Li et Luo, 2006 (Kielan-Jaworowska et al. 2004; Luo and Wible 2005; Ji et al. 2006; Li and Luo 2006; Luo et al. 2007a, b). Synostosed lumbar ribs are found in morganucodontids, monotremes, *Jeholodens* Ji et al., 1999, multituberculates, *Zhangheotherium*, *Maotherium* Rougier et al., 2003, *Vincelestes* Bonaparte, 1986, *Henkelotherium* Krebs, 1991, *Juramaia*, and extant therians (Krebs 1991; Li and Luo 2006; Ji et al. 2009; Luo et al. 2011). Such irregular distribution of this character, with notable variation within symmetrodonts, is best explained by evolutionary plasticity of this trait (Li and Luo 2006). It is likely that synostosis of lumbar ribs is a plesiomorphic for the Theria.

The lumbar ribs or transverse processes are posterolaterally directed in *Pseudotribos*, *Fruitafossor*, *Yanoconodon* Chen et al., 2007, and *Akidolestes* (Luo and Wible 2005; Li and Luo 2006; Luo et al. 2007a, b). They are directed laterally or anterolaterally in multituberculates, *Maotherium*, and most extant therians (Kielan-Jaworowska and Gambaryan 1994; Ji et al. 2009). At least in one of the two lumbar vertebrae from the Bissekty Formation the transverse processes are anterolaterally directed. This character might be a therian plesiomorphy.

The plesiomorphic therian morphotype of the scapula, with the infraspinous fossa positioned medially to the supraspinous fossa and the scapular spine, and an S-shaped cross section of the scapula, has been documented or reported for the stem placentals *Ukhaatherium* and *Maelestes*, and basal cladotherians *Henkelotherium* and *Vincelestes* (Krebs, 1991; Horovitz 2003; Wible et al. 2009). Among zalambdalestids only the proximal fragment of a scapula is known for *Barunlestes* (Kielan-Jaworowska 1978: fig. 9; pl. 7, fig. 2). Based on the stereophotographs of this specimen, it appears that the infraspinous and supraspinous fossae were not coplanar in Zalambdalestidae as in other stem placentals. The scapula of the stem therians *Eomaia* Ji et al., 2002 and *Sinodelphys* Luo et al., 2003 has been interpreted as having a plate-like scapular blade with a flat infraspinous fossa (Ji et al. 2002; Luo et al. 2003; Luo 2015). This interpretation is not supported by detailed description of the

material and photographs and may be affected by the flattened preservation of the specimens. Another stem therian mammal, *Juramaia*, was coded in the data matrix as having the infraspinous and supraspinous fossae in different planes (Luo et al. 2011). Luo (2015) suggested that the trough-like infraspinous fossa of the scapula could reflect fossorial adaptations, as it is present in the fossorial marsupial mole *Notoryctes* Stirling, 1891 and the placental golden mole *Chrysochloris* Lacépède, 1799. Other mammalian postcranial bones from the Bissekty Formation do not show features of fossorial adaptations, so possession of this scapular anatomy might not indicate fossoriality. Moreover, the generalized forelimbs of *Ukhaatherium* and *Maelestes*, which also have the trough-like infraspinous fossa, suggest a terrestrial mode of life (Horovitz 2003; Wible et al. 2009). Most likely, this scapular morphology is plesiomorphic for Theria. As this scapular morphotype is present in all Bissekty specimens, it is likely that zhelestids also had such a morphology.

The preacetabular tubercle for *m. rectus femoris* on the ilium is absent in haramiyidans, docodonts, *Pseudotribos*, *Rugosodon* Yuan et al., 2013, eutriconodonts, symmetrodonts, *Fruitafossor*, and *Ukhaatherium* (Horovitz 2003; Luo and Wible 2005; Luo et al. 2007a, b, 2015; Ji et al. 2009; Chen and Luo 2013; Yuan et al. 2013; Zheng et al. 2013; Bi et al. 2014). In Cimolodonta there is a pit rather than a tubercle for insertion of *m. rectus femoris* in front of the acetabulum (Kielan-Jaworowska and Gambaryan 1994). The preacetabular tubercle is present in monotremes, in the stem marsupial *Herpetotherium* Cope, 1873, in pantodonts, and in many crown group placental mammals (Gambaryan et al. 2002; Horovitz 2003; Horovitz et al. 2008; Muizon et al. 2015). This tubercle is absent on all ilial specimens from the Bissekty Formation except ZIN 103889, where it is very large (Fig. 12d, e).

The three pubic bones participate in the acetabulum almost equally in symmetrodonts and *Vincelestes* (Horovitz 2003; Luo and Ji 2005). In *Ukhaatherium* the pubis articulation is reduced but still larger than in most crown group placentals (Horovitz 2003). No mammalian pubis has been identified from the Bissekty Formation, but it is possible that the pubis was excluded from the acetabulum in these taxa, being replaced by the acetabular bone.

The third trochanter of femur is absent in haramiyidans, *Pseudotribos*, multituberculates, *Yanoconodon*, *Akidolestes*, *Maotherium*, most crown marsupials, and stem placentals (Horovitz 2003; Luo et al. 2007a, b; Ji et al. 2009; Chen and Luo 2013; Bi et al. 2014). It is likely absent on femora from the Bissekty Formation. The third trochanter was reconstructed for *Barunlestes* (Kielan-Jaworowska 1978: fig. 14A1), but it may well have been absent in that taxon. The third trochanter is present in some stem marsupials and many extant placentals, where it likely developed independently in various groups (Marshall and Sigogneau-Russell 1995; Horovitz et al. 2008; Hooker 2014). Absence of the third trochanter of femur is likely a therian plesiomorphy.

The femoral patellar groove and an ossified patella are absent in tritylodonts, morganucodontids, *Pseudotribos*, *Yanoconodon*, *Fruitafossor*, *Maotherium*, and some stem marsupials (Szalay and Trofimov 1996; Luo and Wible 2005; Luo et al. 2007a, b; Horovitz et al. 2008; Ji et al. 2009). In *Pucadelphys* Marshall et de Muizon, 1988 there is a patellar groove on the femur, but the ossified patella was likely absent (Marshall and Sigogneau-Russell 1995; Samuels et al. 2017). The ossified patella and patellar groove are present in monotremes, multituberculates, *Eomaia* (Ji et al. 2002), stem placentals (Horovitz 2003), and extant therians. The patellar groove is absent in one specimen from the Bissekty Formation, referred to a metatherian by Chester et al. (2012), or to *Paranyctoides* in the present study, and is present in all other specimens, referred to the Eutheria (Chester et al. 2012). The absence of an ossified patella was reconstructed as an ancestral trait for the Theria (Samuels et al. 2017). Thus, absence of the patellar groove in *Paranyctoides* could be a plesiomorphic retention rather than a character indicating metatherian affinities.

Among Cretaceous therians the tibia and fibula are separate in *Eomaia*, *Asiatherium* Trofimov et Szalay, 1994 and *Ukhaatherium* and fused distally in *Barunlestes* (Kielan-Jaworowska 1978; Szalay and Trofimov 1996; Horovitz 2000, 2003; Ji et al. 2002). The distal fusion of tibia and fibula is characteristic for some cursorial crown group placentals. It is present in the specimens from the Bissekty Formation referred to *Kulbeckia*. The distal fusion of tibia and fibula is apparently a synapomorphy for zalambdalestids, if this group falls within stem placentals. If Zalambdalestidae is a stem group of Euarchontoglires (Fostowicz-Frelik 2016), this character might be an apomorphy for that clade, as it is widely distributed in rodents and lagomorphs.

In tritylodonts, morganucodontids, monotremes, docodonts, multituberculates, eutriconodonts, symmetrodonts, *Vincelestes*, and *Henkelotherium* there is an extensive contact between fibula and calcaneus (Krebs 1991; Hu et al. 1997; Ji et al. 1999, 2006, 2009; Li and Luo 2006; Luo et al. 2007a). This contact is reduced in stem therians (*Eomaia*) and stem marsupials (*Deltatheridium*) (Horovitz 2000; Ji et al. 2002). In stem placentals, this contact is completely absent (*Ukhaatherium*, *Zalambdalestes*). Among materials from the Bissekty Formation, a reduced calcaneofibular facet was found in two calcanei attributed to *Sulestes*. In other specimens, referred to Eutheria, the contact between fibula and calcaneus is absent. According to Horovitz (2000), contact between fibula and calcaneus is an ancestral trait for the Theria.

In tritylodonts, morganucodontids, *Pseudotribos*, monotremes, docodonts, eutriconodonts, multituberculates, *Zhangheotherium*, *Akidolestes*, *Vincelestes*, *Henkelotherium*, *Eomaia*, *Asioryctes*, and *Ukhaatherium* the fibula contacts the distal end of the femur (Horovitz 2000, 2003; Ji et al. 2002, 2006; Li and Luo 2006; Luo et al. 2007b). This contact is absent in *Fruitafossor*, *Maotherium*, stem marsupials, and *Zalambdalestes* (Luo and Wible 2005; Ji et al. 2009). The absence of fibula-femur contact was considered a synapomorphy for epitherians (Shoshani and McKenna 1998), or the clade *Eomaia* + Theria (O'Leary et al. 2013). The preserved distal fragments of the femur from the Bissekty Formation show no facet for the fibula (Chester et al. 2012). These fragments can be attributed to *Paranyctoides*, Asioryctitheria, and *Kulbeckia*, suggesting that in these taxa the distal femur was not in contact with the fibula.

The presence of the astragalar canal is likely a therian plesiomorphy, as it is present in *Vincelestes* and *Ukhaatherium* (Horovitz 2000). Among stem placentals, the canal is lost in *Zalambdalestes*. The astragalar canal is present in the astragali from the Bissekty Formation referred to *Sulestes* and *Kulbeckia*.

The astragalar head has a flat or concave articular surface for the navicular in tritylodonts, morganucodontids, monotremes, multituberculates, and *Vincelestes* (Horovitz 2000). A convex surface was considered as an exclusive apomorphy for Theria (Horovitz 2000). In the stem therian *Eomaia* the astragalonavicular articulation is restricted and the astragalar head is concave (Luo et al. 2003: fig. 2D). In *Asioryctes* and *Ukhaatherium*, the astragalonavicular articulation is also restricted, but the head is convex, contra Szalay and Sargis (2006). The astragalar head is convex in *Maelestes* (Wible et al. 2009). The astragalar head is convex in all Bissekty astragali, referred to *Sulestes* and *Kulbeckia*.

Horovitz (2000) considered the astragalar head wider than neck in *Ukhaatherium* and *Asioryctes*. This is formally true as there is a slight constriction of the neck before the head, but the astragalonavicular articulation is restricted in these taxa (Luo et al. 2003: fig. 3). The astragalar head is narrower than the neck in *Zalambdalestes*, as well as in some stem marsupials (Horovitz 2000), including USNM 642687 referable to the deltatheroidan *Sulestes*. In contrast with previous accounts, the astragalar neck is present in symmetrodonts, being short and indistinct in *Zhangheotherium* and longer in *Akidolestes*; in both taxa the astragalar head is not wider than the neck (Chen and Luo 2013). It is likely that the narrow astragalar neck, with restricted astragalonavicular articulation, is a therian plesiomorphy.

According to Horovitz (2000), the hypertrophied astragalar medial plantar tuberosity (ampt) is a synapomorphy (observed in *Asioryctes* and *Ukhaatherium*) for asioryctitherians. A similarly large crested ampt was found in the stem therian *Eomaia* (Luo et al. 2003). A large posteriorly extended ampt is present in *Zhangheotherium* and *Akidolestes* (Luo and Ji 2005; Chen and Luo 2013). The ampt is absent in eutriconodont *Yanoconodon* (Luo et al. 2007a). The large crested ampt is likely a eutherian plesiomorphy. In stem metatherians the ampt is reduced (Luo et al. 2003), which is also true for URBAC 04-064 referred to *Sulestes*. The ampt is also reduced in the astragali from the Bissekty Formation referred to *Kulbeckia*.

The medial trochlear ridge (medio-tibial crest) of the astragalus is absent in eutriconodonts and symmetrodonts (Li and Luo 2006; Luo et al. 2007a; Ji et al. 2009). In *Maelestes*, *Ukhaatherium*, and *Zalambdalestes* the medial trochlear ridge is present, but smaller, with a smaller radius of curvature compared to the lateral trochlear ridge (tibio-fibular crest) (Horovitz 2000; Wible et al. 2009). The same is true for the eutherian astragali from the Bissekty Formation. In *Protungulatum* Sloan et Van Valen, 1965 and more derived eutherians both ridges have a similar size and curvature (Szalay and Decker 1974).

The sustentacular and navicular facets of the astragalus are separate in *Vincelestes* but merged in *Ukhaatherium* (Horovitz 2000) and in both metatherian and zalambdalestid astragali from the Bissekty

Formation. Having merged facets is likely a therian apomorphy.

The sustentacular facet of the astragalus does not reach the medial edge of the astragalar neck in *Vincelestes*, metatherians including USNM 642687 referred to *Sulestes*, eutherian astragali from the Bissekty Formation, and some crown group placentals (Horovitz and Sánchez-Villagra 2003; Wible et al. 2009). It reaches the medial side of the neck in *Ukhaatherium* (Horovitz 2000).

The angle between the lateral astragalotibial and astragalofibular facets is close to 180° in tritylodonts, morganucodontids, monotremes, eutriconodonts, symmetrodonts, *Vincelestes*, and metatherians (Horovitz 2000). This angle is between 180° and 90° in multituberculates and stem placentals *Maelestes*, *Asioryctes*, *Ukhaatherium*, and *Deccanolestes* (Prasad and Godinot 1994; Horovitz 2000; Wible et al. 2009). In USNM 642687 referred to *Sulestes* this angle is ~132°. In *Zalambdalestes* and most crown placentals this angle is close to 90° (Wible et al. 2009). The angle close to 180° is a therian plesiomorphy and the angle close to 90° is a placental plesiomorphy according to Horovitz (2000). A similar reduction of angle also occurred between the medial and lateral facets for tibia on astragalus. The angle is between 180° and 90° in *Asioryctes*, *Ukhaatherium*, and *Maelestes* and close to 90° in *Zalambdalestes* and crown placentals. In the two eutherian astragali from the Bissekty Formation both angles are close to 90°, which confirms their attribution to Zalambdalestidae.

In most therians the lateral and medial astragalotibial facets are confluent. These facets are separate in the astragali from the Bissekty Formation referred to *Kulbeckia* (Szalay and Sargis 2006).

Among the calcanei from the Bissekty Formation, the specimens referred to *Paranyctoides*, *Kulbeckia*, and Zhelestidae have the peroneal process (tubercle) that is protruding distally beyond the calcaneocuboid facets. In the specimens referred to *Sulestes* and Asioryctitheria, the peroneal process is not protruding beyond the calcaneocuboid facet, sometimes set at some distance from the distal end of the calcaneus. The latter condition of the peroneal process is also characteristic for the asioryctitherian *Ukhaatherium* (Horovitz 2000), while in *Asioryctes* it protrudes distally beyond the calcaneocuboid facet (Kielan-Jaworowska 1977: fig. 4A). The large distally protruding peroneal process of the calcaneus is likely a therian plesiomorphy (Horovitz 2000). The peroneal process is reduced in *Zalambdalestes* (Horovitz 2000).

The mediodistal orientation of the calcaneocuboid facet is a symplesiomorphic feature for therians (Szalay and Sargis 2006; Horovitz 2000). Among the Bissekty calcanei, it is found in the specimens referred to *Sulestes*, *Paranyctoides*, and Asioryctitheria. In the specimens referred to *Kulbeckia* and Zhelestidae the calcaneocuboid facet is facing distally, perpendicular to the long axis of the bone.

The posterior calcaneoastragalar (ectal) facet is oriented at a negative angle to the long axis of calcaneus, with the anterior end of the facet placed more medial than the posterior end, in Vincelestes, *Deltatheridium*, and some marsupials (Horovitz 2000), as well as in *Sulestes*, *Paranyctoides*, and Asioryctitheria from the Bissekty Formation. This is a plesiomorphic therian morphotype (Horovitz 2000). In *Ukhaatherium*, some stem and crown group marsupials, and some crown group placentals, the ectal facet is parallel to the long axis of the calcaneus (Horovitz 2000). This was considered a eutherian ancestral condition (Horovitz 2000). The orientation of the ectal facet in a calcaneus referred to *Kulbeckia* (USNM 642681) is difficult to assess, because of its unusual cone-like structure. In the calcanei from the Bissekty Formation referred to Zhelestidae the ectal facet is oriented at a positive angle to the long axis of the calcaneus, with the anterior end more lateral than the posterior end. The same orientation is characteristic for *Deccanolestes* and many crown placentals (Prasad and Godinot 1994; Horovitz 2000; Wible et al. 2009).

The calcaneofibular articulation is likely an ancestral trait for Theria (Horovitz 2000). According to Szalay and Sargis (2006), none of the therians from the Bissekty Formation has the calcaneofibular articulation. We did find a calcaneofibular facet on two calcanei referred to *Sulestes*. Among stem placentals and marsupials, the calcaneofibular facet is present in *Asioryctes*, *Deltatheridium*, *Pucadelphys*, and *Mayulestes* de Muizon, 1994, and absent in *Zalambdalestes* and *Deccanolestes* (Horovitz 2000; Wible et al. 2009). The condition of *Ukhaatherium* is uncertain. Among Bissekty eutherians the facet is absent in *Paranyctoides*, asioryctitherians, *Kulbeckia*, and zhelestids. It is variably developed in the crown group placentals (Asher et al. 2003; Wible et al. 2009).

The ventrally curved calcaneal tuber is likely an ancestral therian condition (Horovitz 2000). It is present in *Fruitafossor*, *Vincelestes*, *Deltatheridium*,

Asioryctes, *Ukhaatherium* (Horovitz 2000; Luo and Wible 2005), as well as in *Paranyctoides* and Bissekty asioryctitherians. The tuber calcanei is straight in *Mayulestes*, *Pucadelphys*, *Deccanolestes*, *Zalambdalestes*, *Kulbeckia*, and zhelestids, as well as in crown group marsupials and placentals (Horovitz 2000; Wible et al. 2009).

The calcaneal (anterior, distal) plantar tubercle is absent in *Asioryctes*, *Ukhaatherium*, *Zalambdalestes* (Horovitz 2000; Wible et al. 2009), and all Bissekty therians. It is present in stem placentals *Deccanolestes* and *Protungulatum* (Szalay and Decker 1974; Prasad and Godinot 1994), some stem and crown group marsupials and various crown group placentals. The phylogenetic significance of this character is unclear.

CONCLUSIONS

Isolated therian postcranial bones are abundant in screen-washing samples from the fluvial deposits of the late Turonian Bissekty Formation at Dzharakuduk, Uzbekistan. These bones are mostly fragmentary, but well preserved, which allows detailed morphological study.

Shaft and distal humerus fragments, as well astragalus and calcanei are referable to the deltatheroidan *Sulestes karakshi*. The humerus of this taxon has a large rectangular lateral epicondylar crest and large spherical capitulum. The astragalus lacks a pulley-shaped astragalar trochlea and has a short neck, which is as wide as the astragalar head. The calcaneus has a calcaneal lateral process and a calcaneofibular facet, as in other stem marsupials.

Fragments of distal humerus and femur, and one calcaneus are attributed to the stem placental *Paranyctoides quadrans*. The humerus has a spherical capitulum and groove separating capitulum and trochlea (zona conoidea), similar to that in arboreal euarchontans. The femur lacks a distinct patellar groove and has asymmetrical distal condyles, with flaring lateral side of the bone. These characters are also consistent with an arboreal mode of life for *Paranyctoides*. The calcaneus has a large distally projecting peroneal process and a sustentacular facet extending along the dorsal margin of calcaneocuboid facet.

Several distal humerus fragments and calcanei can be attributed to Zhelestidae. The humeri have no groove separating the trochlea and capitulum. These calcanei are characterized by straight, relatively short and massive tuber calcanei, larger peroneal process, and the calcaneocuboid process perpendicular to the long axis of the calcaneus. Two fragments of the scapula are referred to the zhelestid *Aspanlestes aptap* based on the size. All scapular fragments from the Bissekty Formation are similar in having the trough-like infraspinous fossa, which is placed medially relative to the supraspinous fossa. This is likely a plesiomorphic therian condition. One very large anterior caudal vertebra is referred to *Eoungulatum kudukensis*, the largest zhelestid in the fauna.

Fragments of the axis, distal humerus, distal femur, and several calcanei can be attributed to the Asioryctitheria. The axis has anterior articular surfaces of the centrum confluent with the articular surface of the dens. These articular surfaces are likely separate in the Zhelestidae. A very small ulna fragment is likely belonging to the smallest mammal in the fauna, asioryctitherian *Uchkudukodon nessovi*.

Most postcranial elements attributed to the Zhelestidae and Asioryctitheria show a plesiomorphic therian morphology, which is also present in some stem marsupials. In contrast, some postcranial elements referred to the zalambdalestid *Kulbeckia kulbecke*, have a more derived and specialized morphology. The distal humerus has a deep trochlea, large medial trochlear keel, and large capitular tail separated from a cylindrical capitulum by a shallow groove. The long and distally fused tibia and fibula indicate a cursorial mode of life. The upper ankle joint of *Kulbeckia* has the complete separation of medial and lateral astragalotibial articulations. This character might be also present in *Zalambdalestes*. The astragalar canal is present in *Kulbeckia* but lost in *Zalambdalestes*. The calcaneus has a cone-like calcaneoastragalar facet, long calcaneal tuber, and a large and nearly transversely oriented calcaneocuboid facet. The long calcaneal tuber is another evidence of cursorial specialization of *Kulbeckia*.

ACKNOWLEDGEMENTS

Fieldwork in Uzbekistan was facilitated by and conducted in cooperation with the Zoological Institute of the National Academy of Sciences of Uzbekistan, particularly D.A. Azimov and Y.A. Chikin. For their efforts in the field, scientific expertise, and camaraderie, we thank A.V. Abramov, G.O. Cherepanov, I.G. Danilov, S. Dominguez, C. King, N. Morris, C.M. Redman, A.S. Resvyi, C. Skrabec, P.P. Skutschas, E.V. Syromyatnikova, and D.J. Ward. The field work in 1997–2006 was funded by the National Science Foundation (EAR-9804771 and

EAR-0207004 to J.D. Archibald and H.-D. Sues), the National Geographic Society (#5901-97 and #6281-98 to J.D. Archibald and H.-D. Sues), and the Navoi Mining and Metallurgy Combinat. AA is grateful to H.-D. Sues for loan of the USNM specimens and to O. Makarova for the help with ZIN collection of extant mammals. AA was supported by the Zoological Institute, Russian Academy of Sciences (project AAAA-A17-117022810195-3) and the Russian Foundation for Basic Research (project 16-04-00294), and the Russian Scientific Fund (14-14-00015). The work is performed according to the Russian Government Program of Competitive Growth of Kazan Federal University. We thank two anonymous reviewers for reading the paper.

REFERENCES

Anyonge W. 1993. Body mass in large extant and extinct carnivores. *Journal of Zoology*, **231**: 339–350.

Archibald J.D. and Averianov A.O. 2001. *Paranyctoides* and allies from the Late Cretaceous of North America and Asia. *Acta Palaeontologica Polonica*, **46**: 533–551.

Archibald J.D. and Averianov A.O. 2003. The Late Cretaceous placental mammal *Kulbeckia*. *Journal of Vertebrate Paleontology*, **23**: 404–419.

Archibald J.D. and Averianov A.O. 2005a. Mammalian faunal succession in the Cretaceous of the Kyzylkum Desert. *Journal of Mammalian Evolution*, **12**: 9–22.

Archibald J.D. and Averianov A.O. 2006. Late Cretaceous asioryctitherian eutherian mammals from Uzbekistan and phylogenetic analysis of Asioryctitheria. *Acta Palaeontologica Polonica*, **51**: 351–376.

Archibald J.D. and Averianov A.O. 2012. Phylogenetic analysis, taxonomic revision, and dental ontogeny of the Cretaceous Zhelestidae (Mammalia: Eutheria). *Zoological Journal of the Linnean Society*, **164**: 361–426.

Archibald J.D., Sues H.-D., Averianov A.O., King C., Ward D.J., Tsaruk O.I., Danilov I.G., Rezvyi A.S., Veretennikov B.G. and Khodjaev A. 1998. Précis of the Cretaceous paleontology, biostratigraphy and sedimentology at Dzharakuduk (Turonian?-Santonian), Kyzylkum Desert, Uzbekistan. *Bulletin of the New Mexico Museum of Natural History and Science*, **14**: 21–28.

Argot C. 2003. Functional-adaptive anatomy of the axial skeleton of some extant marsupials and the paleobiology of the Paleocene marsupials *Mayulestes ferox* and *Pucadelphys andinus*. *Journal of Morphology*, **255**: 279–300.

Argot C. 2004. Evolution of South American mammalian predators (Borhyaenoidea): anatomical and palaeobiological implications. *Zoological Journal of the Linnean Society*, **140**: 487–521.

Asher R.J., Novacek M.J. and Geisler J.H. 2003. Relationships of endemic African mammals and their fossil relatives based on morphological and molecular evidence. *Journal of Mammalian Evolution*, **10**: 131–194.

Averianov A.O. and Archibald J.D. 2005. Mammals from the mid-Cretaceous Khodzhakul Formation, Kyzylkum Desert, Uzbekistan. *Cretaceous Research*, **26**: 593–608.

Averianov A.O. and Archibald J.D. 2006. New specimens of the multituberculate mammal *Uzbekbaatar* from the Late Cretaceous of Uzbekistan. *Acta Palaeontologica Polonica*, **51**: 377–380.

Averianov A.O. and Archibald J.D. 2013. New material and reinterpretation of the Late Cretaceous eutherian mammal *Paranyctoides* from Uzbekistan. *Acta Palaeontologica Polonica*, **58**: 17–23.

Averianov A.O. and Archibald J.D. 2016. New evidence on the stem placental mammal *Paranyctoides* from the Upper Cretaceous of Uzbekistan. *Palaeontologia Polonica*, **67**: 25–33.

Averianov A.O., Archibald J.D. and Ekdale E.G. 2010. New material of the Late Cretaceous deltatheroidan mammal *Sulestes* from Uzbekistan and phylogenetic reassessment of the metatherian-eutherian dichotomy. *Journal of Systematic Palaeontology*, **8**: 301–330.

Averianov A.O. and Sues H.-D. 2012. Correlation of Late Cretaceous continental vertebrate assemblages in Middle and Central Asia. *Journal of Stratigraphy*, **36**: 462–485.

Bi S., Wang Y., Guan J., Sheng X. and Meng J. 2014. Three new Jurassic euharamiyidan species reinforce early divergence of mammals. *Nature*, **514**: 579–584.

Bloch J.I., Rose K.D. and Gingerich P.D. 1998. New species of *Batodonoides* (Lipotyphla, Geolabididae) from the Early Eocene of Wyoming: smallest known mammal? *Journal of Mammalogy*, **79**: 804–827.

Boyer D.M., Prasad G.V.R., Krause D.W., Godinot M., Goswami A., Verma O. and Flynn J.J. 2010. New postcrania of *Deccanolestes* from the Late Cretaceous of India and their bearing on the evolutionary and biogeographic history of euarchontan mammals. *Naturwissenschaften*, **97**: 365–377.

Chen M. and Luo Z.-X. 2013. Postcranial skeleton of the Cretaceous mammal *Akidolestes cifellii* and its locomotor adaptations. *Journal of Mammalian Evolution*, **20**: 159–189.

Chester S.G.B., Sargis E.J., Szalay F.S., Archibald J.D. Averianov A.O. 2010. Mammalian distal humeri from the Late Cretaceous of Uzbekistan. *Acta Palaeontologica Polonica*, **55**: 199–211.

Chester S.G.B., Sargis E.J., Szalay F.S., Archibald J.D. and Averianov A.O. 2012. Therian femora from the Late Cretaceous of Uzbekistan. *Acta Palaeontologica Polonica*, **57**: 53–64.

Cifelli R.L. 1983. Eutherian tarsals from the late Paleocene of Brazil. *American Museum Novitates*, **2761**: 1–31.

Coillot T., Smith R., Gigase P. and Smith T. 2013. Tarsal diversity in the earliest Eocene mammal fauna of Dormaal, Belgium. *Geologica Belgica*, **16**: 274–283.

Conroy G.C. 1987. Problems of body-weight estimation of fossil primates. *International Journal of Primatology*, **8**: 115–137.

Evans H.E. 1993. Miller's Anatomy of the Dog. Third Edition. W. B. Saunders Company, Philadelphia. 1113 p.

Fostowicz-Frelik L. 2016. A new zalambdalestid (Eutheria) from the Late Cretaceous of Mongolia and its implications for the origin of Glires. *Palaeontologia Polonica*, **67**: 127–136.

Gambaryan P.P., Aristov A.A., Dixon J.M. and Zubtsova G.Y. 2002. Peculiarities of the hind limb musculature in monotremes: an anatomical description and functional approach. *Russian Journal of Theriology*, **1**: 1–36.

Gingerich P.D. 1974. Size variability of the teeth in living mammals and the diagnosis of closely related sympatric fossil species. *Journal of Paleontology*, **48**: 895–903.

Gingerich P.D. 1990. Prediction of body size in mammalian species from long bones lengths and diameters. *Contributions from the Museum of Paleontology, the University of Michigan*, **28**: 79–92.

Gingerich P.D. and Smith B.H. 1985. Allometric scaling in the dentition of primates and insectivores. In: W.L. Jungers (Ed.). Size and Scaling in Primate Biology. Plenum, New York: 257–272.

Gingerich P.D., Smith B.H. and Rosenberg K. 1982. Allometric scaling in the dentition of primates and prediction of body weight from tooth size in fossils. *American Journal of Physical Anthropology*, **58**: 81–100.

Gradstein F.M., Ogg J.G. and Smith A. 2004. A Geologic Time Scale 2004. Cambridge University Press, Cambridge, New York, Melbourne. 589 p.

Hooker J.J. 2014. New postcranial bones of the extinct mammalian family Nyctitheriidae (Paleogene, UK): Primitive euarchontans with scansorial locomotion. *Palaeontologia Electronica*, **17.3.47A**:1–82.

Horovitz I. 2000. The tarsus of *Ukhaatherium nessovi* (Eutheria, Mammalia) from the Late Cretaceous of Mongolia: an appraisal of the evolution of the ankle in basal therians. *Journal of Vertebrate Paleontology*, **20**: 547–560.

Horovitz I. 2003. Postcranial skeleton of *Ukhaatherium nessovi* (Eutheria, Mammalia) from the Late Cretaceous of Mongolia. *Journal of Vertebrate Paleontology*, **23**: 857–868.

Horovitz I., Ladevèze S., Argot C., Macrini T.E., Hooker J.J., Kurz C., de Muizon C. and Sánchez-Villagra M. 2008. The anatomy of *Herpetotherium* cf. *fugax* Cope, 1873, a metatherian from the Oligocene of North America. *Palaeontographica Abteilung A*, **284**: 109–141.

Horovitz I. and Sánchez-Villagra M.R. 2003. A morphological analysis of marsupial mammal higher-level phylogenetic relationships. *Cladistics*, **19**: 181–212.

Hu. Y., Wang Y., Luo Z.-X. and Li C. 1997. A new symmetrodont mammal from China and its implications for mammalian evolution. *Nature*, **390**: 137–142.

Jenkins F.A., Jr. 1969. The evolution and development of the dens of the mammalian axis. *Anatomical Record*, **164**: 173–184.

Jenkins F.A., Jr. and Parrington F.R. 1976. The postcranial skeletons of the Triassic mammals *Eozostrodon*, *Megazostrodon* and *Erythrotherium*. *Philosophical Transactions of the Royal Society of London Series B, Biological Sciences*, **273**: 387–431.

Ji Q., Luo Z.-X. and Ji S.-A. 1999. A Chinese triconodont mammal and mosaic evolution of mammalian skeleton. *Nature*, **398**: 326–330.

Ji Q., Luo Z.-X., Yuan C.-X. and Tabrum A.R. 2006. A swimming mammaliaform from the Middle Jurassic and ecomorphological diversification of early mammals. *Science*, **311**: 1123–1127.

Ji Q., Luo Z.-X., Yuan C.-X., Wible J.R., Zhang J.-P. and Georg J.A. 2002. The earliest known eutherian mammal. *Nature*, **416**: 816–822.

Ji Q., Luo Z.-X., Zhang X., Yuan C.-X. and Xu L. 2009. Evolutionary development of the middle ear in Mesozoic therian mammals. *Science*, **326**: 278–281.

Kielan-Jaworowska Z. 1977. Evolution of the therian mammals in the Late Cretaceous of Asia. Part II. Postcranial skeleton in *Kennalestes* and *Asioryctes*. *Palaeontologia Polonica*, **37**: 65–83.

Kielan-Jaworowska Z. 1978. Evolution of the therian mammals in the Late Cretaceous of Asia. Part III. Postcranial skeleton in Zalambdalestidae. *Palaeontologia Polonica*, **38**: 5–41.

Kielan-Jaworowska Z., Cifelli R.L. and Luo Z.-X. 2004. Mammals from the Age of Dinosaurs: Origins, Evolution, and Structure. Columbia University Press, New York, 630 p.

Kielan-Jaworowska Z. and Gambaryan P.P. 1994. Postcranial anatomy and habits of Asian multituberculate mammals. *Fossils and Strata*, **36**: 1–92.

Kielan-Jaworowska Z. and Nesov L.A. 1992. Multituberculate mammals from the Cretaceous of Uzbekistan. *Acta Palaeontologica Polonica*, **37**: 1–17.

Krebs B. 1991. Das Skelett von *Henkelotherium guimarotae* gen. et sp. nov. (Eupantotheria, Mammalia) aus dem Oberen Jura von Portugal. *Berliner geowissenschaftliche Abhandlungen, Reihe A: Geologie und Palaeontologie*, **133**: 1–121.

Kristoffersson R. 1971. A note on the age distribution of hedgehogs in Finland. *Annales Zoologici Fennici*, **8**: 554–557.

Lessertisseur J. and Saban R. 1967. Squelette axial. In: P.-P. Grassé (Ed.). Traité de Zoologie. Anatomie, Systématique, Biologie. Tome XVI. Mammifères. Fascicule I: Téguments et Squelette. Maison et Cie, Paris: 584–708.

Li G. and Luo Z.-X. 2006. A Cretaceous symmetrodont therian with some monotreme-like postcranial features. *Nature*, **439**: 195–200.

Luo Z.-X. 2015. Origin of the mammalian shoulder. In: K.P. Dial, N.H. Shubin and E.L. Brainerd (Eds.). Great Transformations: Major Events in the History of Vertebrate Life. The University of Chicago Press, Chicago, London: 167–187.

Luo Z.-X., Chen P., Li G. and Chen M. 2007a. A new eutriconodont mammal and evolutionary development in early mammals. *Nature*, **446**: 288–293.

Luo Z.-X. and Ji Q. 2005. New study on dental and skeletal features of the Cretaceous "symmetrodontan" mammal *Zhangheotherium*. *Journal of Mammalian Evolution*, **12**: 337–357.

Luo Z.-X., Ji Q., Wible J.R. and Yuan C.-X. 2003. An Early Cretaceous tribosphenic mammal and metatherian evolution. *Science*, **302**:1934–1940.

Luo Z.-X., Ji Q. and Yuan C.-X. 2007b. Convergent dental adaptations in pseudo-tribosphenic and tribosphenic mammals. *Nature*, **450**: 93–97.

Luo Z.-X., Meng Q.-J., Ji Q., Liu D., Zhang Y.-G. and Neander A.I. 2015. Evolutionary development in basal mammaliaforms as revealed by a docodontan. *Science*, **347**: 760–764.

Luo Z.-X. and Wible J.R. 2005. A Late Jurassic digging mammal and early mammalian diversification. *Science*, **308**: 103–107.

Luo Z.-X., Yuan C.-X., Meng Q.-J. and Ji Q. 2011. A Jurassic eutherian mammal and divergence of marsupials and placentals. *Nature*, **476**: 442–445.

Marshall L.G. and Sigogneau-Russell D. 1995. Part III. Postcranial skeleton. In: C. de Muizon (Ed.). *Pucadelphys andinus* (Marsupialia, Mammalia) from the early Paleocene of Bolivia (*Memoire du Museum National d'Histoire Naturelle*, **165**): 91–164.

Millien V. and Bovy H. 2010. When teeth and bones disagree: body mass estimation of a giant extinct rodent. *Journal of Mammalogy*, **91**: 11–18.

Moncunill-Solé B., Quintana J., Jordana X., Engelbrektsson P. and Köhler M. 2015. The weight of fossil leporids and ochotonids: body mass estimation models for the order Lagomorpha. *Journal of Zoology*, **295**: 269–278.

Muizon C., de, Billet G., Argot C., Ladevéze S. and Goussard F. 2015. *Alcidedorbignya inopinata*, a basal pantodont (Placentalia, Mammalia) from the early Palaeocene of Bolivia: anatomy, phylogeny and palaeobiology. *Geodiversitas*, **37**: 397–634.

Narita Y. and Kuratani S. 2005. Evolution of the vertebral formulae in mammals: a perspective on developmental constraints. *Journal of Experimental Zoology Part B: Molecular and Developmental Evolution*, **304**: 91–106.

Nesov L.A. 1982. The most ancient mammals of the USSR. *Ezhegodnik Vsesoyuznogo Paleontologicheskogo Obshchestva*, **25**: 228–242. [In Russian].

Nesov L.A. 1985. New mammals from the Cretaceous of Kyzylkum. *Vestnik Leningradskogo Universiteta, Seriya 7*, **17**: 8–18. [In Russian].

Nesov L.A. 1987. Results of search and study of Cretaceous and early Paleogene mammals on the territory of the USSR. *Ezhegodnik Vsesoyuznogo Paleontologicheskogo Obshchestva*, **30**: 199–218. [In Russian].

Nesov L.A., Archibald J.D. and Kielan-Jaworowska Z. 1998. Ungulate-like mammals from the Late Cretaceous of Uzbekistan and a phylogenetic analysis of Ungulatomorpha. *Bulletin of the Carnegie Museum of Natural History*, **34**: 40–88.

Nesov L.A., Sigogneau-Russell D. and Russell D.E. 1994. A survey of Cretaceous tribosphenic mammals from Middle Asia (Uzbekistan, Kazakhstan and Tajikistan), of their geological setting, age and faunal environment. *Palaeovertebrata*, **23**: 51–92.

O'Leary M.A., Bloch J.I., Flynn J.J., Gaudin T.J., Giallombardo A., Giannini N.P., Goldberg S.L., Kraatz B.P., Luo Z.-X., Meng J., Ni X., Novacek M.J., Perini F.A., Randall Z.S., Rougier G.W., Sargis E.J., Silcox M.T., Simmons N.B., Spaulding M., Velazco P.M., Weksler M., Wible J.R. and Cirranello A.L. 2013. The placental mammal ancestor and the post–K-Pg radiation of placentals. *Science*, **339**: 662–667.

Penkrot T.A. and Zack S.P. 2016. Tarsals of Sespedectinae (?Lipotyphla) from the middle Eocene of southern California, and the affinities of Eocene 'erinaceomorphs'. *Journal of Vertebrate Paleontology*, **36**: e1212059.

Prasad G.V.R. and Godinot M. 1994. Eutherian tarsals from the Late Cretaceous of India. *Journal of Paleontology*, **68**: 892–902.

Redman C.M. and Leighton L.R. 2009. Multivariate faunal analysis of the Turonian Bissekty Formation: Variation in the degree of marine influence in temporally and spatially averaged fossil assemblages. *Palaios*, **24**: 18–26.

Samuels M.E., Regnault S. and Hutchinson J.R. 2017. Evolution of the patellar sesamoid bone in mammals. *PeerJ*, **5**: e3103.

Scott K.M. 1990. Postcranial dimensions of ungulates as predictors of body mass. In: J. Damuth and B.J. MacFadden (Eds.). Body Size in Mammalian Paleobiology: Estimation and Biological Implications. Cambridge University Press, Cambridge: 301–336.

Sereno P.C. 2006. Shoulder girdle and forelimb in multituberculates: Evolution of parasagittal forelimb posture in mammals. In: M.T. Carrano, R.W. Blob, T.J. Gaudin and J.R. Wible (Eds.). Amniote Paleobiology: Perspectives on the Evolution of Mammals, Birds, and Reptiles. University of Chicago Press, Chicago: 315–365.

Shoshani J. and McKenna M.C. 1998. Higher taxonomic relationships among extant mammals based on morphology, with selected comparisons of results from

molecular data. *Molecular Phylogenetics and Evolution*, **9**: 572–584.

Slijper E.J. 1946. Comparative biologic-anatomical investigations on the vertebral column and spinal musculature of mammals. *Verhandelingen der Koninklijke Nederlandse Akademie van Wetenschappen, Afdeling Natuurkunde Tweede sectie*, **42**: 1–128.

Smith T., De Bast E. and Sigé B. 2010. Euarchontan affinity of Paleocene Afro-European adapisoriculid mammals and their origin in the late Cretaceous Deccan Traps of India. *Naturwissenschaften*, **97**: 417–422.

Szalay F.S. 1993. Pedal evolution of mammals in the Mesozoic: tests for taxic relationships. In: F.S. Szalay, M.J. Novacek and M.C. McKenna (Eds.). Mammal Phylogeny: Mesozoic Differentiation, Multituberculates, Monotremes, Early Therians, and Marsupials. Springer Verlag, New York: 233–359.

Szalay F.S. 1994. Evolutionary History of the Marsupials and an Analysis of Osteological Characters. Cambridge University Press, Cambridge, 481 p.

Szalay F.S. and Decker R.L. 1974. Origin, evolution, and function of the tarsus in Late Cretaceous Eutheria and Paleocene Primates. In: F.A. Jenkins, Jr. (Ed.). Primate Locomotion. Academic Press, London: 223–259.

Szalay F.S. and Sargis E.J. 2001. Model-based analysis of postcranial osteology of marsupials from the Palaeocene of Itaboraí (Brazil) and the phylogenetics and biogeography of Metatheria. *Geodiversitas*, **23**: 139–302.

Szalay F.S. and Sargis E.J. 2006. Cretaceous therian tarsals and the metatherian-eutherian dichotomy. *Journal of Mammalian Evolution*, **13**: 171–210.

Szalay F.S. and Trofimov B.A. 1996. The Mongolian Late Cretaceous *Asiatherium*, and the early phylogeny and paleobiologeography of Metatheria. *Journal of Vertebrate Paleontology*, **16**: 474–509.

Wible J.R., Rougier G.W., Novacek M.J. and Asher R.J. 2009. The eutherian mammal *Maelestes gobiensis* from the Late Cretaceous of Mongolia and the phylogeny of Cretaceous Eutheria. *Bulletin of the American Museum of Natural History*, **327**: 1–123.

Yuan C.-X., Ji Q., Meng Q.-J., Tabrum A.R. and Luo Z.-X. 2013. Earliest evolution of multituberculate mammals revealed by a new Jurassic fossil. *Science*, **341**: 779–783.

Zheng X., Bi S., Wang X. and Meng J. 2013. A new arboreal haramiyid shows the diversity of crown mammals in the Jurassic period. *Nature*, **500**: 199–202.

Zhou C.-F., Wu S., Martin T. and Luo Z.-X. 2013. A Jurassic mammaliaform and the earliest mammalian evolutionary adaptations. *Nature*, **500**: 163–167.

Submitted October 6, 2017; accepted November 17, 2017.

Supplementary Table 1. List of postcranial mammal specimens in the USNM and ZIN collections.

Collection number	URBAC	Site	Identification	Material
USNM 590598	03-068	CBI-14	Eutheria indet.	anterior caudal vertebra
USNM 594513	04-035	CBI-14	Eutheria indet.	thoracic vertebra
USNM 594518	04-044	CBI-14	Eutheria indet.	thoracic vertebra
USNM 594520	04-026	CBI-14	Eutheria indet.	atlas fragment
USNM 594554	04-056	CBI-14	Eutheria indet.	axis fragment
USNM 594567	03-084	CBI-14	Eutheria indet.	anterior caudal vertebra
USNM 594579	03-138	CBI-14	Eutheria indet.	thoracic vertebra
USNM 594587	03-077	CBI-14	Eutheria indet.	atlas fragment
USNM 594690	04-207	CBI-14	Eutheria indet.	thoracic vertebra
USNM 594693	04-360	CBI-14	Eutheria indet.	left proximal ulna
USNM 594696		CBI-14	Eutheria indet.	right ischium fragment
USNM 594713	06-091	CBI-4e	Eutheria indet.	atlas fragment
USNM 594719	06-102	CBI-14	Eutheria indet.	posterior caudal vertebra
USNM 594720	06-015	CBI-14	Eutheria indet.	posterior caudal vertebra
USNM 605212	06-052	CBI-17	Eutheria indet.	thoracic vertebra
USNM 642630	06-028	CBI-17	*Aspanlestes aptap*	left scapula fragment
USNM 642631	06-115	CBI-4e	Eutheria indet.	right scapula fragment
USNM 642632	04-112	CBI-14	Eutheria indet.	left scapula fragment
USNM 642633	04-183	CBI-14	*Kulbeckia kulbecke*	right scapula fragment
USNM 642634	02-079	CBI-4e	Eutheria indet.	left scapula fragment
USNM 642635	02-002	CBI-4e	Eutheria indet.	posterior caudal vertebra
USNM 642636	02-016	CBI-4e	Eutheria indet.	posterior caudal vertebra
USNM 642637	02-089	CBI-4e	Eutheria indet.	anterior caudal vertebra
USNM 642638	02-098	CBI-4e	Eutheria indet.	anterior caudal vertebra
USNM 642639	03-080	CBI-14	Eutheria indet.	posterior caudal vertebra
USNM 642640	03-135	CBI-14	Eutheria indet.	posterior caudal vertebra
USNM 642641	1997.P9	CBI-14	*Eoungulatum kudukensis*	anterior caudal vertebra
USNM 642642	03-096	CBI-14	*Paranyctoides quadrans*	right femur distal fragment
USNM 642643	00-018	CBI-14	Asioryctitheria indet.	right femur distal fragment
USNM 642644	04-095	CBI-14	*Kulbeckia kulbecke*	left femur distal fragment
USNM 642645	02-052	CBI-4e	Eutheria indet.	right femur proximal fragment
USNM 642646	04-052	CBI-14	*Kulbeckia kulbecke*	right femur proximal fragment
USNM 642647	03-092	CBI-14	Asioryctitheria indet.	right femur distal fragment
USNM 642648	03-055	CBI-14	Eutheria indet.	right humerus proximal fragment
USNM 642649	03-109	CBI-14	Eutheria indet.	left humerus distal fragment
USNM 642650	03-126	CBI-14	Eutheria indet.	left humerus distal fragment
USNM 642651	04-001	CBI-14	Eutheria indet.	left humerus distal fragment

Supplementary Table 1. *Continued.*

Collection number	URBAC	Site	Identification	Material
USNM 642652	04-030	CBI-14	*Kulbeckia kulbecke*	right humerus distal fragment
USNM 642653	04-062	CBI-14	*Sulestes karakshi*	right humerus shaft fragment
USNM 642654	04-174	CBI-14	Eutheria indet.	right humerus proximal fragment
USNM 642655	06-048	CBI-4e	Zhelestidae indet.	left humerus shaft fragment
USNM 642656	02-075		*Paranyctoides quadrans*	right humerus distal fragment
USNM 642657	04-002	CBI-14	*Paranyctoides quadrans*	left humerus distal fragment
USNM 642658	06-103		*Sulestes karakshi*	right humerus distal fragment
USNM 642659	06-062		Asioryctitheria indet.	right humerus distal fragment
USNM 642660	06-057		Zhelestidae indet.	right humerus distal fragment
USNM 642661	97-P04	CBI-14	Zhelestidae indet.	right humerus distal fragment
USNM 642662	03-187		Zhelestidae indet.	right humerus distal fragment
USNM 642663	97-P07	CBI-14	Zhelestidae indet.	left humerus distal fragment
USNM 642664	03-099	CBI-14	Zhelestidae indet.	left humerus distal fragment
USNM 642665	06-072	CBI-4e	Zhelestidae indet.	right humerus distal fragment
USNM 642666	03-126	CBI-14	Zhelestidae indet.	left humerus distal fragment
USNM 642667	00-072		Zhelestidae indet.	right humerus distal fragment
USNM 642668	98-P08	CBI-14	Zhelestidae indet.	left humerus distal fragment
USNM 642669	04-018	CBI-14	Eutheria indet.	left ischium fragment
USNM 642670	04-231	CBI-4e	Eutheria indet.	right ischium fragment
USNM 642671	1998.P4	CBI-14	Eutheria indet.	lumbar vertebra
USNM 642672	00-005	CBI-14	Eutheria indet.	cervical vertebra
USNM 642673	1998.P1	CBI-14	Eutheria indet.	cervical vertebra
USNM 642674	1999.P7	CBI-14	Eutheria indet.	cervical vertebra
USNM 642675	1998.P15	CBI-14	*Kulbeckia kulbecke*	right astragalus
USNM 642676	1999.P17	CBI-14	*Kulbeckia kulbecke*	left astragalus
USNM 642677	00-047	CBI-14	Zhelestidae indet.	right calcaneus
USNM 642678	00-067	CBI-14	Zhelestidae indet.	left calcaneus
USNM 642679	00-P37	CBI-4e	Zhelestidae indet.	left calcaneus
USNM 642680	00-P59	CBI-14	Zhelestidae indet.	left calcaneus
USNM 642681	00-P67	CBI-14	*Kulbeckia kulbecke*	right calcaneus
USNM 642682	02-046	CBI-4e	Asioryctitheria indet.	left calcaneus
USNM 642683	02-054	CBI-4e	Zhelestidae indet.	right calcaneus
USNM 642684	02-097	CBI-4e	Zhelestidae indet.	right calcaneus
USNM 642685	03-097	CBI-14	Sulestes karakshi	right calcaneus
USNM 642686	03-130	CBI-14	Asioryctitheria indet.	right calcaneus
USNM 642687	04-064	CBI-14	*Sulestes karakshi*	right astragalus

Supplementary Table 1. *Continued.*

Collection number	URBAC	Site	Identification	Material
USNM 642688	04-087	CBI-14	Asioryctitheria indet.	left calcaneus
USNM 642689	04-P10		*Sulestes karakshi*	right calcaneus
USNM 642690	04-P85		Zhelestidae indet.	left calcaneus
USNM 642691	04-P86		Zhelestidae indet.	left calcaneus
USNM 642692	04-P87		Asioryctitheria indet.	left calcaneus
USNM 642693	04-P117		*Paranyctoides quadrans*	right calcaneus
USNM 642694	04-P117		Zhelestidae indet.	right calcaneus
USNM 642695	04-P178		Zhelestidae indet.	left calcaneus
USNM 642696	06-011	CBI-14	Zhelestidae indet.	left calcaneus
USNM 642697	06-029	CBI-17	Zhelestidae indet.	right calcaneus
USNM 642698	06-095	CBI-4e	Zhelestidae indet.	left calcaneus
USNM 642699	1999.P8	CBI-14	Zhelestidae indet.	right calcaneus
USNM 642700	03-015	CBI-14	Eutheria indet.	thoracic vertebra
USNM 642702	1997.P8	CBI-14	*Kulbeckia kulbecke*	right distal tibia-fibula
USNM 642703	00-013		Eutheria indet.	femur distal fragment
ZIN 82557		CBI-14	Eutheria indet.	thoracic vertebra
ZIN 82559		CBI-14	Eutheria indet.	left proximal tibia
ZIN 82564		CBI-14	Eutheria indet.	thoracic vertebra
ZIN 85305			*Sulestes karakshi*	left distal humerus
ZIN 85309			*Kulbeckia kulbecke*	left distal humerus
ZIN 85321			Eutheria indet.	right proximal femur
ZIN 85322			Eutheria indet.	right proximal femur
ZIN 85324			Eutheria indet.	left proximal femur
ZIN 85325			Eutheria indet.	right proximal femur
ZIN 85327			*Kulbeckia kulbecke*	right distal femur
ZIN 85344		CBI-14	Zhelestidae indet.	left calcaneus
ZIN 88865		CBI-4b	Eutheria indet.	posterior caudal vertebra
ZIN 88876		CBI-14	Eutheria indet.	right humerus shaft fragment
ZIN 88878		CBI-14	Eutheria indet.	lumbar vertebra
ZIN 88889		CBI-14	Zhelestidae indet.	left calcaneus
ZIN 88890		CBI-14	Zhelestidae indet.	right calcaneus
ZIN 88902		CBI-4a	Asioryctitheria indet.	right calcaneus
ZIN 88903		CBI-14	Eutheria indet.	posterior caudal vertebra
ZIN 88904		CBI-14	Eutheria indet.	posterior caudal vertebra
ZIN 88905		CBI-5a	Eutheria indet.	anterior caudal vertebra
ZIN 88910		CBI-5a	Eutheria indet.	anterior caudal vertebra

Supplementary Table 1. *Continued.*

Collection number	URBAC	Site	Identification	Material
ZIN 88916		CBI-14	Eutheria indet.	right humerus shaft fragment
ZIN 88917		CBI-56	Eutheria indet.	atlas fragment
ZIN 88925		CBI-14	Eutheria indet.	cervical vertebra
ZIN 97885			*Kulbeckia kulbecke*	proximal femur
ZIN 97886			Eutheria indet.	right proximal femur
ZIN 103866		CBI-4b	Eutheria indet.	left scapula
ZIN 103867		CBI-14	*Aspanlestes aptap*	right scapula
ZIN 103868		CBI-14	Eutheria indet.	left scapula
ZIN 103869		CBI-14	Eutheria indet.	right scapula
ZIN 103870		CBI-14	Eutheria indet.	right scapula
ZIN 103871		CBI-14	Eutheria indet.	atlas fragment
ZIN 103872		CBI-5a	Eutheria indet.	des scapula
ZIN 103873		CBI-	Eutheria indet.	atlas fragment
ZIN 103874		CBI-5a	Eutheria indet.	thoracic vertebra
ZIN 103875		CBI-14	Eutheria indet.	thoracic vertebra
ZIN 103876		CBI-14	Eutheria indet.	thoracolumbar neural arch
ZIN 103877		CBI-14	Eutheria indet.	anterior caudal vertebra
ZIN 103878		CBI-17	Eutheria indet.	posterior caudal vertebra
ZIN 103879		CBI-14	Eutheria indet.	posterior caudal vertebra
ZIN 103880		CBI-14	Eutheria indet.	right proximal tibia
ZIN 103881		CBI-14	*Kulbeckia kulbecke*	right distal tibia
ZIN 103882		CBI-14	Eutheria indet.	right proximal radius
ZIN 103883		CBI-14	Eutheria indet.	right proximal ulna
ZIN 103884		CBI-4a	*Uchkudukodon nessovi*	left ulna proximal
ZIN 103885		CBI-14	Eutheria indet.	right ilium
ZIN 103886		CBI-52	Eutheria indet.	right ilium
ZIN 103887		CBI-7b	Eutheria indet.	right ilium
ZIN 103888		CBI-14	Eutheria indet.	left ilium
ZIN 103889		CBI-14	Eutheria indet.	left ilium
ZIN 103890		CBI-4b	Eutheria indet.	left ischium
ZIN 103891		CBI-14	Eutheria indet.	right femur proximal
ZIN 103892		CBI-14	Eutheria indet.	left femur proximal
ZIN 103893		CBI-14	Eutheria indet.	left femur proximal
ZIN 103894		CBI-4	Eutheria indet.	right femur proximal
ZIN 103895		CBI-14	Zhelestidae indet.	left calcaneus
ZIN 104110		CBI-14	Zhelestidae indet.	right calcaneus
ZIN 104111		CBI-14	Zhelestidae indet.	left calcaneus

Supplementary Table 1. *Continued.*

Collection number	URBAC	Site	Identification	Material
ZIN 104112		CBI-14	Zhelestidae indet.	left calcaneus
ZIN 104113		SSHD-8	Zhelestidae indet.	right calcaneus
ZIN 104118		CBI-14	Eutheria indet.	atlas fragment
ZIN 104119		CBI-14	Eutheria indet.	atlas fragment
ZIN 104120		CBI-14	Asioryctitheria indet.	axis fragment
ZIN 104121		CBI-14	Eutheria indet.	left calcaneus
ZIN 104122		CBI-14	Eutheria indet.	left radius proximal
ZIN 104123		CBI-14	Eutheria indet.	left radius proximal
ZIN 104124		CBI-14	Eutheria indet.	left radius proximal

Supplementary Table 2. Body mass estimation based on equation from Bloch et al. (1988).

Taxon	Specimen	Lm1. mm	Wm1. mm	X (Lm1 x Wm1)	lnX	lnY	Y (body mass. g)	Reference	Com-ments
Sulestes karakshi	URBAC 03-009	2.3	1.5	3.45	1.2384	3.7421	42.19	Averianov et al. 2010	m2
Sulestes karakshi	URBAC 04-344	2.3	1.6	3.68	1.3029	3.8471	46.86	Averianov et al. 2010	m2
Sulestes karakshi	URBAC 06-005	2.4	1.5	3.6	1.2809	3.8113	45.21	Averianov et al. 2010	m2
Sulestes karakshi	URBAC 00-001	2.5	1.8	4.5	1.5041	4.1746	65.02	Averianov et al. 2010	m2
Sulestes karakshi	CCMGE 5/12455	2.6	1.7	4.42	1.4861	4.1454	63.15	Averianov et al. 2010	m2
Sulestes karakshi	URBAC 03-194	2.6	1.7	4.42	1.4861	4.1454	63.15	Averianov et al. 2010	m2
Paranyctoides quadrans	URBAC 03-215	1.6	0.8	1.28	0.2469	2.1279	8.4	Averianov and Archibald 2013	m1 or m2
Daulestes kulbeckensis	CCMGE 1/11758	1.3	0.91	1.183	0.1681	2	7.39	Archibald and Averianov 2006	
Daulestes kulbeckensis	URBAC 03-085	1.17	0.9	1.053	0.0516	1.81	6.11	Archibald and Averianov 2006	
Daulestes inobservabilis	URBAC 03-088	1.34	0.94	1.2596	0.2308	2.1017	8.18	Archibald and Averianov 2006	
Bulaklestes kezbe	URBAC 98-141	1.67	1.1	1.837	0.6081	2.716	15.12	Archibald and Averianov 2006	
Bulaklestes kezbe	URBAC 98-132	1.55	1.14	1.767	0.5693	2.6528	14.19	Archibald and Averianov 2006	
Bulaklestes kezbe	URBAC 03-142	1.49	1.06	1.5794	0.4571	2.4701	11.82	Archibald and Averianov 2006	
Uchkudukodon nessovi	ZIN 79066	1.21	0.84	1.0164	0.0163	1.7525	5.77	Archibald and Averianov 2006	left
Uchkudukodon nessovi	ZIN 79066	1.12	0.85	0.952	-0.0492	1.6459	5.19	Archibald and Averianov 2006	right
Aspanlestes aptap	CCMGE 4/12176	2.06	1.63	3.3578	1.2113	3.698	40.37	Archibald and Averianov 2012	
Aspanlestes aptap	URBAC 04-134	2.36	1.59	3.7524	1.3224	3.8789	48.37	Archibald and Averianov 2012	
Aspanlestes aptap	CCMGE 13/12953	2.27	1.61	3.6547	1.296	3.8359	46.34	Archibald and Averianov 2012	
Aspanlestes aptap	URBAC 06-100	2.19	1.57	3.4383	1.235	3.7365	41.92	Archibald and Averianov 2012	
Aspanlestes aptap	URBAC 98-148	1.92	1.41	2.7072	0.9959	3.4374	28.43	Archibald and Averianov 2012	
Aspanlestes aptap	URBAC 04-197	2.27	1.62	3.6774	1.3022	3.846	46.81	Archibald and Averianov 2012	
Aspanlestes aptap	URBAC 99-032	2.22	1.59	3.5298	1.2612	3.7793	43.79	Archibald and Averianov 2012	

Supplementary Table 2. *Continued.*

Taxon	Specimen	Lm1. mm	Wm1. mm	X (Lm1 x Wm1)	lnX	lnY	Y (body mass. g)	Reference	Com-ments
Aspanlestes aptap	URBAC 98-147	2.28	1.64	3.7392	1.3189	3.8731	48.09	Archibald and Averianov 2012	
Parazhelestes mynbulakensis	URBAC 04-402	2.45	1.72	4.214	1.4384	4.0677	58.42	Archibald and Averianov 2012	
Parazhelestes mynbulakensis	URBAC 04-399	2.46	1.95	4.797	1.568	4.2787	72.15	Archibald and Averianov 2012	
Parazhelestes mynbulakensis	URBAC 04-398	2.34	1.77	4.1418	1.4211	4.0396	56.8	Archibald and Averianov 2012	
Parazhelestes mynbulakensis	URBAC 04-227	2.39	1.63	3.8957	1.3599	3.9399	51.42	Archibald and Averianov 2012	
Parazhelestes mynbulakensis	URBAC 03-211	2.39	1.61	3.8479	1.3475	3.9198	50.39	Archibald and Averianov 2012	
Parazhelestes mynbulakensis	URBAC 00-080	2.25	1.69	3.8025	1.3357	3.9005	49.43	Archibald and Averianov 2012	
Parazhelestes mynbulakensis	URBAC 99-109	2.37	2	4.74	1.556	4.2592	70.76	Archibald and Averianov 2012	
Parazhelestes mynbulakensis	URBAC 98-013	2.41	1.87	4.5067	1.5056	4.1771	65.17	Archibald and Averianov 2012	
Zhelestes temirkazyk	URBAC 03-189	2.6	1.94	5.044	1.6182	4.3604	78.29	Archibald and Averianov 2012	
Zhelestes temirkazyk	CCMGE 14/12953	2.6	1.92	4.992	1.6078	4.3436	76.98	Archibald and Averianov 2012	
Zhelestes temirkazyk	URBAC 06-031	2.28	1.58	3.6024	1.2816	3.8125	45.26	Archibald and Averianov 2012	
Zhelestes temirkazyk	URBAC 04-190	2.41	1.61	3.8801	1.3559	3.9333	51.07	Archibald and Averianov 2012	
Zhelestes temirkazyk	URBAC 04-310	2.41	1.73	4.1693	1.4278	4.0504	57.42	Archibald and Averianov 2012	
Zhelestes temirkazyk	CCMGE 37/12000	2.33	1.57	3.6581	1.2969	3.8374	46.41	Archibald and Averianov 2012	
Eoungulatum kudukensis	CCMGE 17/12953	2.73	2.18	5.9514	1.7836	4.6297	102.49	Archibald and Averianov 2012	
Kulbeckia kulbecke	URBAC 00-052	2.1	1.6	3.36	1.2119	3.699	40.41	Archibald and Averianov 2003	
Kulbeckia kulbecke	URBAC 98-002	1.8	1.4	2.52	0.9243	3.2307	25.3	Archibald and Averianov 2003	
Kulbeckia kulbecke	URBAC 00-009	1.9	1.7	3.23	1.1724	3.6348	37.89	Archibald and Averianov 2003	
Kulbeckia kulbecke	CCMGE 60/12455	1.7	1.3	2.21	0.793	3.017	20.43	Archibald and Averianov 2003	
Kulbeckia kulbecke	CCMGE 102/12455	1.8	1.3	2.34	0.8502	3.11	22.42	Archibald and Averianov 2003	
Kulbeckia kulbecke	URBAC 98-001	1.9	1.5	2.85	1.0473	3.431	30.91	Archibald and Averianov 2003	
Kulbeckia kulbecke	URBAC 99-064	1.9	1.5	2.85	1.0473	3.431	30.91	Archibald and Averianov 2003	

Supplementary Table 3. Body mass estimation based on equation from Conroy (1987).

Taxon	Specimen	Lm1. mm	Wm1. mm	X (Lm1 x Wm1)	lnX	lnY	Y (body mass. g)	Reference	Com-ments
Sulestes karakshi	URBAC 03-009	2.3	1.5	3.45	1.2384	4.7493	115.51	Averianov et al. 2010	m2
Sulestes karakshi	URBAC 04-344	2.3	1.6	3.68	1.3029	4.8644	129.59	Averianov et al. 2010	m2
Sulestes karakshi	URBAC 06-005	2.4	1.5	3.6	1.2809	4.8251	124.6	Averianov et al. 2010	m2
Sulestes karakshi	URBAC 00-001	2.5	1.8	4.5	1.5041	5.2233	185.55	Averianov et al. 2010	m2
Sulestes karakshi	CCMGE 5/12455	2.6	1.7	4.42	1.4861	5.1912	179.69	Averianov et al. 2010	m2
Sulestes karakshi	URBAC 03-194	2.6	1.7	4.42	1.4861	5.1912	179.69	Averianov et al. 2010	m2
Paranyctoides quadrans	URBAC 03-215	1.6	0.8	1.28	0.2469	2.9805	19.7	Averianov and Archibald 2013	m1 or m2
Daulestes kulbeckensis	CCMGE 1/11758	1.3	0.91	1.183	0.1681	2.8399	17.11	Archibald and Averianov 2006	
Daulestes kulbeckensis	URBAC 03-085	1.17	0.9	1.053	0.0516	2.6321	13.9	Archibald and Averianov 2006	
Daulestes inobservabilis	URBAC 03-088	1.34	0.94	1.2596	0.2308	2.9517	19.14	Archibald and Averianov 2006	
Bulaklestes kezbe	URBAC 98-141	1.67	1.1	1.837	0.6081	3.6249	37.52	Archibald and Averianov 2006	
Bulaklestes kezbe	URBAC 98-132	1.55	1.14	1.767	0.5693	3.5556	35	Archibald and Averianov 2006	
Bulaklestes kezbe	URBAC 03-142	1.49	1.06	1.5794	0.4571	3.3555	28.66	Archibald and Averianov 2006	
Uchkudukodon nessovi	ZIN 79066	1.21	0.84	1.0164	0.0163	2.5691	13.05	Archibald and Averianov 2006	left
Uchkudukodon nessovi	ZIN 79066	1.12	0.85	0.952	-0.0492	2.4522	11.61	Archibald and Averianov 2006	right
Aspanlestes aptap	CCMGE 4/12176	2.06	1.63	3.3578	1.2113	4.701	110.05	Archibald and Averianov 2012	
Aspanlestes aptap	URBAC 04-134	2.36	1.59	3.7524	1.3224	4.8992	134.18	Archibald and Averianov 2012	
Aspanlestes aptap	CCMGE 13/12953	2.27	1.61	3.6547	1.296	4.8521	128	Archibald and Averianov 2012	
Aspanlestes aptap	URBAC 06-100	2.19	1.57	3.4383	1.235	4.7432	114.81	Archibald and Averianov 2012	
Aspanlestes aptap	URBAC 98-148	1.92	1.41	2.7072	0.9959	4.3167	74.94	Archibald and Averianov 2012	
Aspanlestes aptap	URBAC 04-197	2.27	1.62	3.6774	1.3022	4.8631	129.43	Archibald and Averianov 2012	
Aspanlestes aptap	URBAC 99-032	2.22	1.59	3.5298	1.2612	4.79	120.3	Archibald and Averianov 2012	

Supplementary Table 3. *Continued.*

Taxon	Specimen	Lm1. mm	Wm1. mm	X (Lm1 x Wm1)	lnX	lnY	Y (body mass. g)	Reference	Com-ments
Aspanlestes aptap	URBAC 98-147	2.28	1.64	3.7392	1.3189	4.8929	133.34	Archibald and Averianov 2012	
Parazhelestes mynbulakensis	URBAC 04-402	2.45	1.72	4.214	1.4384	5.1061	165.03	Archibald and Averianov 2012	
Parazhelestes mynbulakensis	URBAC 04-399	2.46	1.95	4.797	1.568	5.3373	207.95	Archibald and Averianov 2012	
Parazhelestes mynbulakensis	URBAC 04-398	2.34	1.77	4.1418	1.4211	5.0752	160.01	Archibald and Averianov 2012	
Parazhelestes mynbulakensis	URBAC 04-227	2.39	1.63	3.8957	1.3599	4.966	143.46	Archibald and Averianov 2012	
Parazhelestes mynbulakensis	URBAC 03-211	2.39	1.61	3.8479	1.3475	4.9439	140.32	Archibald and Averianov 2012	
Parazhelestes mynbulakensis	URBAC 00-080	2.25	1.69	3.8025	1.3357	4.9229	137.4	Archibald and Averianov 2012	
Parazhelestes mynbulakensis	URBAC 99-109	2.37	2	4.74	1.556	5.3159	203.55	Archibald and Averianov 2012	
Parazhelestes mynbulakensis	URBAC 98-013	2.41	1.87	4.5067	1.5056	5.226	186.05	Archibald and Averianov 2012	
Zhelestes temirkazyk	URBAC 03-189	2.6	1.94	5.044	1.6182	5.4269	227.44	Archibald and Averianov 2012	
Zhelestes temirkazyk	CCMGE 14/12953	2.6	1.92	4.992	1.6078	5.4083	223.25	Archibald and Averianov 2012	
Zhelestes temirkazyk	URBAC 06-031	2.28	1.58	3.6024	1.2816	4.8264	124.76	Archibald and Averianov 2012	
Zhelestes temirkazyk	URBAC 04-190	2.41	1.61	3.8801	1.3559	4.9589	142.44	Archibald and Averianov 2012	
Zhelestes temirkazyk	URBAC 04-310	2.41	1.73	4.1693	1.4278	5.0872	161.94	Archibald and Averianov 2012	
Zhelestes temirkazyk	CCMGE 37/12000	2.33	1.57	3.6581	1.2969	4.8537	128.21	Archibald and Averianov 2012	
Eoungulatum kudukensis	CCMGE 17/12953	2.73	2.18	5.9514	1.7836	5.7219	305.5	Archibald and Averianov 2012	
Kulbeckia kulbecke	URBAC 00-052	2.1	1.6	3.36	1.2119	4.702	110.17	Archibald and Averianov 2003	
Kulbeckia kulbecke	URBAC 98-002	1.8	1.4	2.52	0.9243	4.1889	65.95	Archibald and Averianov 2003	
Kulbeckia kulbecke	URBAC 00-009	1.9	1.7	3.23	1.1724	4.6316	102.67	Archibald and Averianov 2003	
Kulbeckia kulbecke	CCMGE 60/12455	1.7	1.3	2.21	0.793	3.9547	52.18	Archibald and Averianov 2003	
Kulbeckia kulbecke	CCMGE 102/12455	1.8	1.3	2.34	0.8502	4.0568	57.79	Archibald and Averianov 2003	
Kulbeckia kulbecke	URBAC 98-001	1.9	1.5	2.85	1.0473	4.4083	82.14	Archibald and Averianov 2003	
Kulbeckia kulbecke	URBAC 99-064	1.9	1.5	2.85	1.0473	4.4083	82.14	Archibald and Averianov 2003	

Supplementary Table 4. Body mass estimation based on Bloch et al. (1998) and Conroy (1987).

Taxon	Minimum	Maximum	Mean	Standard error	N
Bloch et al. 1998					
Sulestes karakshi	42.19	65.02	54.26	4.31	6
Paranyctoides quadrans			8.4		1
Aspanlestes aptap	28.43	48.37	43.02	2.32	8
Parazhelestes mynbulakensis	49.43	72.15	59.32	3.21	8
Zhelestes temirkazyk	45.26	78.29	59.24	6.08	6
Eoungulatum kudukensis			102.49		1
Uchkudukodon nessovi	5.19	5.77	5.48	0.29	2
Daulestes kulbeckensis	6.11	7.39	6.75	0.64	2
Daulestes inobservabilis			8.18		1
Bulaklestes kezbe	11.82	15.12	13.71	0.98	3
Kulbeckia kulbecke	20.43	40.41	29.75	2.86	7
Conroy 1987					
Sulestes karakshi	115.51	185.55	152.44	13.22	6
Paranyctoides quadrans			19.7		1
Aspanlestes aptap	74.94	134.18	118.13	6.89	8
Parazhelestes mynbulakensis	137.4	207.95	167.97	9.97	8
Zhelestes temirkazyk	124.76	227.44	168.01	18.91	6
Eoungulatum kudukensis			305.5		1
Uchkudukodon nessovi	11.61	13.05	12.33	0.72	2
Daulestes kulbeckensis	13.9	17.11	15.51	1.61	2
Daulestes inobservabilis			19.14		1
Bulaklestes kezbe	28.66	37.52	33.73	2.64	3
Kulbeckia kulbecke	52.18	110.17	79	8.3	7